Composite nanocarriers for nucleic acid delivery

Dissertation

zur

Erlangung des Doktorgrades

der Naturwissenschaften

(Dr.rer.nat.)

dem

Fachbereich Pharmazie

der Philipps-Universität Marburg

vorgelegt von

Shashank Reddy Pinnapireddy

aus **Hyderabad, India**

Marburg/Lahn **2017**

Erstgutachter: **Prof. Dr. Udo, Bakowsky**

Zweitgutachter: **Prof. Dr. Achim, Aigner**

Drittgutachter: **Prof. Dr. Marc, Schneider**

Eingereicht am **19.04.2017**

Tag der mündlichen Prüfung am **31.05.2017**

Hochschulkennziffer: 1180

Composite nanocarriers for nucleic acid delivery

Thesis

Submitted in the fulfilment of the requirements of degree of

Doctor of Natural Sciences (Dr.rer.nat.)

equivalent to

Doctor of Philosophy (Ph.D.)

To

The Faculty of Pharmacy,

University of Marburg.

by

Shashank Reddy Pinnapireddy

from **Hyderabad, India**

Marburg/Lahn **2017**

First Supervisor: **Prof. Dr. Udo, Bakowsky**

Second Supervisor: **Prof. Dr. Achim, Aigner**

Third Supervisor: **Prof. Dr. Marc, Schneider**

Date of Submission **19th April 2017**

Defense date **31st May 2017**

Hochschulkennziffer: 1180

E I D E S S T A T T L I C H E E R K L Ä R U N G

Ich versichere, dass ich meine Dissertation

„**Composite nanocarriers for nucleic acid delivery**“

selbständig ohne unerlaubte Hilfe angefertigt und mich dabei keiner anderen als der von mir ausdrücklich bezeichneten Quellen bedient habe. Alle vollständig oder sinngemäß übernommenen sind Zitate als solche gekennzeichnet.

Die Dissertation wurde in der jetzigen oder einer ähnlichen Form noch bei keiner anderen Hochschule eingereicht und hat noch keinen sonstigen Prüfungszwecken gedient.

Marburg, den 19.04.2017

.....

(**Shashank Reddy Pinnapireddy**)

AUTHOR'S DECLARATION

I declare that this thesis titled

"Composite nanocarriers for nucleic acid delivery"

has been written entirely by myself and is a record of work performed by myself. The research was carried out at the Institut für Pharmazeutische Technologie und Biopharmazie, University of Marburg, at the campus Ketzerbach 63 (old location) and Robert-Koch-Straße. 4 (new location) under the supervision of Professor Udo Bakowsky

This thesis has not been submitted in any form elsewhere for a higher degree

Marburg, 19th April 2017

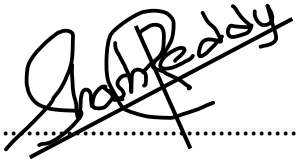

.....

(**Shashank Reddy Pinnapireddy**)

A C K N O W L E D G E M E N T S

This work was performed between August 2013 and January 2017 in the Research Group of Prof. Dr. Udo Bakowsky, Department of Pharmaceutics and Biopharmaceutics, Faculty of Pharmacy, Philipps-Universität Marburg.

I would like to thank my supervisor Prof. Dr. Udo Bakowsky, whose profound knowledge, ideas, advice, support and invaluable guidance helped me throughout my Doctoral studies.

I would also like to thank Prof. Dr. Achim Aigner for his fruitful scientific discussions during my visits to his lab in Leipzig. I would like to acknowledge the help of Mrs Eva Maria Mohr who has supported me and motivated me with her discussions and expertise throughout the course of my studies. I would also like to thank the past and the present members at the Department of Pharmaceutics and Biopharmaceutics for their friendship and help. Most importantly, I would like to thank Dr. Jarmila Jedelská and Dr. Jens Schäfer for their outstanding support, sensible advice and willingness to help. Sincere thanks to my colleagues at the Research Group Bakowsky especially Dena Akbari, Lili Duse, Sandra Ditzler, Boris Strehlow, Elias Baghdan and Konrad Engelhardt for helping me out with my studies. Special thanks to Julia Michaelis for her patience and eagerness to help.

I am extremely grateful to my family and my parents who have supported me all the way and whose encouragement has made this possible. Thank you so much, I dedicate this to you both!

Die vorliegende Arbeit entstand auf Anregung und unter Leitung von

Herrn Prof. Dr. Udo Bakowsky

am Institut für Pharmazeutische Technologie und Biopharmazie
der Philipps-Universität Marburg

TABLE OF CONTENTS

LIST OF FIGURES

LIST OF TABLES

Part I: Introduction

1.1 Gene therapy

Gene therapy is a clinical approach to treat diseases and correct disorders at a genetic level. Historically, this approach has been used to treat genetic disorders, but after several advancements in the field of genetic engineering, it is also possible to cure acquired diseases, cancer and infections. Such a therapy would restore proper functioning of the diseased organ or tissue. The main objectives of gene therapy are expression of a deficit gene, knockdown of an over-expressing gene, or replacement of a defective gene in considerable number of target cells. Gene therapy can be performed *ex vivo* which involves isolation of cells isolated from patients, introduction of genetic material using suitable vectors and injecting back into the patients. Alternatively, in *in vivo* gene therapy, the patient is directly injected with vectors containing genetic material [1]. Over years, gene therapy has garnered interest from researchers in various fields. A lot of progress has been made in the development of viral and non-viral vectors for gene therapy [2].

In the plethora of gene delivery strategies available today, internalisation of the delivery vehicle, protection of its cargo against degradation in the extracellular milieu, and its subsequent release are the major factors determining the success of the treatment regimen. Nucleic acids such as DNA (especially plasmid DNA) and siRNA have long been experimented with for the treatment of a comprehensive range of diseases [3].

To achieve the desired effect, nucleic acids need to be delivered into the cells bypassing various hindrances [4]. Of these, blood is a major barrier due to its complexity in terms of composition followed by cellular entry by bypassing the cell wall. Once the delivery vehicles enter the cells, they need to withstand the endosomal and lysosomal environments. This can only be achieved with delivery vehicle designed to sustain the extracellular and intracellular environments. Numerous factors such as cytotoxicity, cell penetrability, degradation and intracellular dissociation of the delivery vehicles are responsible for a reliable therapy. Viral vectors which fulfil the above requirements, have been employed in the past and have also shown some promising results *in vivo* [5-7]. Unfortunately, after a series of clinical trials their use was frowned upon owing to their toxic side effects, risk of undesired immune reactions, harmful mutations and cost of treatment [8-10]. Subsequent focus was hence laid upon development of alternatives to viral vectors for *in vitro*, *in vivo* and *ex vivo* delivery.

Among others, liposomes, polymers and nanoparticles have been the most studied non-viral vectors for gene therapy. With the aspect of achieving the delivery efficiency similar to viruses, in this work, focus was laid upon developing hybrid vectors utilising physical means to enhance the gene transfer.

1.2 RNA interference

Majority of the gene delivery strategies involve addition of a specific functionality to the target organ or tissue to overcome its deficiencies. With the discovery of gene silencing ability of short interfering RNA (siRNA) by Fire and Mello in 1998, new horizons were opened in the field of gene therapy [11]. siRNA's ability to knock down the production of corresponding proteins is known as RNA interference (RNAi). The mechanism with which siRNA works is through a multiprotein RNA induced silencing complex (RISC). After entering a cell, double stranded siRNA is unwound into two single strands by the RISC complex. Of these two strands, the guide strand remains bound to the complex which acts as template to its complementary mRNA. Upon recognition of the complementary mRNA, Argonuate (AGO), a protein found in the RISC complex, cleaves the mRNA inhibiting protein translation (
Figure 1) [12, 13].

While DNA's can go up to several kilo base pairs (bp), siRNA is a relatively small biomolecule comprising 21-23 bp. A new class of 27-mer siRNA termed dicer-substrate siRNA (dsiRNA) having a dicer sequence has been found to be more efficient. dsiRNA works by mimicking the features of naturally occurring dicer substrates thereby promoting an efficient incorporation into the RISC complex [14, 15]. Due to its small size, siRNA is highly susceptible to enzymatic degradation, necessitating the use of an appropriate delivery system [16].

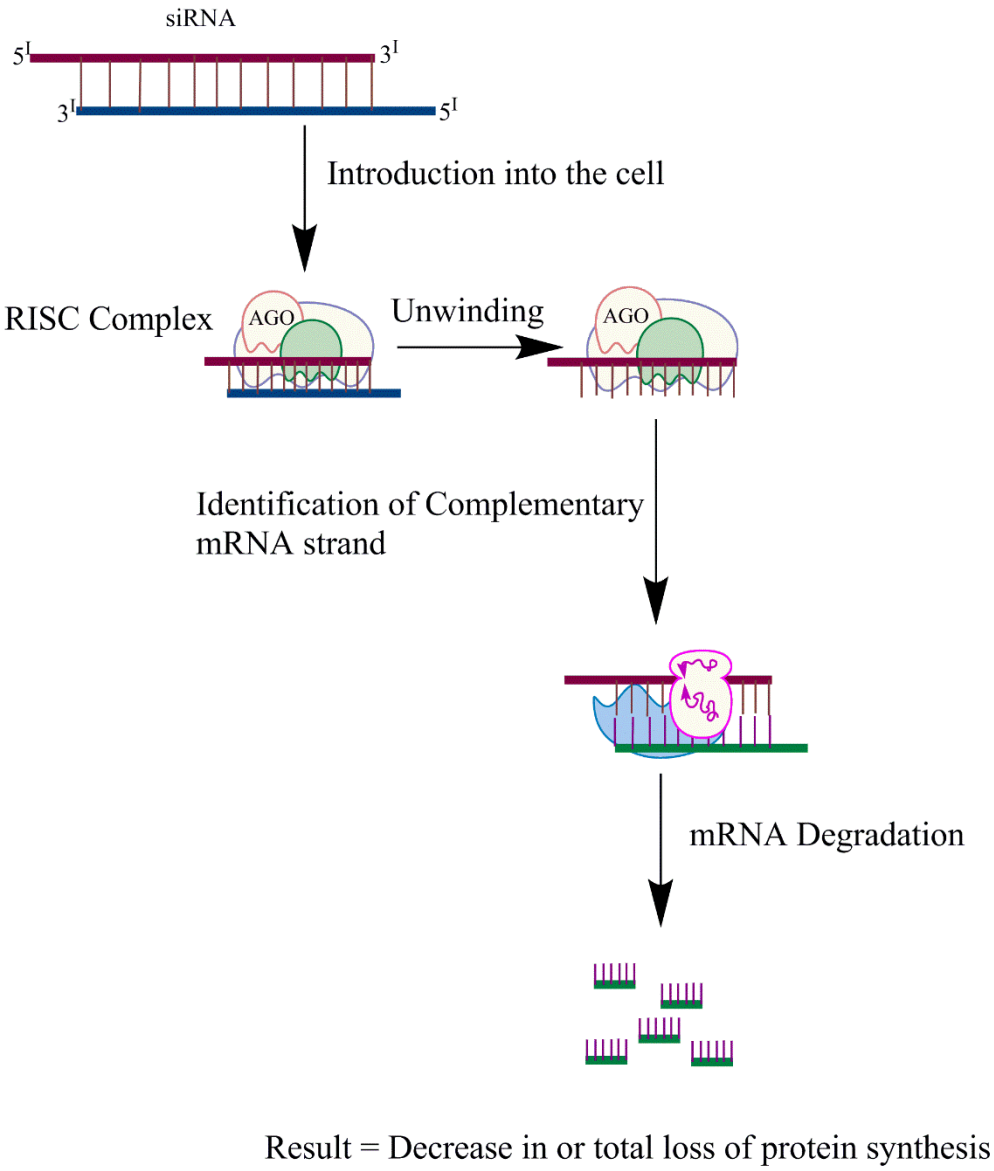

Figure 1: Graphical illustration of the RNA induced silencing complex

1.3 Non-viral Vectors

The success of non-viral gene therapy depends on the application form or the delivery vehicle. An ideal delivery vehicle should possess significant delivery efficiency and should be relatively non-toxic and biocompatible. Delivery of nucleic acid devoid of vectors i.e. naked nucleic acid delivery has been employed with varying success. The commonly used methods for naked delivery are electroporation, micro needle injection and ballistic delivery which are all limited to an *in vitro* set up and have never made their way into clinical therapeutics [17]. On the other

hand, delivery of nucleic acids using delivery vehicles such as liposomes, polymers and nanoparticles has been met with considerable success [18-20]. 1,2-dioleoyl-3-trimethylammonium-propane (DOTAP), 1,2-di-O-octadecenyl-3-trimethylammonium propane (DOTMA), (1-[2-(9-(Z)-octadecenoyloxy)ethyl] -2-(8-(Z)-heptadecenyl) -3 (hydroxyethyl) imidazolinium chloride (DOTIM), N-methyl-4(dioleyl)methylpyridiniumchloride (SAINT), 1,2-dimyristyloxy-propyl-3-dimethyl-hydroxy ethyl ammonium bromide (DMRIE), 1,2-di-(9Z-octadecenoyl)-*sn*-glycero-3- [(N- (5-amino-1-carboxypentyl) iminodiacetic acid) succinyl (DOGS), and 1,2-dioleoyl-sn-glycero-3-phosphoethanolamine (DOPE) are the most frequently used lipids for delivery of nucleic acids [21, 22]. Among polymers, polyethylenimine (PEI; linear and branched) of various molecular weights, poly-L-lysine (PLL), chitosan, polyamidoamine (PAMAM) are widely used [23, 24]. Poly (lactic-co-glycolic acid) (PLGA) and silica particles have been proven to be indispensable for formulation of nanoparticles for gene delivery [20]. Several therapies which are under clinical evaluation are based upon one of these vectors [25].

Size, surface charge, stability and rigidness are the main factors influencing the delivery efficiency of non-viral vectors [26]. These parameters laid the foundation for this study which was aimed at developing a non-viral vector system capable of effectively delivering the genetic material with minimal effects on cell viability.

1.4 Liposomes

Though it has been more than a century since their first mention by Otto Lehmann in his book ‘Die Flüssige Kristalle’, it wasn’t until the 60’s, where Alec Bangham along with his colleagues at the Babraham Institute, discovered the beneficial properties of liposomes [27]. Since then, several research groups have been involved in studying liposomes from structure to interactions with biological systems.

Based on their lamellarity, liposomes may be classified into two major groups, multilamellar and unilamellar vesicles; unilamellar liposomes are further divided into small and large unilamellar vesicles [28]. Simple as they might seem, many factors come into play in the formation of a liposome. Physicochemical factors such as van der Waals forces, phase transition temperature, chemical composition of the lipids used, solvents employed, rehydration buffers,

pH, presence or absence of inorganic salts etc. all play a vital role in shaping a liposome [21, 29, 30].

Liposomal delivery of drugs and nucleic acids is an evolving field comprising of several research disciplines ranging from biophysics to medicine. Hydrophilic, hydrophobic, amphiphilic substances, antibodies, and genetic material can be delivered using liposomes (Figure 2).

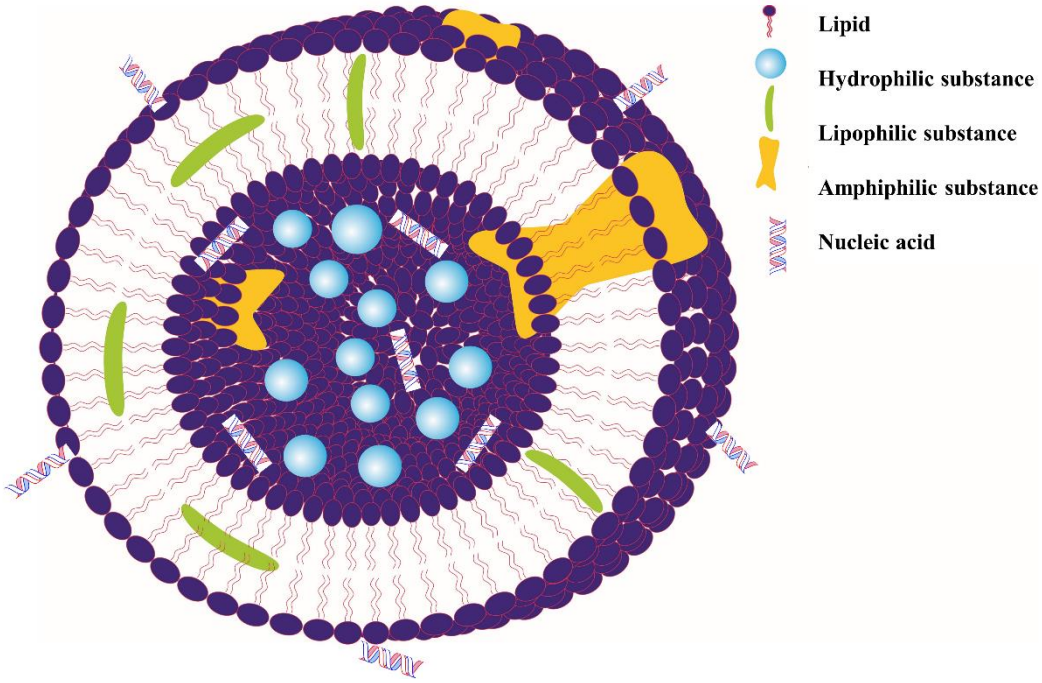

Figure 2: Illustration of a liposome with different types of cargo [31]

Formulation of an optimal liposomal delivery system requires knowledge in various fields like physical, analytical, organic and colloidal chemistry, theoretical, structural and surface physics, physiology, pharmacology, pharmacokinetics and toxicology to name a few [32]. An ideal liposomal delivery system should be able to deliver its cargo to the target organ with minimal loss and without being immunogenic. In practice, this is an extremely challenging task to achieve considering the complexity of the biological fluids which pose a major challenge between their administration and reaching of the therapeutic target.

Among the biological fluids, blood plays a pivotal role in determining the fate of the liposomes. Plasma, which makes up 55 % of blood‘s volume, consists of numerous ions, proteins, lipases, glucose, antibodies, salts, vitamins and amino acids which all interact with the liposomes and are detrimental to its stability [33].

Upon reaching their target, liposomes interact with the cells of the target tissue or organ, which forms the basis for the therapy. There are many ways in which liposomes interact with cells viz. intermembrane transfer i.e. transfer between the phospholipid bilayers of the cells and liposomes; contact release, which is the release of the aqueous contents of the liposome upon cellular contact due to an apparent increase in the permeability of the liposomal membrane; adsorption; cellular fusion, in which liposomes and cell membranes fuse together; phagocytosis and endocytosis [34-38]. The size, shape, surface charge and composition of the liposomes are the determining factors for cellular interactions and uptake.

Due to similarities in composition with biological membranes and ease of optimisation, liposomes make a popular choice for delivery of drugs and genetic material. Biocompatibility, bioavailability, circulation time and solubility of the cargo can be improved using liposomes. Depending upon their application, either cationic, anionic or zwitterionic lipids maybe employed in liposomal formulation [39-41]. Due to their electrostatic interactions with nucleic acids, cationic liposomes are the first choice for gene delivery [42-44]. However, without appropriate shielding of the surface charge, cationic liposomes tend to be cytotoxic and have low storage stability [45-47].

On the other hand, anionic liposomal formulations tend to be less cytotoxic and when formulated using zwitterionic phospholipids (e.g. Dipalmitoylphosphatidylcholine; DPPC) and helper lipids (e.g. DOPE and cholesterol), offer more room for optimisation in terms of surface charge and mechanical stability which have a significant effect on endosomal escape and binding of nucleic acids [48-51]. With cytotoxicity, delivery efficiency, stability being the driving forces, this study was directed to develop a novel formulation wherein emphasis was laid upon controlled release of the liposomal contents.

1.5 Polymers

Cationic polymers have a long-standing history in gene delivery. Most of the cationic polymers rely on the ability of the amines to protonate in physiological environment which electrostatically attracts the oppositely charged phosphate groups of nucleic acids to form nano-complexes or polyplexes [52, 53].

Beginning with PLL, research into cationic polymers as condensing and gene transfer agents has made many breakthroughs [54, 55]. Worth mentioning is PEI which has set a gold standard as a transfection agent after its beneficial properties as a gene transfer agent were realised. PEI has a high charge density which condenses the nucleic acids and protects them against nucleases (Figure 3) [56]. Though the exact mechanism of action is still debated, the endosome rupturing 'proton-sponge effect' has been proposed as the main mode of action [57]. During endosome maturation, the pH inside begins to acidify. Starting with early endosome at around 6, the pH falls to 5 in late endosomes, this fall in pH protonates the secondary and tertiary amines of PEI which causes increased influx of protons. This increases the osmotic pressure leading to swelling and eventual rupture of the endosome [58, 59].

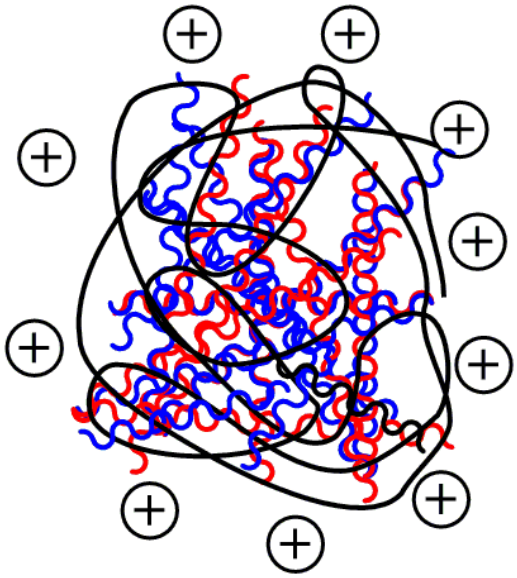

Figure 3: Representation of a cationic polymer-PEI based polyplex

Since the discovery of its ability to condense genetic material, PEI has been the most studied polymer in gene therapy [60-62]. Various modifications such as grafting, coupling, cross-linking, PEGylation have been done to improve the transfection efficiency of PEI and to reduce its cytotoxicity [63-70].

Soon after PEI, other synthetic polymers like PAMAM, PLL, poly (2-dimethylaminoethyl methacrylate) (pDMAEMA) and naturally occurring polymers such as chitosan made their way into gene delivery [71-74].

1.6 Composite liposome-polymer lipopolyplexes

Utilising the biocompatible property of liposomes and combining it with the (nucleic acid) condensation and protective properties of cationic polymers, a hybrid delivery vehicle has been developed. The combination of cationic polymers and liposomes have shown promising transfection and knockdown efficiencies *in vitro* [75]. Since the cell membrane is also composed of phospholipids, encapsulation of cationic nanoparticles in phospholipid based liposomes enhances the biocompatibility [76].

A deacylated variant of linear PEI (lPEI) was used to prepare the polyplexes used in the study. Deacylation dramatically improves transfection efficiency and the absence of primary amines in linear PEI renders it less cytotoxic than its branched counterpart [77]. The primary amines are responsible for the higher charge density of branched PEI (bPEI) which is often associated with destabilisation of cell wall and cellular necrosis [78-80].

Using lPEI, several formulations were developed to simplify the design of the complexes and to improve transfection efficacy and cytotoxicity. Due to their cationic nature, lPEI/nucleic acid complexes often invoke immune responses [79]. To shield the cationic charge and to address the most frequent problem with polyplexes i.e. aggregation, polyplexes were encapsulated with various liposomal combinations using DPPC, DOTAP, DOPE, and cholesterol to form lipopolyplexes.

When liposomes are added to nucleic acid-polycation complexes, an extensive reorganisation of the lipid membranes takes place following the initial contact, resulting in polymer-nucleic acid complexes with lipid coatings (Figure 4). This strategy overcomes the surface charge issue

associated with cationic polymers. The extracellular cytotoxicity of the complexes is reduced, making room for receptor-mediated targeting without interference of nonspecific charge-charge interaction.

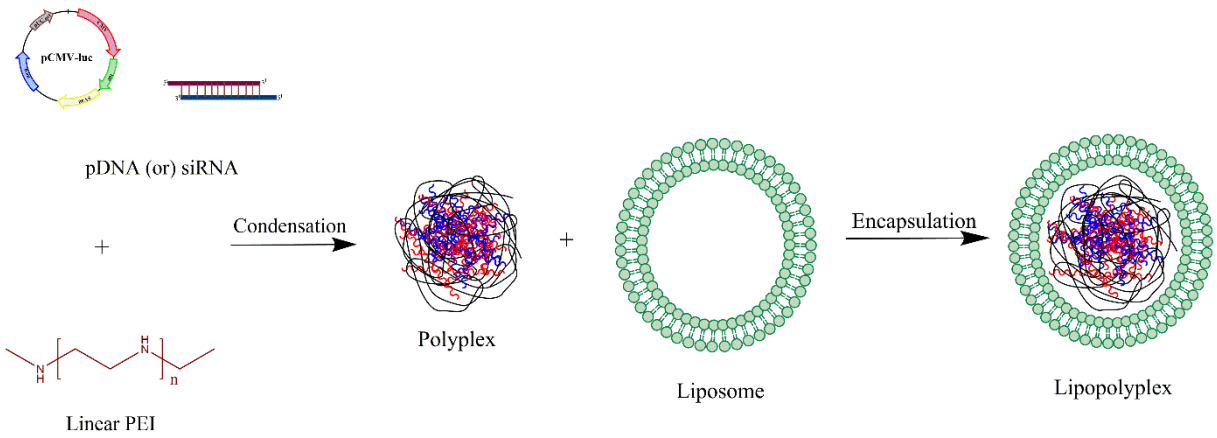

Figure 4: Illustration of lipopolyplex formation

The transfection efficiency of gene delivery vehicles depends upon their surface charge, size, rigidity and stability, especially in the physiological environment [26, 81]. A unique combination of lipids was therefore selected for formulation of lipopolyplexes. To obtain the desired physicochemical characteristics, viz. slight positive charge and a size range in between 100 and 200 nm along with improved stability, helper lipids were incorporated into the liposomal formulations. These have a considerable influence on the electrostatics, lipid self-assembly, level of hydration, packing parameter and surface charge [21, 82]. DOPE and cholesterol were chosen as helper lipids after a series of experiments. The most common problem faced by gene delivery vehicles is the escape of the delivery vehicle from the endosome and other cellular compartments [83]. To tackle this problem, focus was laid upon physical methods for enhancement of gene transfer in this thesis work. Light and ultrasound have been used as the preferred methods due their minimally invasive nature.

1.7 Photo activation

Light has been used since ages as a therapeutic agent in ancient Indian and Egyptian civilisations for the treatment of psoriasis, vitiligo, rickets and skin cancer [84]. Photodynamic therapy (PDT) is a process which induces localised tissue necrosis. An otherwise inert photosensitiser delivered to the target tissue is activated using light of a specific wavelength. In presence of molecular oxygen, reactive oxygen species are generated which selectively destroy the tumour tissue [85, 86]. PDT has been approved by the European medicines agency (EMA) and Food and drug administration (FDA) for the treatment of certain pre-malignant and malignant diseases [87-89]. Photo-chemical internalisation (PCI) is a subclass of photodynamic therapy wherein light is used to trigger breakdown of the endo/lysosomal membranes (Figure 5). This process is based on photosensitisers localised inside these membranes. Photo-activation initiates photochemical reactions, causing rupture of the vesicles leading to release of endocytosed compounds [90-93]. PCI could be used for both triggered release of substances and biomolecules and for enhancing the therapeutic efficacy [94-96]. PCI strategy has been successfully utilised for enhancing the release of polymer-DNA complexes [97, 98]. For enhancing the endosomal release, liposomes containing curcumin, a proven therapeutic agent and a photosensitiser, were used for the lipopolyplex formulation.

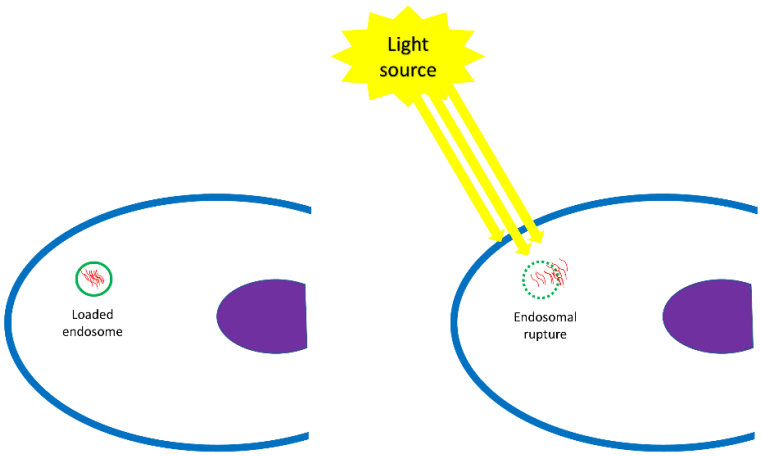

Figure 5: PCI; Endosomal rupture and subsequent release of contents following irradiation

1.8 Ultrasound

Since its inception in the late 50's, ultrasound has made countless breakthroughs in the field of medical diagnostics. It is a gentle and non-invasive tool which has been proven valuable in the diagnosis of a variety of diseases [99]. Ultrasound has excellent patient compliance and a remarkable safety track record [100, 101]. Nanocarriers have been successfully employed in ultrasound mediated drug delivery and as theranostic agents for enhancing ultrasound contrast [102-104]. The use of ultrasound in gene transfer, termed as ultrasound enhanced gene transfer (UEGT), began after individual research groups observed enhanced permeation of delivery vehicles into the cell and subsequent release [105, 106]. It is a known fact ultrasound permeabilises the cell membrane which is the underlying mechanism of ultrasound enhanced cellular uptake of nanocarriers [107]. Among others, gas-filled microbubbles are the most commonly used delivery vehicles for UEGT [108, 109]. Upon application of ultrasound, these bubbles blast and the propulsion created from this effect enhances their delivery into the cells. Enhancement of liposomal gene delivery using ultrasound has already been reported, the exact mechanism of action is however, still unclear.

1.9 Anti-Inflammatory gene therapy

Advancements in RNAi research have paved a new dimension in therapeutic targets for gene delivery, which was otherwise confined to transfer of therapeutic genetic material for replacing defective genes. RNAi has provided a means of downregulating expression of various overexpressed genes [110]. The therapeutic aspects of RNAi have extended to treatment of anti-inflammatory disorders [111]. E-selectin is expressed by the SELE gene in humans. It is responsible for inflammatory activity in endothelial cells and mediates the adhesion of tumour cells to the endothelial cells thereby playing a major role in tumour metastasis [112, 113]. Delivery vehicles loaded with siRNA directed against SELE can mediate knockdown of E-selectin thereby inhibiting inflammatory activity and tumour cell metastasis [114].

Aims and scope

This work was aimed at developing non-viral vectors for anti-inflammatory gene therapy capable of overcoming the extracellular and cellular barriers. The ambit of this study included development of a potent multicomponent delivery system with low cytotoxicity without compromising on delivery efficiency.

The key aspects covered in this work include:

- Designing a delivery system capable of dealing with the shortcomings of non-viral vectors - A relatively low toxic vehicle with high gene transfer efficiency
- Optimising the parameters determining the physicochemical properties of the lipopolyplexes
- Detailed physical characterisation of the lipopolyplexes in terms of structure and morphology
- Electron microscopic elucidation of the polyplex-in-liposome structure
- Establishing a reproducible method for preparation of lipopolyplexes and transfection
- Determination of the mechanism of cellular uptake
- Physically enhancing gene transfer by improving endosomal escape of the lipopolyplexes using light and ultrasound
- Selective knockdown of the inflammatory gene SELE by means of RNAi.

Part II: Experimental

2.1 Materials

List of materials

Materials or substances	Source
∅ 15 mm cover slips	Gerhard Menzel B.V. & Co. KG., Braunschweig, Germany
0.2 µm PES Syringe Filters	Whatman plc, Buckinghamshire, UK
0.2 cm Electroporation Cuvettes	Bio-Rad Laboratories GmbH, Munich, Germany
10 kDa MWCO Centrifugal Concentrators; Vivaspin 6	Sartorious Stedim GmbH; Göttingen, Germany
12-well plates; Nunclon Delta	Nunc GmbH & Co. KG., Wiesbaden, Germany
2-iminothiolane hydrochloride; Traut's Reagent	Sigma Aldrich Chemie GmbH, Taufkirchen, Germany
3,3',5,5'-Tetramethylbenzidine	Sigma Aldrich Chemie GmbH, Taufkirchen, Germany
96-well microtiter plates; CytoOne®	Starlab International GmbH, Hamburg, Germany
A549 cell line	ATCC®, Manassas, USA
Adhesive plate seals	Boehringer Mannheim GmbH, Mannheim, Germany
AFM Probe; HQ:MSC16/Al BS	µmasch, Tallinn, Estonia
Agar	Merck KGaA, Darmstadt, Germany
Agarose	Merck KGaA, Darmstadt, Germany
Ampicillin	Sigma Aldrich Chemie GmbH, Taufkirchen, Germany
Anti-human E-selectin monoclonal antibody	Sigma Aldrich Chemie GmbH, Taufkirchen, Germany
Anti-luc siRNA 1	GE Dharmacon, Lafayette, USA
Argon Ion Laser; Enterprise II	Coherent Inc., Santa Clara, USA
Atomic force microscope; Nanowizard® 1	JPK Instruments AG, Berlin, Germany
Autoclave, Tuttnauer 3850 ELC	Tuttnauer GmbH, Linden, Germany
Bath Sonicator; Transonic Digital S	Elma Schmidbauer GmbH, Singen, Germany
Beetle luciferin	Synchem UG & Co. KG, Felsberg, Germany

Carbon Tabs	PLANO GmbH, Wetzlar, Germany
CCD-Camera; Gatan MegaScan 794	Gatan Inc., Pleasanton, USA
Cell Culture Lysis Reagent	Promega GmbH, Mannheim, Germany
Centrifuge; Beckman J2-21	Beckman Coulter GmbH, Krefeld, Germany
Specific Pathogen Free Eggs	Valo Biomedia GmbH, Osterholz-Scharmbeck, Germany
Chlorpromazine	Alfa Aesar GmbH & Co. KG., Karlsruhe, Germany
Cholesterol	Sigma Aldrich Chemie GmbH, Taufkirchen, Germany
CO_2 incubator, HeraCell	Heraus GmbH & Co. KG., Hanau, Germany
Coagulation analyser; Coatron M1	Teco GmbH, Neufahrn, Germany
Confocal laser scanning microscope; LSM 510/Axiovert 100M	Carl Zeiss Microscopy GmbH, Jena, Germany
Critical Point Dryer; Bal-Tec CPD 030	Bal-Tec AG, Balzers, Liechtenstein
Cryo Transfer System; Alto 2500	Gatan Inc., Pleasanton, USA
Culture Tubes; Pyrex	Corning Inc., Corning, USA
Curcumin	Sigma Aldrich Chemie GmbH, Taufkirchen, Germany
DAPI	Sigma Aldrich Chemie GmbH, Taufkirchen, Germany
Digital image acquisition system; DISS 5	Point Electronic GmbH, Halle, Germany
DMEM-HG	Biochrom GmbH, Berlin, Germany
DMEM-LG	Biochrom GmbH, Berlin, Germany
DNA ladder; GeneRuler 1 kb	Fermentas Life Sciences, Vilnius, Lithuania
DMSO; ≥ 99 %	Acros Organics B.V.B.A., Geel, Belgium
DOPE	Lipoid GmbH, Ludwigshafen, Germany
DOTAP	Avanti Polar Lipids Inc., Alabaster, USA
DPPC	Lipoid GmbH, Ludwigshafen, Germany
Dynasore	Cayman Chemical Company, Ann Arbor, USA
EA.hy926 cell line	ATCC®, Manassas, USA
Electrophoresis chamber; Thermo Hybaid Electron 4	Thermo Electron GmbH, Ulm, Germany

Electroporator; Gene Pulser™	Bio-Rad GmbH, Munich, Germany
Endothelial cell growth kit; PCS-100-041™	ATCC®, Manassas, USA
Ethanol	Carl Roth GmbH + Co. KG., Karlsruhe, Germany
Ethidium Bromide	Sigma Aldrich Chemie GmbH, Taufkirchen, Germany
Extruder; Avanti Mini	Avanti Polar Lipids Inc., Alabaster, USA
Field emission SEM; JSM-7500F	JEOL Ltd., Tokyo, Japan
Filipin III	Sigma Aldrich Chemie GmbH, Taufkirchen, Germany
Foetal bovine serum	PAA Laboratories GmbH, Cölbe, Germany
Formaldehyde	Alfa Aesar GmbH & Co. KG., Karlsruhe, Germany
Freeze Drier; Christ Beta I	Martin Christ Gefriertrocknungsanlagen GmbH, Osterode am Harz, Germany
Glow Discharger; Edwards S150B	Edwards Vacuum, Crawley, UK
Glutaraldehyde	Alfa Aesar GmbH & Co. KG., Karlsruhe, Germany
Gold Nanospheres	Sigma Aldrich Chemie GmbH, Taufkirchen, Germany
Hatching incubator; Ehret KMB 6	Dipl. Ing. W. Ehret GmbH, Emmendingen, Germany
HeLa cell line	Clontech Laboratories Inc., Saint-Germain-en-Laye, France
Heparin	AppliChem GmbH, Darmstadt, Germany
Human E-selectin standard	Sigma Aldrich Chemie GmbH, Taufkirchen, Germany
IMDM	Biochrom GmbH, Berlin, Germany
INTERFERin®	Polyplus-transfection® SA, Illkirch, France
Isotonic NaCl	B.Braun Melsungen AG, Melsungen, Germany
Escherichia Coli; JM109	Clontech Laboratories Inc., Saint-Germain-en-Laye, France
Kanamycin	Sigma Aldrich Chemie GmbH, Taufkirchen, Germany
L929	ATCC®, Manassas, USA
Laminar Flow Hood; Labgard Class II	NuAire Inc., Plymouth, USA

LDH assay Kit	Roche Diagnostics AG, Basel, Switzerland
LED Irradiator	Lumundus GmbH, Eisenach, Germany
Liquid CO_2	Praxair Deutschland GmbH, Düsseldorf, Germany
Constant Power Supply; LKB 2197	LKB Produkter AB, Bromma, Sweden
Luciferase GL3 duplex	Dharmacon Inc., Lafayette, USA
Magnetic Stirrer; MCS 66	CAT Scientific, Paso Robles, USA
MCDB 153	Biochrom GmbH, Berlin, Germany
Medical ultrasound device; eZono® 3000	eZono AG, Jena, Germany
Micro reagent tubes	Sarstedt AG & Co., Nümbrecht, Germany
MilliQ® Water	Millipore Corporation, Billerica, USA
Mounting medium; FluorSave™	Calbiochem Corporation, San Diego, USA
MTT dye	Sigma Aldrich Chemie GmbH, Taufkirchen, Germany
N-2-Hydroxyethylpiperazine-N′-2-ethanesulfonic acid; HEPES ≥ 99 %	VWR International GmbH, Darmstadt, Germany
Osmium Tetroxide	Alfa Aesar GmbH & Co. KG., Karlsruhe, Germany
pCMV-luc	PlasmidFactory GmbH & Co. KG., Bielefeld, Germany
PCS-100-012™ cell line	ATCC®, Manassas, USA
pEGFP-N1	Clontech Laboratories Inc., Saint-Germain-en-Laye, France
PEI MAX; Linear PEI 22 kDa	Polysciences Europe GmbH, Hirschberg, Germany
Petri Dishes; Tissue Culture grade and Suspension type	Sarstedt AG & Co., Nümbrecht, Germany
Piece BCA assay kit	Thermo Fisher Scientific GmbH, Dreieich, Germany
Plasmid Isolation Kit; QIAfilter Giga	Qiagen GmbH, Hilden, Germany
Polycarbonate membranes	Whatman plc, Buckinghamshire, UK
Polymin®; Branched PEI 25 kDa	BASF AG, Ludwigshafen, Germany
RNAse free water	GE Healthcare Europe GmbH, Freiburg, Germany
Rotary Evaporator; Laborota 4000	Heidolph Instruments GmbH & Co. KG., Schwabach, Germany

Scanning electron microscope; Hitachi S-510	Nissei Sangyo Co. Ltd., Tokyo, Japan
SELE dsiRNA 27mer	OriGene Technologies, Rockville, USA
SELE siRNA	Santa Cruz Biotechnology Inc., Santa Cruz, USA
SEM Specimen Stubs	PLANO GmbH, Wetzlar, Germany
Shaking Incubator; IKA KS4000 IC	IKA Werke & Co. KG., Staufen, Germany
siRNA dilution buffer	GE Healthcare Europe GmbH, Freiburg, Germany
siRNA No. 2; siCtrl	Dharmacon Inc., Lafayette, USA
SK-OV-3 cell cline	ATCC®, Manassas, USA
SK-OV-3-luc cell line	Gift from Prof. Dr. Aigner
Microscopy Slides	Gerhard Menzel B.V. & Co. KG., Braunschweig, Germany
SOC	Carl Roth GmbH + Co. KG., Karlsruhe, Germany
Sodium citrate	Eifelfango Werk GmbH & Co. KG., Bad Neuenahr-Ahrweiler, Germany
Luminometer; FLUOstar® Optima	BMG Labtech, Ortenberg, Germany
Spectrophotometer; Ultrospec 3000	Pharmacia Biotech AG, Uppsala, Sweden
Sputter Coater; Edwards S150	Edwards Vacuum, Crawley, UK
TEClot aPTT-S Kit	Teco GmbH, Neufahrn, Germany
TEM 300 mesh grids	PLANO GmbH, Wetzlar, Germany
Trans-Illuminator; BioDoc Analyse Ti5	Whatman Biometra GmbH, Göttingen, Germany
Transmission electron microscope; JEM-3010	JEOL Ltd., Tokyo, Japan
Tris	Merck KGaA, Darmstadt, Germany
Triton™ X-100	Sigma Aldrich Chemie GmbH, Taufkirchen, Germany
Uranyl acetate	Sigma Aldrich Chemie GmbH, Taufkirchen, Germany
Vacuum Pump; SC 920	KNF Neuberger GmbH, Freiburg, Germany
Water Bath	Kottermann GmbH & Co. KG., Hänigsen, Germany
White opaque 96-well plates	Brand GmbH + Co. KG., Wertheim, Germany
Zetasizer Nano ZS	Malvern Instruments Ltd, Malvern, UK

2.1.1 Lipids

2.2.1.1 DPPC

Dipalmitoylphosphatidylcholine is a fatty acid containing a polar phosphate head group and a nonpolar fatty acid chain. DPPC is an amphiphilic molecule with a molecular weight of 734.039 g/mol and a phase transition temperature T_c of 41 °C. The molecules of DPPC can arrange in favour of polar and nonpolar interactions to a phospholipid bilayer which can form spherical vesicles [115]. It is often employed together with cholesterol which acts a membrane stabiliser. DPPC is found abundantly in eggs and is a prominent lipid found in cell membrane and in lung surfactant. The DPPC used for this work was however synthetically produced with a purity ≥ 99 %. The lipid was dissolved in 2:1 (v/v) chloroform: methanol mixture at a concentration of 10 mg/mL and stored in glass vials at -20 °C.

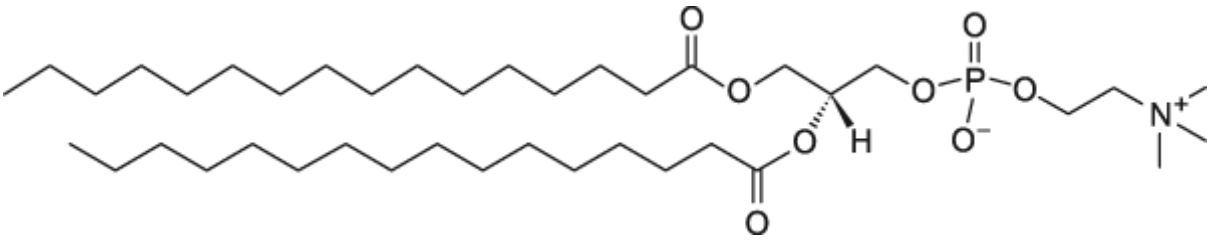

DPPC

2.2.1.2 DOPE

Dioleoylphosphoethanolamine is a conical unsaturated non-bilayer synthetic phospholipid. DOPE forms an inverted hexagonal phase due to its negative spontaneous curvature [116]. It is often employed as a co-lipid or a helper lipid in liposome formulation. DOPE is a neutral lipid with a molecular weight of 744.034 g/mol and a T_m of -16 °C and known to enhance the fusion of liposomes with endosomes facilitating incorporation into the cellular membrane [117]. The DOPE used for this work was of a purity ≥ 99 %. Aliquots of 10 mg/mL of the lipid were dissolved in 2:1 (v/v) chloroform: methanol mixture and stored in glass vials at -20 °C.

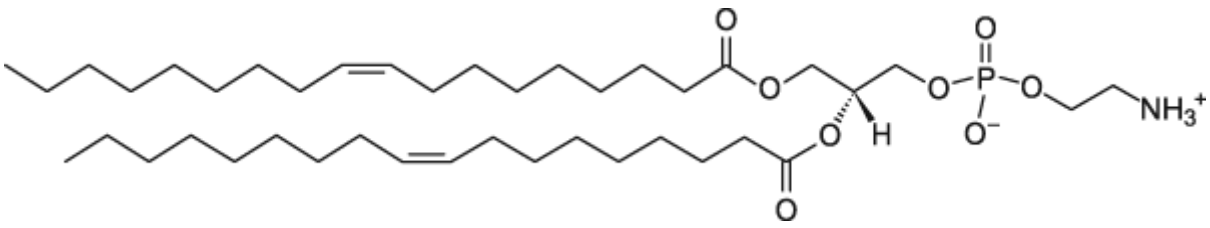

DOPE

2.2.1.3 DOTAP

Dioleoyltrimethylammoniumpropane is a synthetic unsaturated cationic lipid with a molecular weight of 698.542 g/mol and a T_m of < 5 °C. It is widely regarded as a standard for lipofection i.e. liposomal transfection. A DOTAP of ≥ 99 % purity was used for this work. The lipid was dissolved in 2:1 (v/v) chloroform: methanol mixture at a concentration of 10 mg/mL and stored in glass vials at -20 °C.

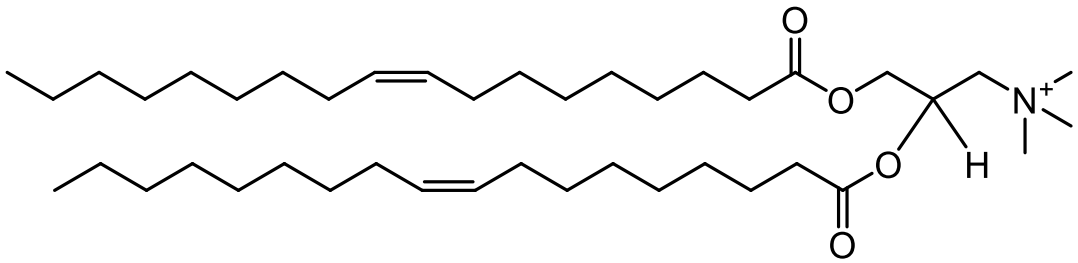

DOTAP

2.2.1.4 Cholesterol

Cholesterol is a lipophilic molecule with a single polar hydroxyl group. It has a molecular weight of 386.65 g/mol. Cholesterol stabilises bio-membranes and liposomes by imparting mechanical strength and flexibility. Furthermore, it improves phosphatidylcholine vesicle resistance and prevents vesicle aggregation [118]. Cholesterol in liposomal formulations is also known to increase the transfection efficiency [119]. Cholesterol was dissolved in 2:1 (v/v) chloroform: methanol mixture at a concentration of 10 mg/mL and stored in glass vials at -20 °C.

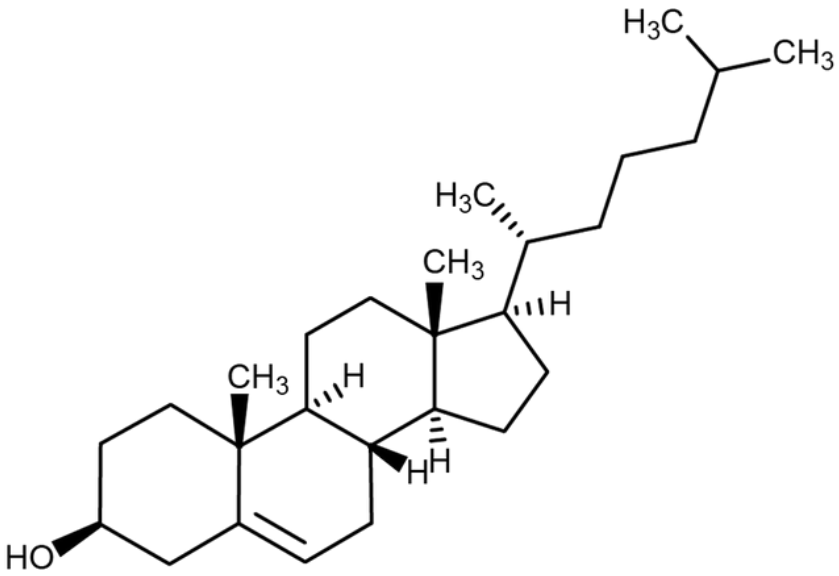

Cholesterol

2.1.2 Polymers

2.1.2.1 Branched Polyethylenimine

Polyethylenimine (PEI) is a polymer obtained by the polymerisation of aziridine. bPEI consists of repeating units composed of an amine group and two carbon aliphatic CH_2-CH_2 spacer [120]. It is an organic macromolecule with a high cationic charge-density potential. Every third atom in bPEI is an amine which can be protonated. Due to the close neighbourhood of the many linker amino groups, PEI retains a substantial buffering capacity at virtually any pH [121]. bPEI has been used successfully for delivering plasmids both *in vitro* and *in vivo* [56]. For this work, bPEI with a molecular weight of 25 kDa was used. 100 mg of the polymer was added to a beaker glass containing 80 mL of milliQ® water. pH was adjusted to 2.0 using 6M HCl. The solution was stirred for 4 h at 500 rpm on a magnetic stirrer at RT. Finally, the pH was adjusted to 7.0 using 6 M NaOH and the volume was made up to 100 mL using milliQ® water. The solution was filter sterilised using 0.2 µm syringe filter (Whatman). Aliquots of 1mg/mL were stored at -20 °C until further use.

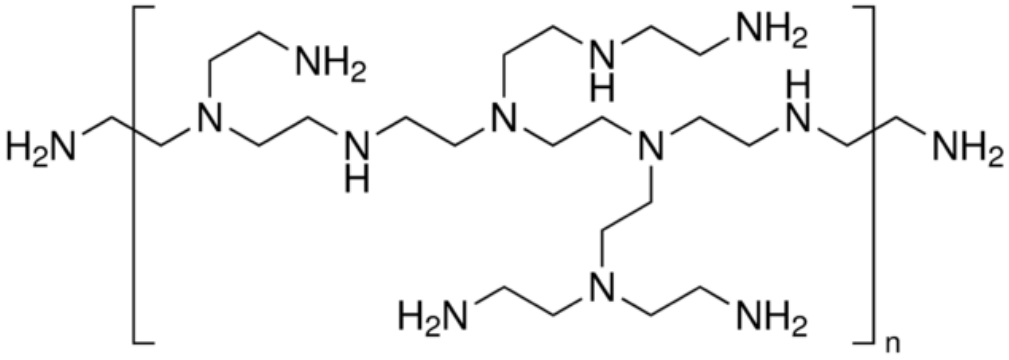

Branched PEI

2.1.2.2 Linear Polyethylenimine

Linear PEI is a linear variant of PEI containing only secondary amines. The lPEI used in this work is a commercially available fully deacylated variant. Deacylation of PEI is reported to increase the transfection efficiency [77]. lPEI contains larger neighbouring ethylenimine segments resulting in 11 % increase in the amount of protonable nitrogen. A hydrochloride salt form of lPEI, PEI MAX 40 kDa was used for this work. 50 mg of the powder was dissolved in a beaker containing 40 mL of milliQ® water. The solution was stirred on a magnetic stirrer and was neutralised to a pH of 7.0 with 6 M NaOH to obtain a 22 kDa linear polyethylenimine. The solution was made up to 50 mL with milliQ® water and filter sterilised using 0.2 µm syringe filter (Whatman). Aliquots of 1 mg/mL were stored at -20 °C.

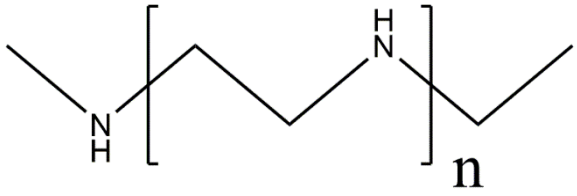

Linear PEI

2.1.3 Curcumin

Curcumin (1,7-bis(4-hydroxy-3-methoxyphenyl)-1,6-heptadiene-3,5-dione) is a naturally occurring phenolic compound obtained from the alcoholic extracts of *Curcuma longa*. The rhizome of this plant, turmeric, has been extensively used for its culinary and anti-bacterial properties. Being excitable with light at 420 nm, is extensively used as a photosensitiser for photodynamic therapy. In this work, curcumin loaded liposomes have been used for photo-chemical internalisation studies.

2.1.4 Nucleic acids

2.1.4.1 HT-DNA

For the experimental practice purposes, herring testes DNA (HT-DNA) was used. 625 mg of HT-DNA (1500 bp) was added to a beaker containing 125 mL milliQ® water. The DNA solution was left to swell for 1 h followed by overnight stirring on a magnetic stirrer at RT. DNA samples were analysed by gel electrophoresis and quantified spectrophotometrically (Ultrospec 3000, Pharmacia Biotech) by determination of $OD_{260/280}$ ratio. The solution was filter sterilised through 0.2 µm syringe filters (Whatman) and stored in 5 mg/mL aliquots at -20 °C.

2.1.4.2 pCMV-luc

pCMV-luc is a plasmid DNA 6233 bp is size. It encodes for firefly luciferase under cytomegalovirus (CMV) promoter. It is used frequently for reporter gene assays to quantify the gene expression. In the present work, pCMV-luc was extensively used to determine transfection efficiencies of various delivery vehicles. pCMV-luc was transformed using JM109 competent *Escherichia Coli (E. Coli)*. The plasmid confers ampicillin resistance to the transformed bacteria. SOC broth was prepared by dissolving 27 g of the nutrient mixture in 1 L of milliQ® water. In case of SOC agar plates, 15 g of agar was added to the above. The mixture was autoclaved and left in a water bath at 60 °C. 100 mg ampicillin was added to make a final concentration of 100 µg/mL. SOC agar was pipetted onto sterile Petri dishes and let to settle. *E. Coli* was thawed on ice and re-suspended into a culture tube (Pyrex®; 16x125 mm) containing SOC broth and incubated for 1 h in a shaking incubator (IKA KS4000 IC) at 37 °C. 20 µL of bacterial suspension was added to 20 µL 10 mM Tris buffer (pH 8.0) containing 1 µg plasmid DNA. The mixture was transferred into electroporation cuvettes (Bio-Rad, 0.2 cm)

placed on ice. The cuvette was pulsed (Bio-Rad Gene Pulser™) once at 2.5 kV (capacitance 25 µF, resistance 200 Ω) [122]. The mixture was immediately transferred into SOC medium containing culture tubes and incubated for 1 h on a shaking incubator (IKA KS4000 IC). Bacteria were inoculated onto selective SOC agar plates and incubated overnight at 37 °C. A single colony of *E. Coli* was selected and transferred into an Erlenmeyer flask containing 1 L of SOC broth and incubated at 37 °C in a shaking incubator. Plasmid DNA from the resulting bacteria was isolated using QIAfilter Plasmid Giga Kit (Qiagen). Plasmid DNA was analysed by agarose gel electrophoresis using a DNA ladder as a control. Quantification was performed by determining the $OD_{260/280}$ ratio (Ultrospec 3000). pCMV-luc was filter sterilised and 1 mg/mL aliquots were stored at -20 °C.

2.1.4.3 pEGFP-N1

Plasmid DNA pEGFP-N1 of 4700 bp expressing green fluorescence protein was used for visualisation of gene expression in this work. pEGFP-N1 was transformed and isolated in the same manner as pCMV-luc (section pCMV-luc) with the only difference being the selective antibiotic i.e. kanamycin. Samples were filter sterilised and stored in 1 mg/mL aliquots at -20 °C.

2.1.4.4 siRNA

Different kinds of siRNAs were used for this work depending upon the gene intended to be downregulated. Anti-luc siRNA 1 directed against firefly luciferase (siLuc, 5´-GAUUAUGUCCGGUUAUGUA-3´) and luciferase GL3 duplex siRNA directed against GL3 luciferase (siGL3, 5´-GCCAUUCUAUCCUCUAGAGGAUG-3´) were used for targeting the luc gene. For downregulation of SELE gene, SELE siRNA duplex directed against E-selectin (siSELE) and three unique dsiRNA 27mer duplexes targeted against E-selectin (Trilencer) were employed. As negative control for the knockdown experiments, a non-targeting, non-specific siRNA designed to have no silencing effects on rat, mouse and human genes, siRNA No. 2 (siCtrl) and Trilencer-27 universal scrambled negative control siRNA duplex was used.

2.1.5 Cell lines

For *in vitro* transfection, knockdown and toxicity experiments, different cell lines were used depending upon the experiment. For transfection and knockdown experiments, SK-OV-3 human epithelial ovarian adenocarcinoma cells, A549 human epithelial lung cancer cells, HeLa human epithelial cervical cancer cells, lentiviral transformed HeLa luc+GFP cells co-expressing firefly luciferase and GFP under CMV promoter, transformed SK-OV-3-luc cells expressing GL3 luciferase, PCS-100-012™ primary human coronary artery endothelial cells and EA.hy926 human endothelial hybrid cells obtained by fusion of primary human umbilical vein cells (HUVEC) with thioguanine resistant A549 by exposure to polyethylene glycol were used [123]. For toxicity studies a sensitive mouse fibroblast cell line, L929, considered as a standard for toxicity testing, was used [124-126].

2.1.6 Chorioallantoic membrane

For the *in vivo* studies, a well-established chorioallantoic membrane (CAM) model was used [127-129]. For this purpose, specific pathogen free fertilised chicken eggs each weighing 50-60 g were used.

2.2 Experiments

2.2.1 Formulation

2.2.1.1 Preparation of liposomes

Depending upon the lipids used in liposomal formulation, appropriate amounts of lipids dissolved in 2:1 (v/v) chloroform: methanol mixture were added to a 5 mL round bottom flask containing 2 mL of 2:1 (v/v) chloroform: methanol to facilitate homogenous mixing. Using a rotary evaporator (Laborota 4000) equipped with a vacuum pump, the lipids were evaporated at 40 ºC to obtain a thin film. The lipid cake was freeze dried (Christ Beta I) overnight to remove any remaining solvent. The lipid film was rehydrated using 20 mM HEPES buffer (pH 7.4) and sonicated in a bath sonicator to obtain a uniform suspension of liposomes. The liposomes were then extruded 21 - 23 times through 400 and 200 nm polycarbonate membranes (Whatman) using an extruder (Avanti Mini Extruder) to reduce their size. Liposomes were filtered through 0.2 µm syringe filters prior to use.

Similar procedure was followed for curcumin loaded liposomes with the exception that curcumin dissolved in 2:1 (v/v) chloroform: methanol was added to the lipids in the round bottom flask at a ratio of 1:300 (curcumin: lipid)

2.2.1.2 PEI-Au conjugation

For structural elucidation, PEI was labelled with gold nanoparticles. For this purpose, branched PEI (25 kDa) was pre-activated with Traut's reagent (2-iminothiolane hydrochloride; Sigma Aldrich) in a similar method described previously with slight modifications [130]. Briefly, 0.2 mM iminothiolane was added dropwise to 22 mM PEI (dissolved in PBS; pH 7.4) under constant stirring at room temperature for 24 h. The reaction was stopped by addition of 0.1M NaOH. Unreacted Traut's reagent was removed using a centrifugal concentrator (Vivaspin 6, cut-off 10 kDa). The mixture was centrifuged (Beckman) at 3000 x g for 15 min. The supernatant thiolated PEI was then freeze dried (Christ Beta I) overnight. The lyophilised product was weighed and reconstituted to 1 mg/mL with milliQ® water. The introduced thiol groups were then used for binding the gold nanoparticles (10-20 nm diameter in citrate buffer).

2.2.1.3 Polyplex preparation

Polyplexes (PP) were prepared according to their charge ratio (N/P ratio) which is the ratio of nitrogen atoms in PEI to phosphate atoms in nucleic acids. N/P ratios ranging from 2 to 30 were used for preparing the polyplexes. For the formation of polyplexes, either branched or linear PEI was used. PEI diluted in 10 mM HEPES (pH 7.4) was pipetted into micro reagent tubes containing either HT-DNA or pDNA diluted in 10 mM HEPES (pH 7.4) or siRNA diluted in 1x siRNA dilution buffer and incubated for 25 min under a laminar airflow hood at RT. To facilitate homogenous mixing, equal volumes of PEI and DNA/siRNA solutions were used.

2.2.1.4 Formation of lipopolyplexes

For the formation of lipopolyplexes (LPP), appropriate amounts of liposomes depending upon liposome to PEI mass ratio were diluted in 10 mM HEPES. Equal volume of the diluted liposomal solution and polyplexes were triturated vigorously in a micro reagent tube and incubated for different time periods ranging from 1 h to 4 h under a laminar airflow hood at RT.

2.2.2 Physicochemical characterisation

2.2.2.1 Dynamic light scattering

The diameter of the liposomes, polyplexes and lipopolyplexes was analysed by dynamic light scattering (DLS) using a Zetasizer Nano ZS (Malvern Instruments) in a clear disposable folded capillary cell (DTS1060; Malvern Instruments). Prior to measurement, liposomes were diluted 1:100; polyplexes and lipopolyplexes were diluted to a ratio of 1:20 with 10 mM HEPES (pH 7.4). For analysis of the data, viscosity (0.88 mPa.s) and refractive index (1.33) of water at 25 ºC were considered. The instrument is equipped with a 10 mW HeNe laser. Measurements were performed at a wavelength of 633 nm and a detection angle of 173º backscatter. Measurement position and laser attenuation were automatically adjusted by the instrument depending upon the sample. The instrument performs 15 size runs per measurement with each lasting 10 s. Three independent formulations were measured and the mean of the measurements is reported.

2.2.2.2 Laser Doppler velocimetry

The zeta potential measurements were performed by laser Doppler velocimetry (LDV) using the Zetasizer Nano ZS in a clear disposable folded capillary cell (DTS1060; Malvern Instruments). The complexes (polyplexes and lipopolyplexes) were diluted as described in section 2.2.2.1. Depending upon the sample, the instrument automatically performs 15-100 runs per measurement. Three independent formulations were measured and the mean of the measurements is reported.

2.2.2.3 Storage stability

For evaluating the storage stability, lipopolyplexes with lPEI (N/P 9.5) were prepared as described in sectionFormation of lipopolyplexes. The lipopolyplexes were then stored at 4 °C for 1, 3, 7, 14, 21 and 30-day time periods and evaluated using dynamic light scattering and laser Doppler velocimetry. The effect of extended storage periods on transfection was evaluated at similar time intervals.

2.2.3 Complex stability studies

2.2.3.1 Gel retardation assay

Polyplexes and lipopolyplexes were subjected to gel electrophoresis to evaluate their integrities. Both polyplexes and lipopolyplexes containing 0.4 µg of pDNA were prepared as described in the sections 2.2.1.3 and 2.2.1.4 respectively. 0.4 µg unbound pDNA and milliQ® water were used as positive and negative controls respectively. The samples were loaded together with 1x loading buffer onto 1 % agarose gel containing ethidium bromide and electrophoresis was carried out in 1x TBE buffer (pH 8.3) on a Thermo Hybaid Electro 4 gel electrophoresis chamber equipped with LKB 2197 constant power supply unit set at 80 V for 1 h. The gels were then analysed at a wavelength of 312 nm under trans-illuminator (BioDoc Analyse Ti5).

2.2.3.2 Heparin assay

The stability of the complexes was analysed in presence of a naturally occurring polyanion in biological systems, heparin. For this assay, polyplexes and lipopolyplexes were prepared with 1 µg pDNA (as described in the sections 2.2.1.3 and 2.2.1.4 respectively) and incubated

together with decreasing concentrations (30, 20, 15, 10, 5, 1 IU) of heparin. After 30 min of incubation in heparin, the samples were packed together with 1x loading buffer on 1 % agarose gel containing ethidium bromide and electrophoresis was carried out (Thermo Hybaid Electro 4) in 1x TBE buffer at 80 V for 1 h (LKB 2197 power supply). The gels were analysed under a trans-illuminator (BioDoc Analyse Ti5) at 312 nm.

2.2.3.3 Ethidium bromide intercalation assay

Polyplexes and lipopolyplexes containing 0.5 µg pDNA were prepared as described in the sections 2.2.1.3 and 2.2.1.4 respectively. 50 µL of the complexes were added to a white opaque bottom 96-well plate (Brand). To these, 50 µL of ethidium bromide (0.4 µg/mL) was added and incubated in dark for a further 30 min at 200 rpm in an orbital shaker (IKA KS4000 IC). As controls, pDNA, ethidium bromide and milliQ® water were used. The fluorescence was measured (FLUOstar® Optima) with an excitation wavelength of 280 nm and emission wavelength of 610 nm [131].

2.2.4 Structural, morphological and surface characterisation

2.2.4.1 Scanning electron microscopy

Scanning electron microscopy (SEM) was performed using a Hitachi S-510 scanning electron microscope. Polyplexes with an N/P ratio of 9.5 containing 3 µg pDNA were briefly incubated for 25 min. After this incubation time, they were added to an equal volume of liposomes diluted with 10 mM HEPES (pH 7.4) and further incubated for a period of 45 min. 10 µL of the lipopolyplexes was pipetted onto specimen stubs with conductive carbon tabs (PLANO Leit-Tabs; Ø 9 mm) and left to dry under a laminar airflow hood. 10 - 15 µL of 2 % glutaraldehyde was pipetted onto the sample in such a manner that it covered the entire sample and incubated for 40 min. Samples were immersed thrice in milliQ® water and then fixed using 10 - 15 µL 2 % osmium tetroxide for 1 h. The samples were immersed again thrice in milliQ® water, and then dehydrated using ascending concentrations (10, 25, 50, 75, and 95 %) of ethanol ending with absolute ethanol with each step lasting 5 min. The samples were then completely dehydrated by supercritical drying (Bal-Tec CPD 030 Critical Point Dryer) using liquid CO_2 as transition liquid. The samples were immediately sputtered (Edwards S150 Sputter Coater) with gold at 1.3 x 10^{-4} bar vacuum and 10 mA current. The samples were examined (WD 15 - 17.5 mm) at an accelerating voltage of 5 kV and 30 µA emission current under 4 x 10^{-7} bar

vacuum. The microscope was retrofitted with a digital image acquisition system (DISS 5) and the micrographs were recorded digitally.

2.2.4.2 Cryo-field emission scanning electron microscopy

Cryo-SEM was performed using a field emission scanning electron microscope JSM-7500F equipped with a lanthanum hexaboride (LaB_6) cathode. Freeze fracture technique was utilised for analysing the samples [132]. Liposomes and lipopolyplexes (lPEI; N/P 9.5) prepared as described in the sections 2.2.1.1 and 2.2.1.4 respectively were pipetted into specimen rivets and shock froze in a slush chamber containing liquid nitrogen. Samples were transferred into a liquid nitrogen cryo transfer system (Alto 2500). The upper half of the rivet was knocked off with an integrated cold knife to create a fracture. Samples were sublimated at -95 °C and sputtered with platinum at -140 °C. The samples were then transferred into the specimen chamber maintained at -140 °C and observed between 2 - 5 kV accelerating voltages and an emission current of 10 µA.

2.2.4.3 Transmission electron microscopy

Structural investigation of the lipopolyplexes was performed using a JEM-3010 ultra-high resolution transmission electron microscope (TEM) equipped with a retractable high-resolution slow scan CCD-Camera (Gatan MegaScan 794). Complexes (lPEI, N/P 9.5) prepared as described in the sections 2.2.1.3 and 2.2.1.4 were diluted to 1:10 ratio with 10 mM HEPES buffer (pH 7.4) and mounted onto 300 mesh carbon coated copper grids which were glow discharged (Edwards S150B) for 1 min to render them hydrophilic. After 15 min, the grid was bought in contact with a drop of milliQ® water thrice to remove the residual buffer. A drop of 2 % uranyl acetate solution was placed onto the grid to negatively stain the sample for 5 min. The sample was examined at an accelerating voltage of 300 kV and 110 µA emission current with current densities between 50-60 pA/cm^2.

2.2.4.4 Atomic force microscopy

AFM was used to determine the morphology of the particles and to confirm the particle size. 10 µL of lipopolyplexes prepared as described in the section 2.2.1.4 were pipetted onto silica wafers which were glued to glass slides. The samples were washed gently with milliQ® water to remove excess of buffer and allowed to dry before being flushed with a stream of compressed

air. Surface analysis was performed under ambient conditions using a Nanowizard® 1 AFM with an aluminium coated pyramidal silicon nitride probe (HQ:NSC16/Al BS) having a 170 kHz resonance frequency and a force constant of 40 N/m. Images were acquired with constant amplitude attenuation at scan rates between 0.5 to 1 Hz. The raw images were processed using JPKSPM data processing software.

2.2.5 Cell culture studies

2.2.5.1 Maintenance of cells

SK-OV-3 and SK-OV-3 luc, cell lines were cultivated at 37 ºC and 7 % CO_2 under humid conditions in IMDM medium (Biochrom) supplemented with 10 % foetal bovine serum (PAA Laboratories). HeLa, HeLa luc+GFP, A549, EA.hy926 were maintained at 37 ºC and 8.5 % CO_2 under humid conditions in DMEM-High Glucose medium (Biochrom) supplemented with 10 % foetal bovine serum (PAA Laboratories). L929 cells were maintained at 37 ºC and 8.5 % CO_2 under humid conditions in DMEM-Low Glucose medium (Biochrom) supplemented with 10 % foetal bovine serum (PAA Laboratories) PCS-100-012™ cells were grown in MCDB 153 medium (Biochrom) supplemented with endothelial cell growth kit VEGF (PCS-100-041™) constituting to 5 ng/mL rh VEGF, 5 ng/mL rh EGF, 5 ng/mL rh FGF basic, 15 ng/mL rh IGF-1, 10 mM L-glutamine, 0.75 Units/mL heparin sulphate, 1 µg/mL hydrocortisone, 50 µg/mL ascorbic acid, 2 % foetal bovine serum in final medium. PCS-100-012™ cells were maintained at 5 % CO_2 at 37 °C. All cells were maintained under humid conditions. Cells were grown as monolayers in ∅ 100 mm tissue culture grade Petri dishes and passaged upon reaching 80 % confluency.

2.2.5.2 Transfection experiments

For transfection and knockdown experiments, the cells were seeded onto 96-well microtiter plates (CytoOne®) with a density of 10,000 cells per well and incubated for 24 h before transfection. The complexes were prepared as described in sections 2.2.1.3 and 2.2.1.4 in a manner such that the concentration of pCMV-luc per well would be 0.2 µg. Medium from the microtiter plates was aspirated and 75 µL of fresh serum containing medium was added. 25 µL of complexes were added in quadruplicates to the wells and the plates were gently swirled. Medium was either changed or fresh medium containing serum was added additionally to the

wells after 4 h depending upon the experiment. The cells were left in the incubator for 48 h before they were further assayed. All the transfection experiments were performed thrice and the results are mean values of the luciferase expression normalised in regard to the protein concentration.

2.2.5.3 RNAi experiments

RNAi experiments were performed similar to transfection experiments (section 2.2.5.2) with the difference that the complexes were prepared with siRNA to give a final concentration of 7.2 pmol per well. RNAse free water and buffers have been used for RNAi experiments. All RNAi experiments have been performed thrice and the knockdown is expressed as percentage of siCtrl control siRNA.

2.2.5.4 Photo-chemical internalisation

Enhancement of the transfection via photo-chemical internalisation was performed using a custom-made prototype Generation I LED irradiator (Lumundus GmbH) with an array of LED lights designed to irradiate a 96-well microtiter plate was used (Figure 6). The LED irradiator was equipped with LED's capable of emitting light at 457 and 620 nm wavelengths with an option to vary time and current intensity (which together correspond to radiation intensity). Transfection experiments were performed as described in section 2.2.5.2 using curcumin loaded lipopolyplexes (lPEI; N/P 9.5) containing 0.2 µg pCMV-luc prepared as described in section 2.2.1.4. 4 h after the transfection, cells were irradiated at 457 nm at various radiation intensities and additional medium was added to the cells and incubated for a further 48 h. Luciferase activity was determined using luciferase assay.

Figure 6: Prototype LED irradiation device; clockwise: control unit, bottom side of the irradiating head with LEDs and top view of the irradiating head during irradiation [133]

2.2.5.5 Ultrasound enhanced release

The use of ultrasound to enhance the release of the delivery vehicles was performed using an eZono 3000 portable medical ultrasound device. SK-OV-3 and PCS-100-012™ cells were seeded onto a ∅ 60 mm Petri dish at a seeding density of 100,000 cells per dish. Transfection experiments were performed as described in section 2.2.5.2 using complexes (with lPEI; N/P 9.5) containing 1 µg pCMV-luc prepared as described in sections 2.2.1.3 and 2.2.1.4 . 1 and 4 h post transfection, the petri dishes were placed on a rotatable petri dish holder and the cells were treated with ultrasound at a frequency of 15 Mhz with a penetration depth of 1.1 cm and a mechanical index (MI) of 1.5 while being rotated on the petri dish holder (Figure 7: Ultrasound enhanced gene transfer).

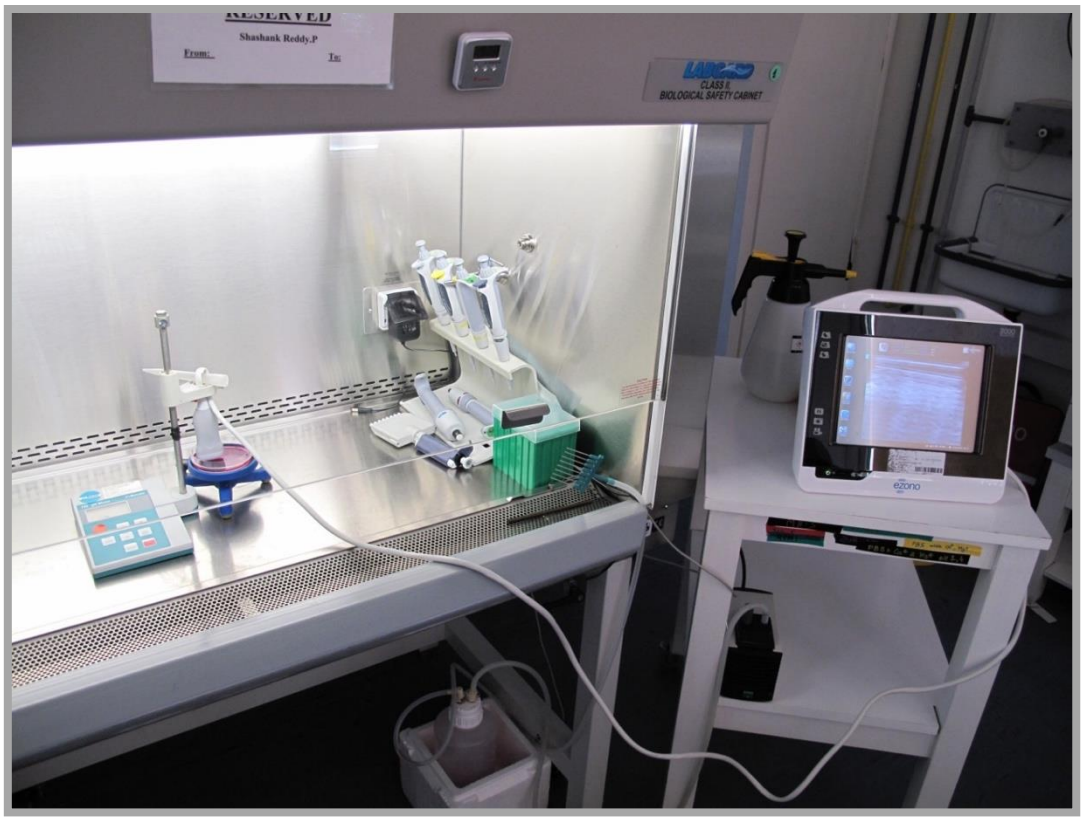

Figure 7: Ultrasound enhanced gene transfer; setup showing the portable ultrasound device with the transducer placed in petri dish

2.2.5.6 Pathway analysis

To determine the exact mechanism of cellular uptake, pathway analysis was carried out. Chlorpromazine, Dynasore, Filipin III were used as pathway inhibitors. SK-OV-3 and HeLa luc+GFP cells were seeded at a cell density of 10,000 cells per well and incubated overnight. On the following day, medium was aspirated and the cells were washed with PBS containing Ca^{+} and Mg^{+} (pH 7.4) to remove any serum residues which can inactivate the effect on the inhibitors. Fresh medium without serum containing the either 80 µM Dynasore, 5 µM of chlorpromazine or 3 µM Filipin III was pipetted into the wells and incubated for 30 min. The cells washed with PBS containing Ca^{+} and Mg^{+} (pH 7.4) and the complexes (with lPEI; N/P 9.5) prepared as described in 2.2.1.3 and 2.2.1.4 containing either 0.2 µg pCMV-luc or 7.2 pmol siRNA were added to the wells and the luciferase activity was determined after 48 h.

2.2.5.7 Luciferase assay and protein quantification

Luciferase expression was determined 48 h post transfections. The cells were washed twice with PBS containing Ca^{+} and Mg^{+} (pH 7.4) and 50 µL of 1x cell culture lysis reagent (Promega) was added to each well. Cells were incubated in a shaking incubator (IKA KS4000 IC) at 200 rpm for 30 min. 20 µL of the lysate was added to a white 96-well opaque plate (Brand). The plate was measured in a luminometer (FLUOstar® Optima) equipped with a pump used for injecting the luciferase assay mixture. Aliquots of luciferase assay reagent and the beetle luciferin were freshly thawed, mixed and primed into the pump. A protocol was created with a 10 s integration time for luminescence detection. The instrument automatically pumped the luciferase assay mixture into each well and measured before proceeding to the next. The results are expressed in relative luminescence units (RLU).

Protein quantification was performed using the Pierce protein BCA assay kit [134]. 25 µL of the cell lysate from the lysis step (section 2.2.5.7) was added to a transparent 96-well microtiter plate for protein quantification. 25 µL of serial dilutions of standard bovine serum albumin (2000 µg/mL - 25 µg/mL) were added to the microtiter plate. 200 µL of the working reagent containing bicinchoninic acid was added to each well and the plate was incubated in a shaking incubator (IKA KS4000 IC) at 200 rpm for 30 min at 37 °C. The plate was let at RT for 15 min and the protein quantification was performed by measuring the absorbance at 570 nm using a plate reader (Tecan Spectra III). The protein values were used to normalise the luciferase expression and the final values were expressed in RLU / mg protein.

2.2.5.8 E-selectin ELISA

ELISA was performed to determine the knockdown of E-selectin expression in endothelial EA.hy926 cells. To enable expression of endothelial leukocyte adhesion molecule 1; E-selectin, 100 µL of medium containing 350 U/mL Tumour Necrosis Factor-α (TNF-α) was added to each well and the cells were incubated to 4 h [135]. Knockdown was performed (with complexes containing lPEI; N/P 9.5) as described in 2.2.5.3 using 16 pmol SELE siRNA or 25 pmol Trilencer dsiRNA 27mer pools (per well) with Trilencer scrambler siRNA and siCtrl as controls. Prior to use, dsiRNA was diluted with 1x siRNA dilution buffer and heated to 94 °C for 2 min to enable duplex formation. After 48 h, the supernatant from each well was collected. A 96-well plate was coated with 50 µl of 10 µg/mL anti-human E-selectin monoclonal antibody

diluted in PBS (pH 7.4) and incubated for 16 h at 4 °C. Plates were washed twice with 300 µL PBS (pH 7.4) to remove unbound antibodies and tapped on a paper towel. Plates were blocked with 1 % BSA containing PBS buffer (pH 7.4), sealed with adhesive plate seals and incubated for 2 h at RT. 20 µl of supernatant from the cells was added to the corresponding wells of the antibody coated plate containing 80 µl PBS (pH 7.4). 100 µL of human E-selectin standard diluted with PBS (pH 7.4) was added to the wells in serial dilutions (50 ng/ml - 0.4 ng/mL) as a standard reference. As a negative control, 100 µL PBS buffer (pH 7.4) was used. 50 µL of 10 µg/mL HRP conjugated anti-human E-selectin monoclonal antibody was added to each well. Plates were sealed with an adhesive plate seal and incubated for 2 h at RT in a shaking incubator (IKA KS4000 IC) at 100 rpm. Following incubation, plate was washed four times with PBS (pH 7.4). 100 µL of 3,3',5,5'-Tetramethylbenzidine substrate solution was added to the wells and incubated for 10 min at RT in a shaking incubator (IKA KS4000 IC) at 100 rpm. 100 µL of 0.16 M sulphuric acid was added to each well and the absorbance was read immediately at 450 nm in a plate reader (FLUOstar™ Optima). The E-selectin expression was compared against the standard and the results are expressed as ng E-selectin expression.

2.2.5.9 Transfection visualisation

To qualitatively visualise the transfections, confocal laser scanning microscopy was employed. SK-OV-3 cells were seeded at a seeding density of 90,000 cells per well onto 12-well plates (Nunclon Delta) containing ∅ 15 mm cover slips. The plates were incubated for 24 h before being used for transfection. Complexes prepared (with lPEI; N/P 9.5) as described in 2.2.1.3 and 2.2.1.4 containing 1.75 µg of pEGFP-N1 were added drop wise to each well containing 400 µL medium containing serum; the plates were gently swirled and incubated. After 4 h, 500 µL of medium containing serum was added to the wells and incubated for a further 48 h. The cells were then washed twice with PBS containing Ca^{+} and Mg^{+} (pH 7.4) and fixed with 4 % formaldehyde solution for 20 min after which the cell nucleus was counterstained with 0.1 µg/mL DAPI (4',6-diamidino-2-phenylindole) for 20 min. Finally, the cells were washed with PBS (pH 7.4) and the cover slips were mounted onto slides with a mounting medium (FluorSave™) and sealed using a transparent nail polish.

The cells were examined under a Confocal Laser Scanning Microscope (Zeiss Axiovert 100M/LSM 510). A class 4 argon ion laser (Coherent Enterprise II) laser with 364 and 488 nm excitation wavelengths for observing nuclear counterstaining and GFP expression respectively

was used. Detector equipped with band pass filters of 505-530 nm for GFP and 385-470 nm for DAPI was used for recording the micrographs. Similar detector gain (master gain) and pinhole size was used across all the samples.

2.2.6 Cytotoxicity studies

2.1.6.1 MTT assay

Cytotoxicity of the complexes was determined by MTT assay using thiazolyl blue tetrazolium bromide. A cell density of 10,000 L929 cells per well were seeded onto 96-well plates. pCMV-luc containing complexes were prepared in a similar manner like in transfection experiments (section 2.2.5.2) and pipetted into the wells. As a positive control 0.1 % Triton™ X-100 was used and untreated cells were used as negative control (Blank). The plates were gently swirled and incubated. After 4 h, additional medium was added to the wells and incubated for another 48 h. After the incubation time, the plates were washed twice with PBS containing Ca^{+} and Mg^{+} and then medium containing MTT assay reagent was added to each of the 96 wells. The cells were incubated for another 4 h during which the viable cells metabolize the MTT dye and reduce it to formazan crystals [136]. The remaining medium was aspirated and 200 µL of dimethyl sulphoxide was added to each well to dissolve the formazan crystals. Absorbance was measured using FLUOstar™ Optima plate reader at 570 nm.

2.1.6.2 LDH Assay

Cellular toxicity as a function of membrane integrity was determined by lactate dehydrogenase assay (LDH) in L929 cells. A density of 10,000 cells per well were seeded onto 96-well plates and incubated overnight. The medium was changed and complexes containing pCMV-luc were prepared in a similar manner to the transfection experiments (section 2.2.5.2) and pipetted dropwise into the wells. As a positive control 0.1% Triton™ X-100 was used. Untreated cells were used as negative control (Blank) and wells with only medium were used as a background control. The plates were gently swirled and incubated. After 4 h additional medium to the wells and incubated for another 48 h. After incubation time, 100 µL of medium from the assay plates was transferred onto corresponding wells of a clear 96-well microtiter plate. 100 µL of freshly prepared reaction mixture (LDH kit, Roche) was added to the plate and incubated for 30 min after which the absorbance was determined at 485 nm using a FLUOstar™ Optima plate reader.

2.2.7 Haemocompatibility studies

2.1.7.1 Haemolysis assay

To determine the haemolytic potential of the complexes on blood, erythrocytes isolated from fresh human blood were used [137]. Fresh blood was drawn into tubes containing 3.8 % sodium citrate (9:1) followed by centrifugation at 500 x g for 20 min. The obtained red blood cell pellet was washed thrice with PBS buffer (pH 7.4) and diluted to 1:50 with PBS (pH 7.4). Complexes (with lPEI and bPEI; N/P 9.5 and 15 respectively) containing to 1 µg pCMV-luc were prepared as described in sections 2.2.1.3 and 2.2.1.4. The samples were diluted 1:1 with erythrocytes to reach a final volume of 200 µL [138]. Samples were incubated for 1 h in at 150 rpm in a shaking incubator (IKA KS4000 IC) at 37 ºC. The samples were subsequently centrifuged and the absorbance of the collected supernatant was determined at 540 nm in a FLUOstar® Optima plate reader. PBS buffer (pH 7.4) and 0.1 % Triton™ X-100 were used as controls and the absorbance values of Triton™ X-100 were considered as 100 % haemolysis.

2.1.7.2 Activated partial thromboplastin time test

Activated partial thromboplastin time (aPTT) test was used to determine the effect of the complexes on coagulation. Fresh blood was drawn into tubes containing 3.8 % sodium citrate (9:1) followed by centrifugation at 1500 x g for 10 min to separate the plasma fraction. Normal aPTT values of plasma were checked and the plasma was stored at -80 °C until further use. The aPTT test was performed in a coagulation analyser (Coatron M1) using the TEClot aPTT-S Kit as per the manufacturer's protocol with slight modifications. 25 µL of plasma was mixed with 25 µL of complexes (with lPEI and bPEI; N/P 9.5 and 15 respectively) prepared as described in sections 2.2.1.3 and 2.2.1.4 containing 1 µg pDNA. 25 µL of prewarmed 0.025 M calcium chloride was added to this mixture followed by addition of equal volume of aPTT reagent to activate coagulation. Coagulation was confirmed spectrophotometrically and the time was recorded in seconds

2.2.8 *In vivo* chorioallantoic membrane model

Specific pathogen free fertilised chicken eggs were incubated (Ehret KMB 6 hatching incubator) at 37 °C in a humidified atmosphere (>60 % RH). The CAM experiments were performed according to established protocols with slight modifications [129, 139]. On egg development day (EDD) 3, a 3 mm ∅ hole was bored into the basal part of the shell and approximately 3 mL of albumin was drawn out of the egg using a syringe to prevent the adhesion of the CAM to the apical part of shell. The apical part of the shell was cut open (∅ 30 mm) to expose the CAM. The bottom end was sealed using a cellophane tape and the apical part using a paraffin film. The eggs were further incubated on a frame designed to hold them upright to facilitate the development of CAM. On EDD 11, 100 µL mL of the lipopolyplexes (with lPEI; N/P 9.5) prepared as described in section 2.2.1.4 containing 0.8 µg pEGFP-N1 was injected into the mesoderm of the CAM using a glass cannula. Eggs were further incubated until EDD 12. Images of the microvasculature were acquired using a Stemi 2000-C stereo microscope equipped with a Moticam 5 CMOS camera. Approximately 1 cm^2 of the CAM was cut out and washed once with isotonic NaCl (0.9 %). Depending upon the analysis, the cut out was either supercritically dried (Bal-Tec CPD 030) for electron microscopy (Hitachi S-510) or mounted onto a slide for confocal fluorescence microscopy (Zeiss Axiovert 100M/LSM 510).

2.2.9 Statistical analysis

All experiments were performed in triplicates and the values are presented as mean ± standard deviation, unless otherwise stated. Two-tailed Student's t-test was performed to identify statistical significance differences. Probability values of $p < 0.05$ were considered significant. Statistical differences are denoted as "*" $p < 0.05$, "**" $p < 0.01$, "***" $p < 0.001$. Results have been plotted in graphs using Origin graphing program (OriginLab Corporation, Northampton, USA).

Part III: Results and discussion

3.1 Physicochemical properties

The most vital criteria for efficient gene delivery are nano-sized, slightly cationic and physiologically stable complexes. Size of the complexes suspended in aqueous solutions determined by Dynamic light scattering called hydrodynamic diameter due to the fact that the complexes are in a hydrated, aspherical state. To correlate the physiological conditions with that of the measurements and to facilitate an ion rich environment for the laser Doppler velocimetry, all measurements were performed at physiological pH using 20 mM HEPES containing 150 mM NaCl (pH 7.4) as a dilution buffer [140].

3.1.1 Hydrodynamic diameter

Hydrodynamic diameter of the liposomes and complexes was determined using dynamic light scattering (DLS) using the size by intensity function. In agreement with previous studies, the hydrodynamic diameter of the polyplexes increased decreased with increasing N/P ratios for both branched and linear variants [141, 142]. This effect however diminished after an N/P ratio of 27 and 25 for bPEI and lPEI respectively. At higher N/P ratios, the polyplexes formed aggregates immediately after complexation. In case of bPEI, the complex size decreased from 298.7 ± 9.3 nm to 188.3 ± 6.4 nm from N/P ratios 3 to 20. lPEI showed a decrease from 210.5 ± 5.5 nm at N/P ratio 2.5 to 124.9 ± 8.2 nm at an N/P ratio of 22. As previously reported, regardless of their sizes, there was no significant difference in the diameter of polyplexes formed from pDNA or siRNA [61].

Two different liposomal formulation containing DOTAP, DPPC and cholesterol (DODC); and DOPE, DPPC and cholesterol (DDC) were investigated. Considering its charge related cytotoxicity, a maximum of 50 % DOTAP was incorporated into the DODC liposomal formulations. To reduce the size of the liposomes and to obtain a homogenous unilamellar population, the liposomal formulations were extruded [143]. Since the polyplex formulations were in the size range of 150 - 180 nm, extrusion was preformed through 400 and 200 nm polycarbonate membranes to obtain liposomes in the corresponding size range. Hence all liposomes formulated were in a size range of 150 - 170 nm (formulations involving DODC) to 160 - 180 nm (formulations involving DDC) and were monodisperse (Polydispersity index (PDI) of 0.1). Since DOPE readily takes on its hexagonal phase when used solely conditions under physiological, DDC liposomes containing high amount of DOPE (≥ 80 %) were highly

unstable and aggregated immediately following vesicle preparation. To avoid this problem without compromising on its fusogenic properties, amount of DOPE was kept to a maximum of 70 mol % in the DDC formulation [144]. After thorough investigations involving different N/P ratio of the polyplexes and the mass ratios of liposomes to polyplexes, a consensus was reached regarding the size of the lipopolyplexes. A complex size of 200 nm and less is a size prerequisite for endocytosis and efficient cellular uptake [145]. Bearing in mind this number, all other formulations exceeding this size range were excluded from further studies. Lipopolyplexes formed using DODC liposomes with bPEI and lPEI were in a size range of 180 - 200 nm and those with DDC liposomes were in a size range of 170 - 210 nm.

3.1.2 Zeta Potential

The other crucial factor effecting cellular interaction is the zeta potential of the complexes. pH and ionic strength are the two main factors influencing the zeta potential. For the success of gene delivery, the delivery vehicles need to have a minute positive charge [146, 147].

Liposomal formulations involving DODC showed a positive zeta potential. The zeta potential increased with increasing DOTAP molar ratios. On the other hand, liposomal formulations involving DDC showed a neutral to negative zeta potential. DOPE molar ratio was the determining factor the negative charge of the formulations. Negative charge increased with an increase in the amount of DOPE.

In case of polyplexes, both bPEI and lPEI showed an increase in the zeta potential with increasing N/P ratios. The branched variant of PEI showed a dramatic increase in the zeta potential with increasing the amount of polymer, whereas the linear variant showed only slight increase in the zeta potential. Since the cytotoxicity of PEI is attributed to its high cationic charge, N/P ratios with zeta potential above + 30 mV were not considered for lipopolyplex formation [148].

Complexation of liposomes with nucleic acids, complexes and nanoparticles involves either electrostatic interactions, mechanically induced interactions, rearrangement of the lipids or the combination of these [42, 149]. Lipopolyplexes formed using DODC liposomes showing the highest zeta potential (+ 43.9 mV) whereas their DDC counterparts showed a zeta potential less than + 4 mV. Therefore, DDC liposomes having highest negative charge were considered for

lipopolyplex formation, due to their ability to shield the positive charge of PEI to an extent. Not only PEI, but also liposomes used in the formulation of lipopolyplexes play an important role in its physicochemical properties which is in agreement with previous studies [75].

Table 1: Physicochemical properties of liposomes, polyplexes and lipopolyplexes. Size and zeta potential are expressed as a mean ± standard deviation of three independent measurements (n=3)

Formulation	Size (nm) ± SD	Zeta Potential (mV) ± SD	PDI
Liposomes (mol %)			
DOTAP:DOPE:Cholesterol (35:50:15) **DOPE:DPPC:Cholesterol (70:15:15)**	168.4 ± 2.5 174.7 ± 3.3	+40.9 ± 4.6 -30.9 ± 2.0	0.11 0.09
Polyplexes			
Branched PEI (N/P 15) **Linear PEI (N/P 9.5)**	180.5 ± 11.6 166.2 ± 8.7	+ 27.3 ± 4.4 + 19.1 ± 2.7	0.35 0.24
Lipopolyplexes with lPEI polyplexes			
DOTAP:DOPE:Cholesterol (35:50:15) **DOPE:DPPC:Cholesterol (70:15:15)**	181.3 ± 7.5 201.1 ± 5.9	+ 43.9 ± 2.3 + 3.7 ± 2.1	0.23 0.19
Lipopolyplexes with bPEI polyplexes			
DOTAP:DOPE:Cholesterol (35:50:15) **DOPE:DPPC:Cholesterol (70:15:15)**	224.6 ± 15.1 194.0 ± 17.3	+ 51.5 ± 3.5 + 9.5 ± 3.7	0.33 0.38

3.1.3 Storage stability

Unlike the polyplexes, lipopolyplexes did not tend to form aggregates upon storage. There was no significant increase in the size of the complexes upon storage thereby making them suitable for *in vivo* application where size is an important parameter affecting the bio-distribution and uptake of the particles [26]. The storage stability study revealed that the loss in biological activity of the DDC-lPEI lipopolyplexes after 30 days (at 4 °C) was minimal at 20 % (Figure 8). The loss in the biological activity could be attributed to the degradation of plasmid DNA upon extended storage at 4 °C.

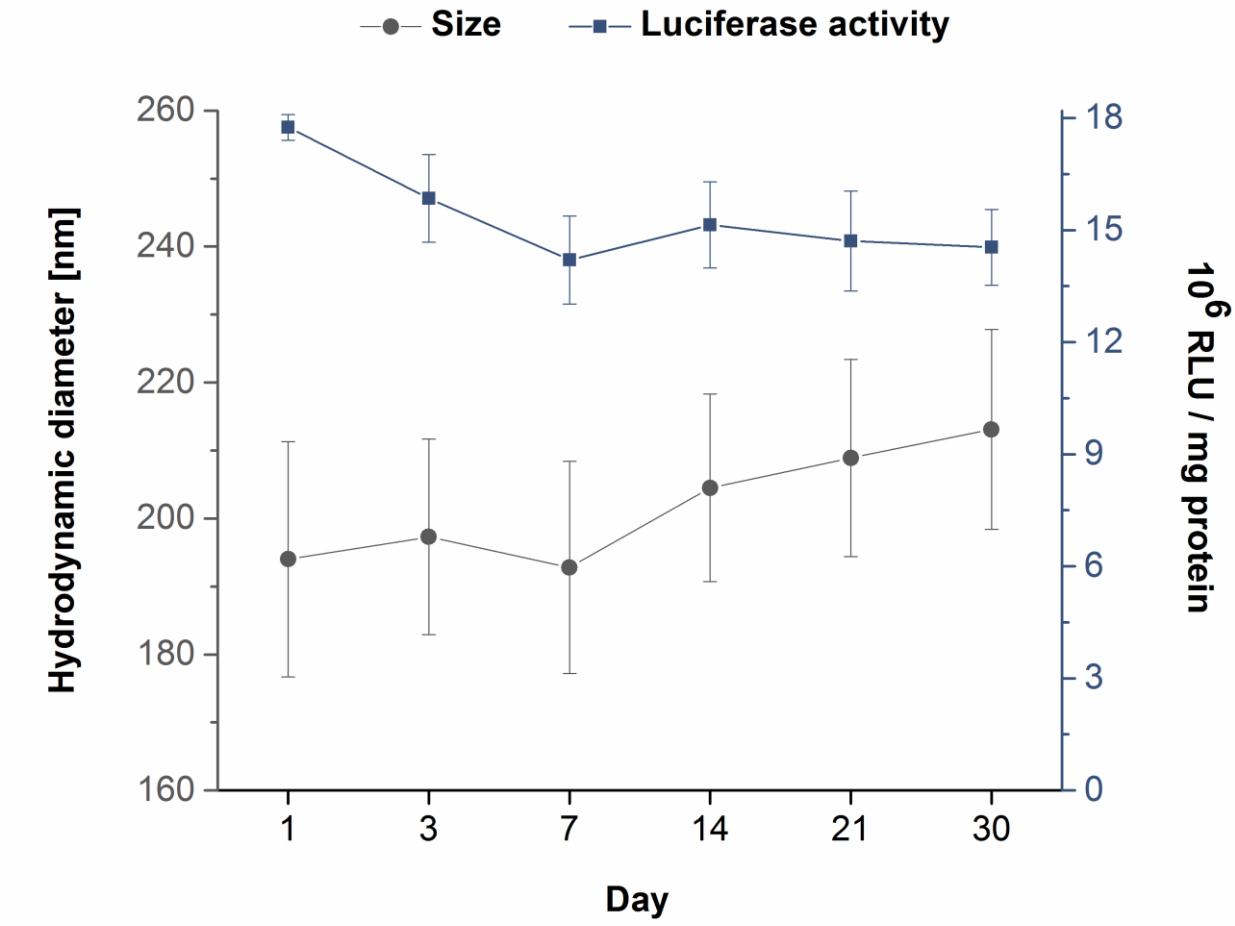

Figure 8 : Storage stability of the lipopolyplexes (DDC-lPEI; N/P 9.5). x-axis represents the storage period in days and y-axes represents size (left) and luciferase expression (right) respectively

3.2 Structural and morphological analysis

Microscopy is a valuable tool in science for the analysis of structures not visible to the naked human eye. Different forms of microscopy have proved to be invaluable for the characterisation of micro and nano-sized structures. The most common microscopes used for structural analysis are optical microscopes. Nanoparticles need to possess certain characteristics to able to be viewed under an optical microscope. Due to Abbe's diffraction limit, optical microscopic analysis of nano-sized structures is limited to either birefringent samples (polarising microscopy), opaque samples (dark field microscopy) or fluorescent samples (confocal microscopy) which all give only a vague representation of the actual structure.

3.2.1 Electron microscopy

Electron microscopy was used to determine the morphology and structure of the formulations. Electron microscopy enables analysis of the samples beyond optical microscopic limit with a much higher resolution. However, unlike optical microscopy, electron microscopy required special sample preparation techniques and a certain amount of experience in handling of the chemicals used for sample preparation which are often toxic. Certain level of training, appropriate skills and thorough knowledge in fundamental physics in required to visualise and analyse the micrographs in electron microscopy. Since each sample preparation technique has its own advantages and disadvantages, a combination of different techniques was employed to obtain the best possible result.

3.2.1.1 Scanning electron microscopy

SEM was performed to elucidate the morphological characteristics of the lipopolyplexes. Since SEM analysis involves exposure of samples to high voltage electron beams and a high vacuum chamber, the samples need to be prepared appropriately. This was enabled by fixation with 2 % glutaraldehyde solution in PBS which helps retain the structural characteristics of the outer lipid membrane. Glutaraldehyde, a slowly penetrating fixative preserves the fine structural details of the lipopolyplexes in the high vacuum environment of the SEM. Samples for electron microscopy need to possess a certain level of contrast to differentiate them from the background. Due to its affinity to polar head groups of the phospholipids and due to its high electron scattering rate, osmium tetroxide was used as a staining agent of choice [150]. Samples devoid of aqueous media is a basic requirement of electron microscopy under high vacuum. To render the sample dry without compromising their structure and to avoid shrinkage, supercritical drying was employed. After ethanol dehydration of the samples, the samples were subjected to supercritical drying using CO_2 as a supercritical fluid to remove residual ethanol from the samples. The other requirement for scanning electron microscopy is that the samples need to be conductive. To achieve this, samples were sputtered with a fine layer of gold. The SEM was equipped with an Everhart-Thornley detector to obtain secondary electron images.

a

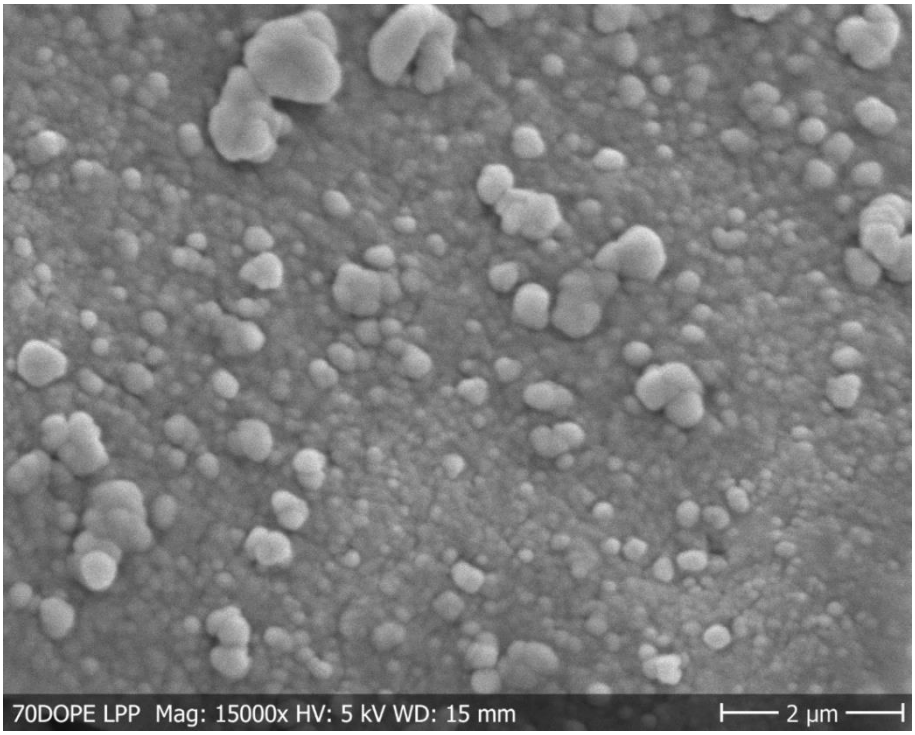

b

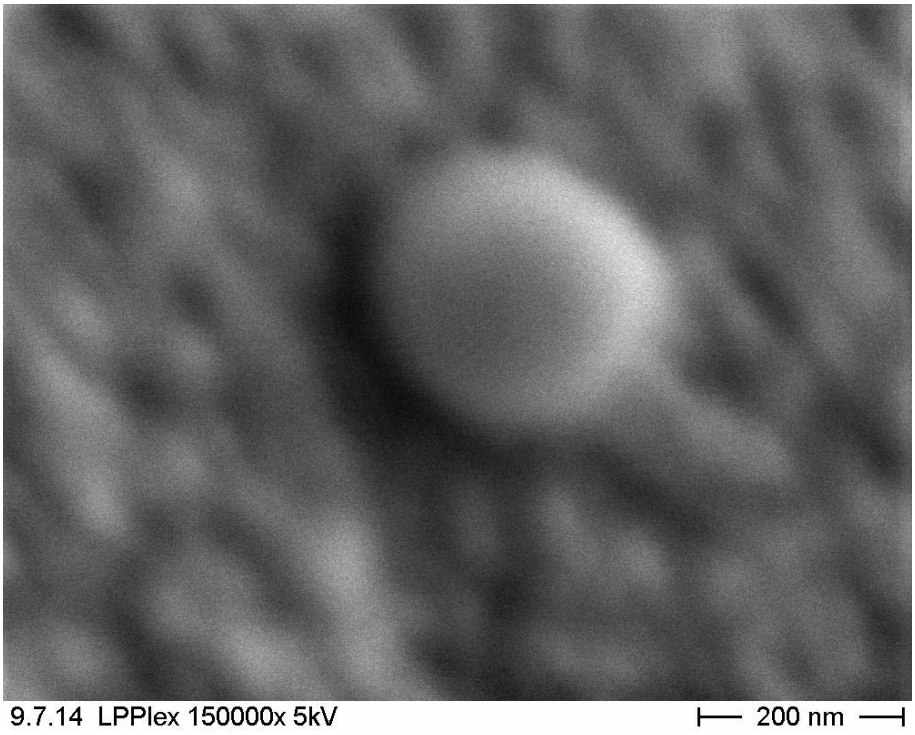

Figure 9: a.) SEM micrograph of DDC-lPEI (N/P 9.5) lipopolyplexes. b.) A closer view of a single lipopolyplex

Since the lipopolyplexes were left to dry on the conductive carbon tabs for scanning electron microscopy, lipopolyplexes tend to come closer and form clumps or pseudo-aggregates (Figure 9. a). The SEM micrograph of a lipopolyplex (Figure 9. b) corresponds to the size measured using DLS. A gross approximation of the shape and morphological features could be made from the micrographs. The micrograph (Figure 9. a) reveals a defined spherical shape of the lipopolyplexes and a lot of small clusters of lipopolyplexes joined together and above each other. Due to the presence of an aqueous core, under normal conditions, it is rather difficult to image liposomes with a normal SEM, despite cumbersome preparation techniques. The fact that the SEM micrographs in this study showing distinct structures could be attributed to the presence of a polyplex inside liposomes thereby stabilising the structure.

3.2.1.2 Freeze fracture cryo scanning electron microscopy

Another exceptional method used in the study of liposomes and liposomal formulations is freeze fracture method. This method involves using aqueous solutions of liposomes which are rapidly froze to temperatures below 100 K using liquid nitrogen. The sample holder containing this frozen liposomal mixture broken (freeze fracture) to reveal the structure within. The images obtained from such samples often show the so-called replicas of the structures which have been removed during the freeze fracture process. This enables imaging of a three-dimensional structures of the samples. Freeze fracture allows imaging of the liposomal formulation in their original form without any additional preparation techniques.

Much higher image resolution could be obtained using the field emission scanning electron microscopy together with a LaB_6 cathode as opposed to the tungsten filament in SEM. The LaB_6 crystals have a lower work function (2.66 eV) than tungsten (4.7 eV) and therefore readily emit electrons offering higher brightness and current densities which reduces the background noise. The cryo-SEM was equipped with a proprietary gentle beam technology which decelerates the incident electrons. A negatively charged stage bias is employed in gentle beam which reduces incident electron penetration of the sample and subsequent charging. This offered visualisation of the samples at much lower accelerations voltages without compromising the resolution.

a

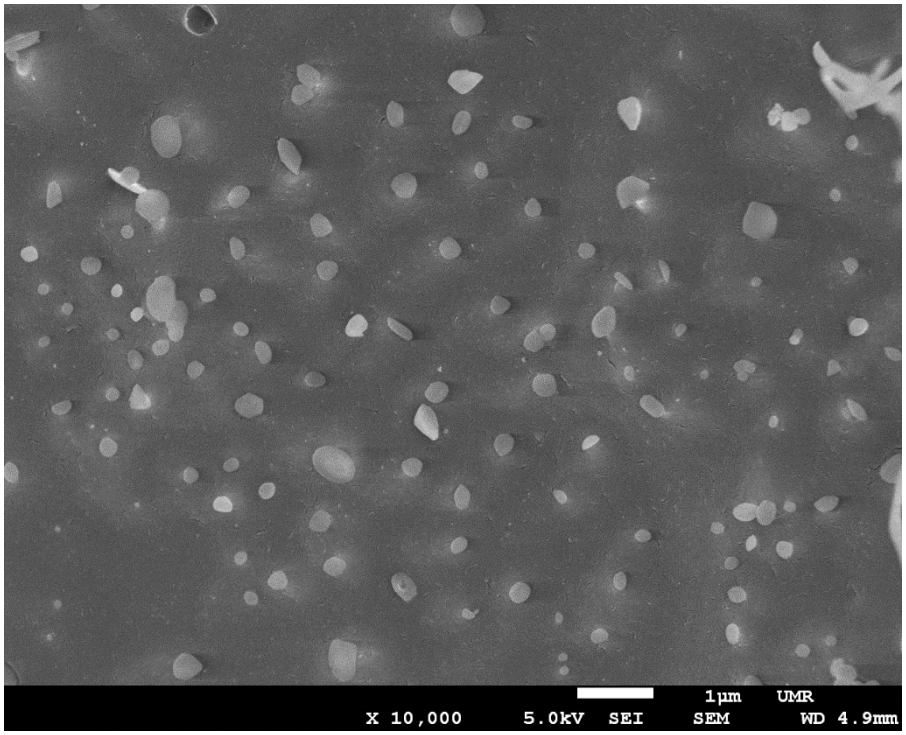

b

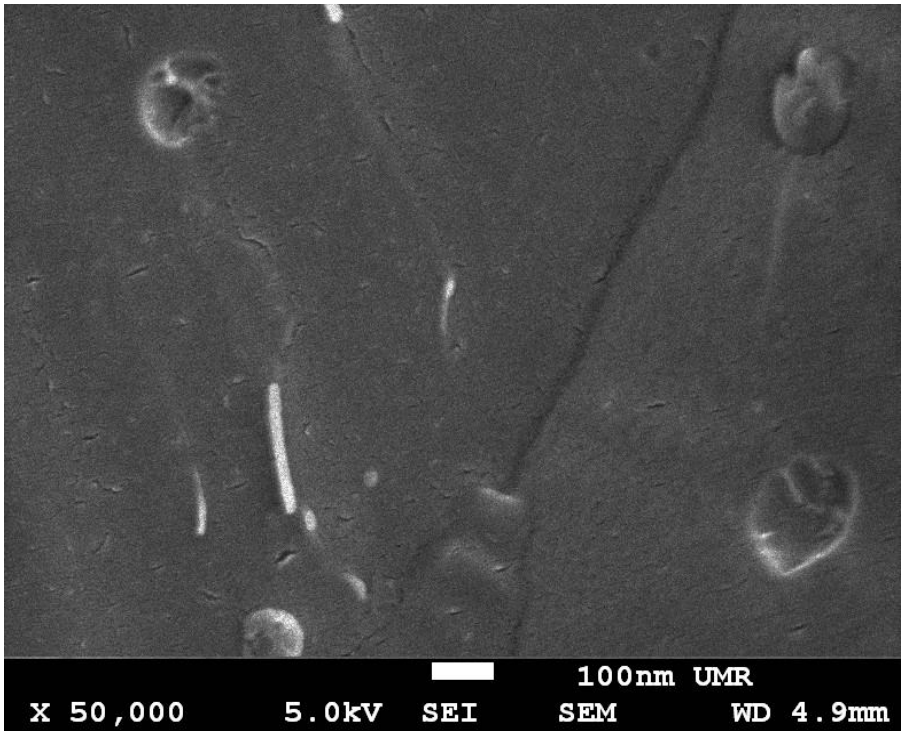

Figure 10: Cryo-SEM micrographs of a.) lipopolyplexes showing distinct shape of the lipopolyplexes and b.) a replica left by the lipopolyplexes

Platinum was used to sputter the samples for cryo-SEM which offers a smaller grain size and a thinner deposition compared to gold. Background noise in the form of grain is significantly reduced using platinum as a target material for sputtering the samples which greatly enhances the signal to noise ratio. The cryo-SEM micrographs confirmed the spherical structure of the lipopolyplexes from the SEM with a much better resolution (Figure 10. a). Since this technique did not require drying of the lipopolyplex suspension, the lipopolyplexes did not form clumps. This enabled effective imaging of the samples even at higher magnifications. The replica of the lipopolyplexes, a consequence of freeze fracture technique, visualised by depositing a layer of platinum could be clearly seen (Figure 10. b). This gave a detailed insight into the morphological features of the lipopolyplexes and their distinctive spherical appearance. The distorted appearance of the replicas in the micrograph could be inferred to the fact that more than a single liposome was removed during the process of freeze fracture giving its replica a wrinkled appearance.

3.2.1.3 Transmission electron microscopy

To elucidate the structure of lipopolyplexes and to confirm the hypothesised polyplex-in-liposome structure, TEM analysis was performed. TEM was performed using an ultra-high resolution microscope equipped with a tungsten cathode capable of delivering 300 kV of accelerating voltages. For the sample preparation, a heavy metal salt, uranyl acetate was employed. At lower concentrations, uranyl acetate acts as a negative stain. Due to its high electron density, its interaction with the incident electron beam is minimal, therefore creating its signature dark background against a light sample which greatly enhances the contrast. Carbon coated copper grids were used for TEM due to better mechanical strength compared to uncoated copper grids. Mounting of hydrophilic lipopolyplexes onto hydrophobic carbon coated grids effects sample preparation, since much of the sample is easily washed away. Therefore, the grids were glow discharged to render them hydrophilic. Since lipopolyplexes were present in buffered aqueous solutions, the grids with samples were carefully washed with water to remove excess of buffer before negative staining with uranyl acetate. At the low concentration used in this study, uranyl acetate does not react with the samples and acts only as a background contrast enhancer.

a

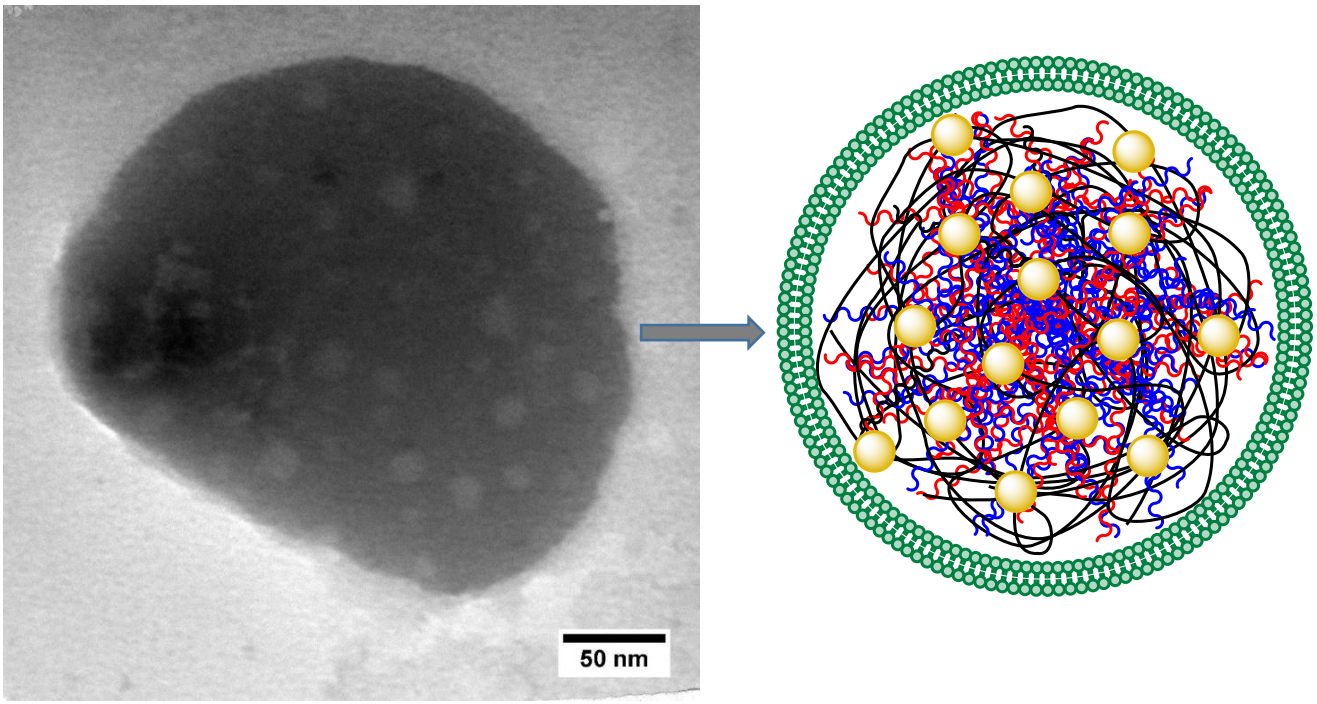

b

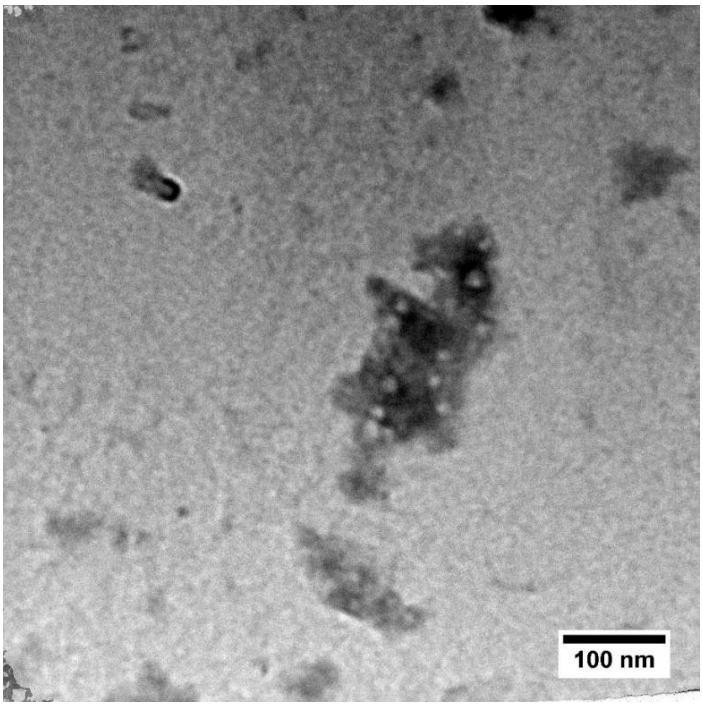

Figure 11: TEM micrographs of a.) lipopolyplex containing gold coupled PEI polyplex (with pictorial representations of the same) and b.) gold coupled PEI polyplex

Coupling of PEI with gold created the opportunity to visualise within the lipopolyplex. Gold particles are easily visible under an electron microscope. Therefore, 20 nm gold spheres were used for coupling with thiolated PEI. Polyplexes could be easily identified due to the presence of gold nanospheres (Figure 11. a). The hypothesis of a composite nanocarrier system i.e. the presence of a polyplex inside a liposome was confirmed with the micrograph showing electron dense gold coupled PEI inside a liposomal structure (Figure 11. b). The illustration of the lipopolyplex represents the arrangement of the gold labelled polyplexes inside the liposomes giving a clear picture about the actual structure. The size range of both polyplexes and lipopolyplexes could be confirmed with the TEM micrographs.

3.2.2 Atomic Force Microscopy

To better understand the surface characteristics of lipopolyplexes, atomic force microscopy was employed. The advantage of atomic force microscopy over other microscopic techniques is the interaction of the scanning tip with the sample thereby giving a clear picture of the actual structure of the sample including minute details. This form of microscopy enables resolution at atomic levels allowing further interpretation of the samples. However, without substantial knowledge about the operation of an AFM, hardness of the cantilever, composition, coating and physical characteristics of the scanning tip it is quite impossible to obtain perceivable micrographs. This often leads to formation of artefacts and misinterpretation of the results.

Since AFM is a surface scanning technique which employs a pyramidal scanning tip (composed of metal or metal alloys) moving across the surface of the sample, soft samples involving liposomes are often damaged. Liposomal formulations often tend to stick to the scanning tip leading to artefacts on the digitally transformed image. To avoid this, intermittent contact mode (also referred to as tapping mode) was used for scanning the lipopolyplexes. In this mode, the piezo element of the cantilever holder constantly oscillates up and down at amplitudes in the range of nanometres. The tip of the cantilever scans close enough to the sample without actually touching it. Electrostatic forces, dipole-dipole interactions and van der Waals forces cause the amplitude of the tip to change, this change is detected and transformed digitally into a micrograph [151, 152]. Lipopolyplexes were image using intermittent contact mode to prevent damage to the liposomal surface.

Similar to SEM, the samples were let dry on a silica wafer followed by washing steps for visualisation under an AFM. Due to this process, the lipopolyplexes tend to clump together forming pseudo-aggregates. AFM micrograph shows individual lipopolyplexes which are distributed freely together clusters of lipopolyplexes attached to each other or stacked above each other (Figure 12). The lipopolyplexes exhibit a smooth, round shape which is a characteristic of its parent liposomes. The shape of lipopolyplexes is in agreement with previously conducted studies confirming the structure of lipopolyplexes [18, 75]. Comparison of electron microscopy images with that of AFM show a clear correlation between the shape and size of lipopolyplexes across the imaging techniques used. The size of the images from the micrographs is in clear agreement with the size obtained from DLS results. The positive zeta potential obtained regardless of the anionic liposomes used points towards an excess of positive charge of PEI radiating outside the liposomal bilayer. Backed by the data obtained from the physicochemical, structural and morphological characterisations, it could be confirmed with certainty that the PEI polyplexes sit inside the liposome.

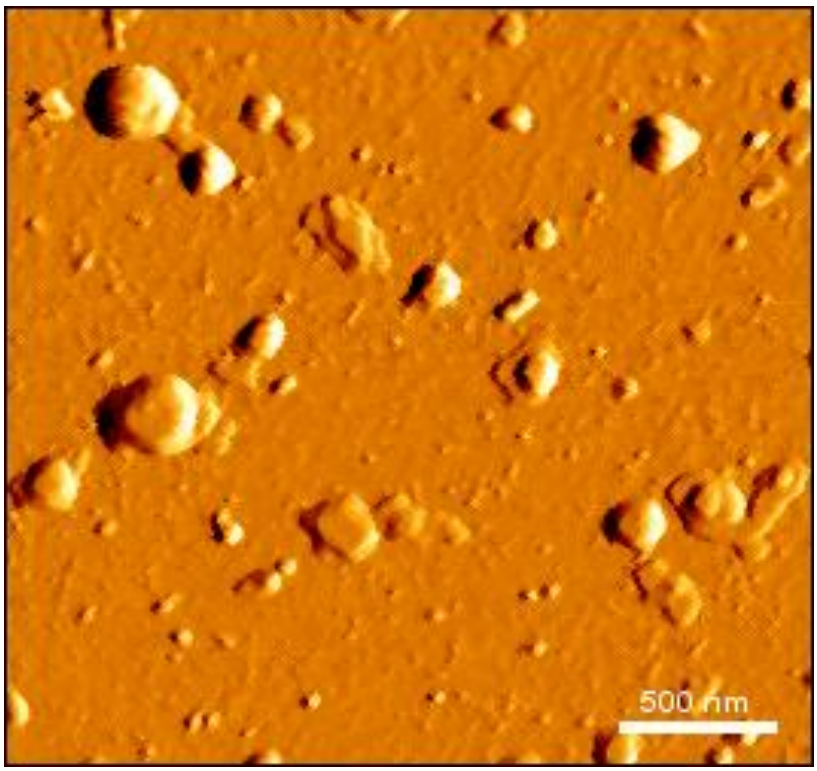

Figure 12: Topographic pseudo-coloured AFM micrograph of linear PEI lipopolyplexes

3.3 Stability studies

In order to deliver the genetic material into the cells, gene delivery vehicles need to be able to protect the cargo from extracellular and intracellular degradation, most importantly against nucleases. The main reason for the decrease in the biological activity is due to insufficient protection of the nucleic acids. Premature degradation of the delivery vehicles in biological fluids often exposes the nucleic acids to nucleases which has a detrimental effect on the delivery efficiency. Delivery vehicles, on the other hand should be able to release their cargo at the site of action, failing to do so would also result in a loss in the biological activity and delivery efficiency. Therefore, delivery vehicles should be formulated in such a manner so that they effectively prevent their cargo against degradation, and readily release the cargo at the site of action.

3.3.1 Complex integrity

To confirm the condensation of pDNA with PEI, gel retardation assay was performed on 1 % agarose gels containing ethidium bromide as a DNA intercalator. Different charge ratios of lPEI and bPEI were used to analyse the interactions between pDNA and PEI.

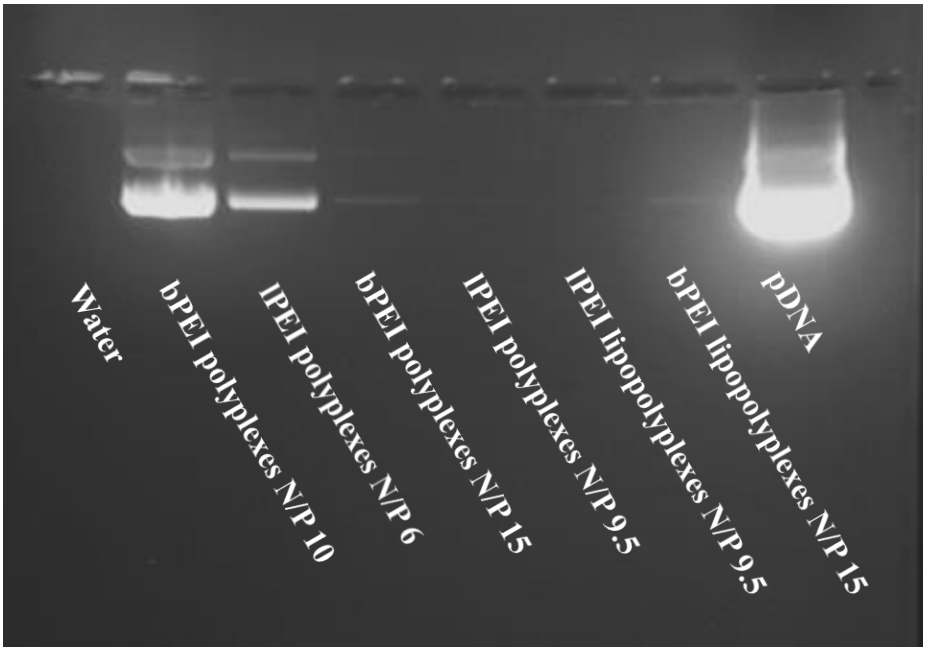

Figure 13: Gel retardation assay of the branched and linear PEI polyplexes and lipopolyplexes

The results obtained from the assay show that condensation efficiency of bPEI is less than that of lPEI (Figure 13). Even at an N/P ratio of 10, bPEI polyplexes release certain amount of pDNA whereas lPEI polyplexes are intact showing no signs of pDNA leakage. At an N/P ratio of 6, lPEI polyplexes showed leakage of a fraction of pDNA which was still less than the N/P ratio 10 of bPEI. A complete retardation of the mobility of the pDNA could be seen in case of both bPEI and lPEI lipopolyplexes, suggesting a more efficient protection of the cargo.

3.3.2 Complex dissociation assay

To simulate physiological conditions, heparin assay was performed. Biological fluids, especially blood, which directly interacts with gene delivery vehicles comprises of a lot of polyanions which may be undermine the stability of the complexes. To reproduce this effect, heparin, a naturally occurring competing polyanion was used.

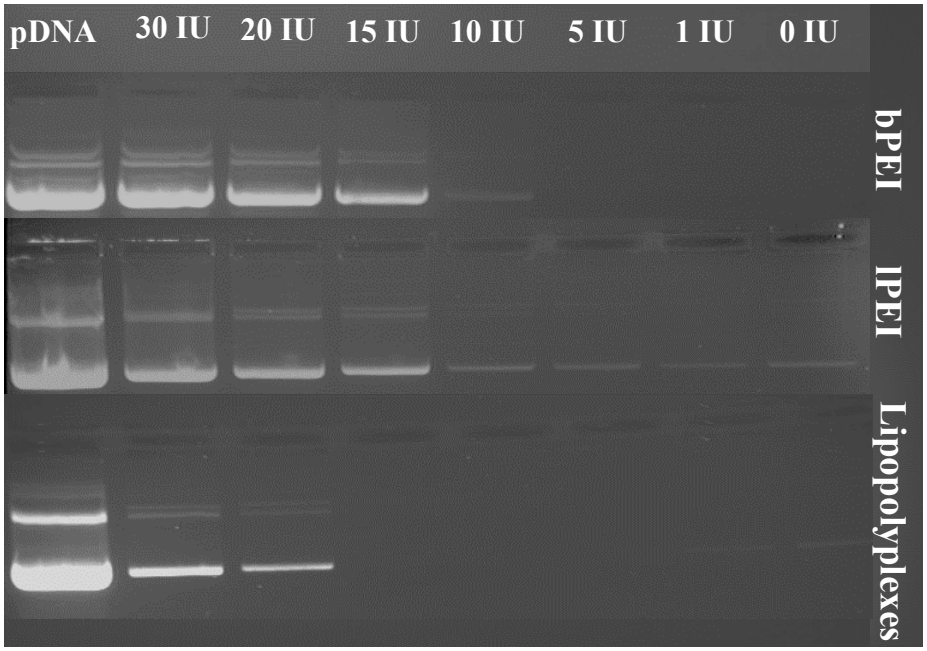

Figure 14: Heparin competition assay of branched and linear PEI polyplexes and lipopolyplexes

Being a polyanion, heparin competes with the complexes and displaces the condensed DNA. The data obtained from the assay, suggests lipopolyplexes to be far more stable in the presence

of polyanions compared to polyplexes from lPEI and bPEI (Figure 14). The lPEI polyplexes also show better stability than those of bPEI. bPEI polyplexes showed the least stability in presence of heparin. All the complexes released pDNA in presence of 20 IU/100 mL of heparin (1 mg = 100 IU) but the amount of pDNA released by the lPEI lipopolyplexes was the lowest. Lipopolyplexes were stable at normal concentration range of heparin in a healthy adults i.e. 15-17 IU/100 mL [153]. The outcome of this assay suggests that the liposomal layer around the polyplexes is offers better protection against heparin.

3.3.3 Binding affinity assay

Binding affinity of ethidium bromide to pDNA was measured as a function of complex integrity. To quantify the amount of free pDNA or prematurely released pDNA from the complexes intercalation assay was performed using fluorescence spectroscopy.

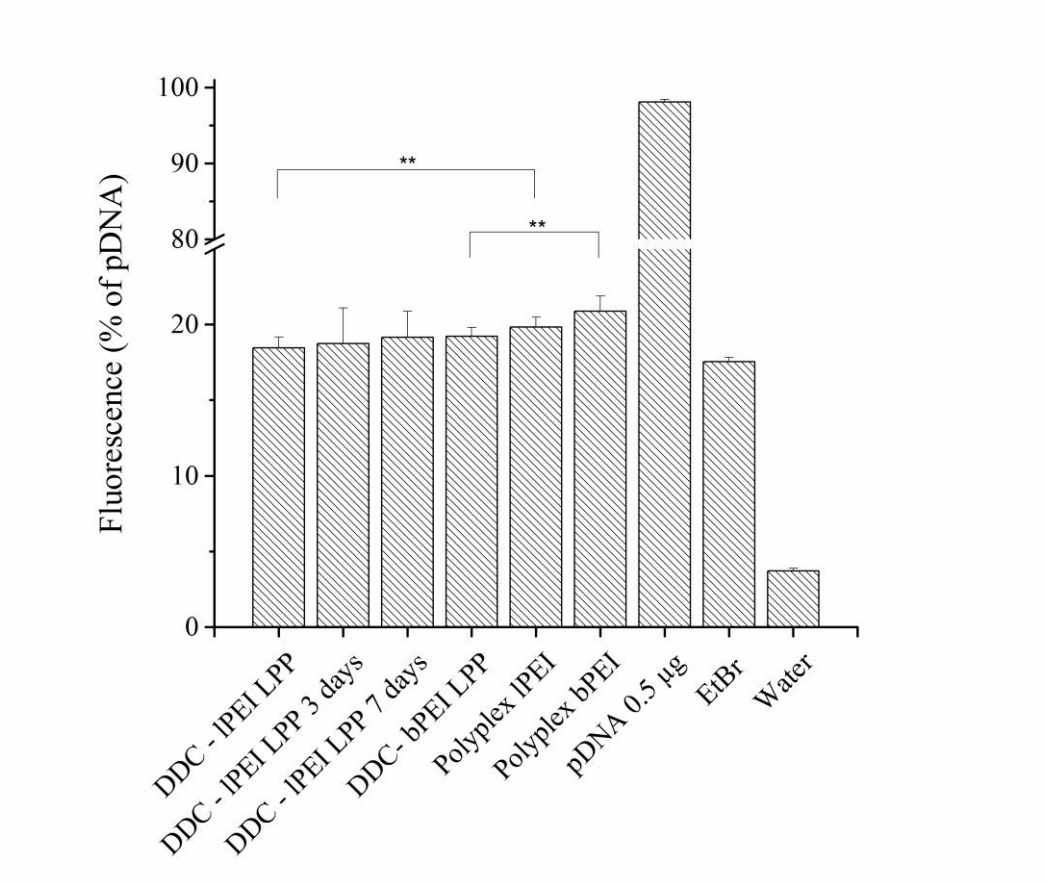

Figure 15: Ethidium bromide intercalation assay of DOPE:DPPC:Cholesterol (DDC) lipopolyplexes and polyplexes.

As seen in the graph, a shift in the fluorescence intensity is observed in case of lipopolyplexes, pointing towards an increased complexation of the genetic material inside (Figure 15). DDC-lPEI-pDNA (N/P 9.5) lipopolyplexes stored at room temperature also tested negative for DNA release. Interestingly the lipopolyplexes were found to be intact even after a week of storage showing no DNA release. The background fluorescence of an empty well was subtracted from the results and the fluorescence is reported as a % of free pDNA bound with ethidium bromide. The data obtained is compatible to the theory that a finite number of ethidium bromide binding sites in DNA that become gradually unavailable with increasing complexation [154].

3.4 *In vitro* studies

In vitro experiments offer a first line of testing for any new delivery system which is intended to be utilised in an organism. In an era where *in vivo* studies are strictly regulated, procuring a grant for the same is often cumbersome. Taking into consideration the ethical issues involved with animal studies, *in vitro* studies with suitable models offer a convenient solution as a preliminary step in evaluating any new delivery vehicle. *In vitro* studies are a cost-effective solution which asses the performance of the delivery vehicles in a more direct manner. In terms of anti-cancer gene therapy, investigating the tumour cells of their respective tissues is an excellent way to evaluate the efficacy of delivery system on the particular tumour. Artificially inducing inflammation using inflammatory factors in cells is has been used to study inflammatory effects in cells [135]. This approach was employed in this work to evaluate the anti-inflammatory gene therapy using lipopolyplexes as delivery vehicles.

3.4.1 Transfection

A direct method of assessing the efficiency of gene delivery vehicles is through transfection experiments. Transfections involve introduction of a nucleic acids into cells via delivery vehicles to alter their genetic sequence or to up or down-regulate certain cellular expressions. In this study, a plasmid DNA pCMV-luc encoding for firefly luciferase upon successful integration with the host DNA was used. Luciferase expression could be monitored using bioluminescent assays and is a direct measure of the efficiency of the gene delivery vehicles. Since expression of transfected gene in the cells is dependent on several factors such as cell health, mycoplasma contamination, cell growth phase, passage number, the results are almost

always irreproducible. Hence all the above factors need to be taken into consideration while evaluating the results.

Polyplexes prepared using various N/P ratios were evaluated in terms of transfection efficiency. The results were consistent with the studies conducted previously in this regard [67, 155]. Data from the polyplexes, suggested than an N/P ratio of 9.5 and 15 for lPEI and bPEI respectively were appropriate for further complexation experiments with liposomes.

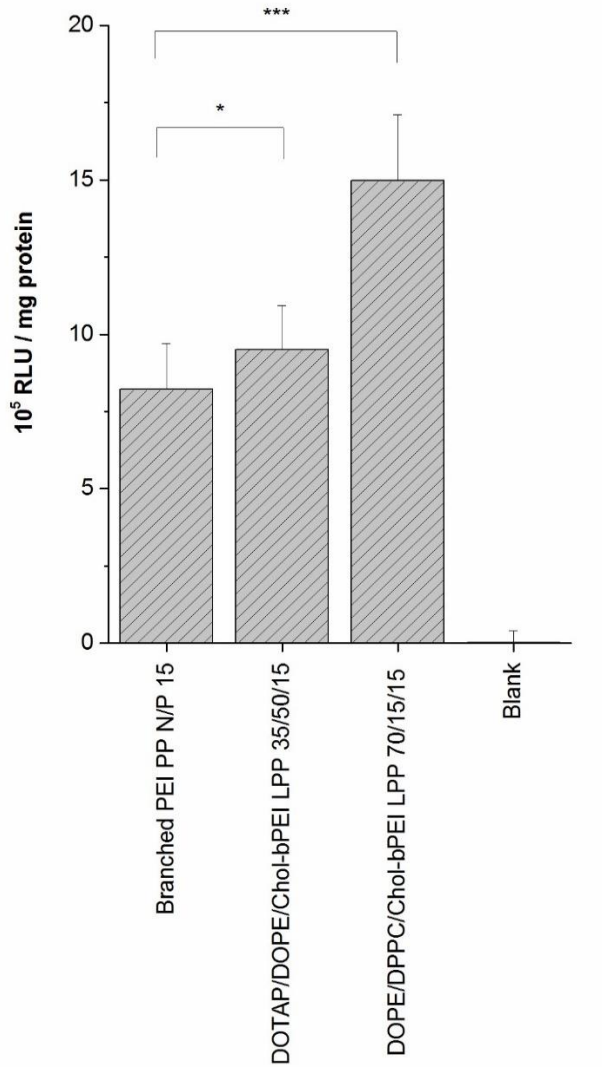

Figure 16: Transfection efficiency of bPEI polyplexes and lipopolyplexes in SK-OV-3 cells.

bPEI polyplexes with an N/P ratio of 15 were used to form lipopolyplexes with both DODC and DDC liposomes. DDC lipopolyplexes showed better transfection compared to DODC lipopolyplexes with bPEI (Figure 16). The increase in the transfection efficiency with DODC lipopolyplexes compared to bPEI polyplexes was not significantly high. 0.2 µg of pDNA per well was found to be effective for both the complexes.

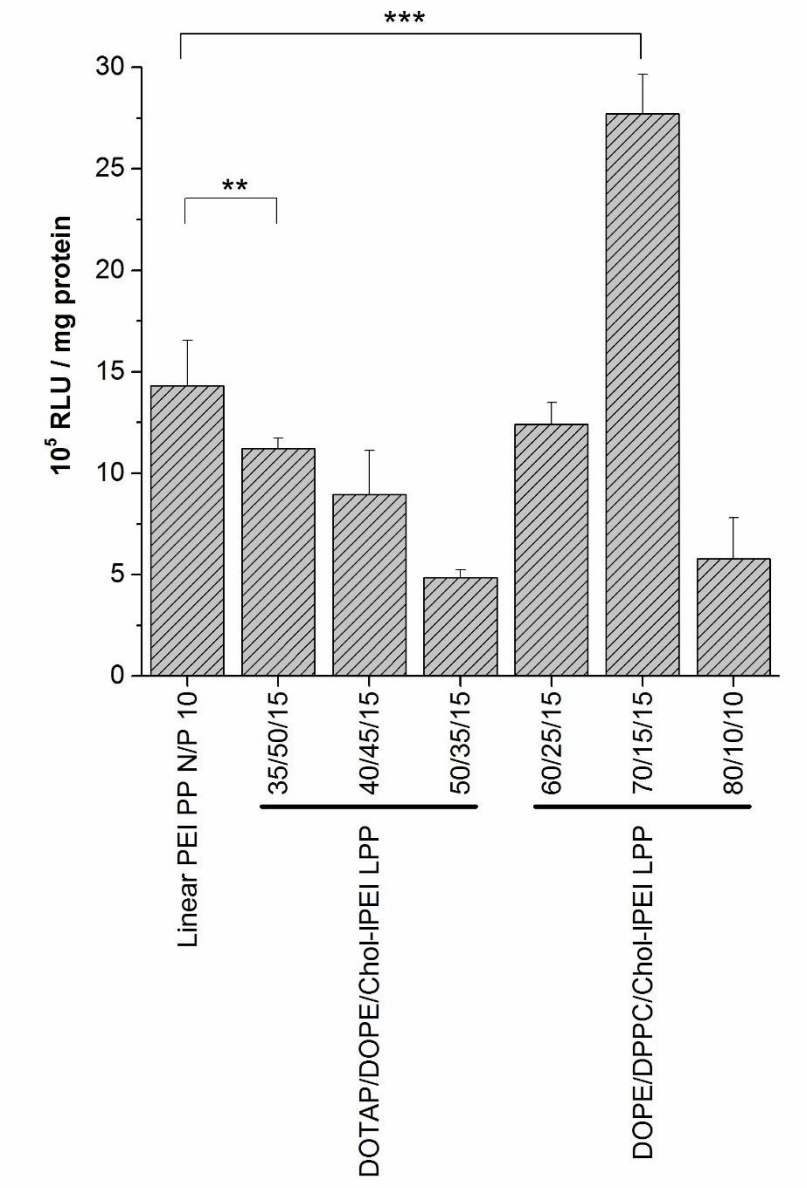

Figure 17: Transfection efficiency of lPEI polyplexes and lipopolyplexes in SK-OV-3 cells.

lPEI complexes show better transfection efficiency than their bPEI counterparts. As was the case with bPEI DODC lipopolyplexes, lPEI DODC lipopolyplexes were also much less efficient than DDC lipopolyplexes (Figure 17). Transfection efficiency has increased at least twofold upon addition of DDC liposomes. A liposome/PEI mass ratio of 1.2 for DDC and 3 for DODC lipopolyplexes was used for the initial experiments. Since DDC lipopolyplexes have been far more efficient than their DODC counterparts, they were solely used for the further experiments. Higher pDNA amounts yielded better transfection results with polyplexes, but the results were inconsistent. Furthermore, unbound free pDNA has been proven toxic to the cell in previous studies, and hence the concentration was kept as low as possible without compromising the transfection efficiency [156].

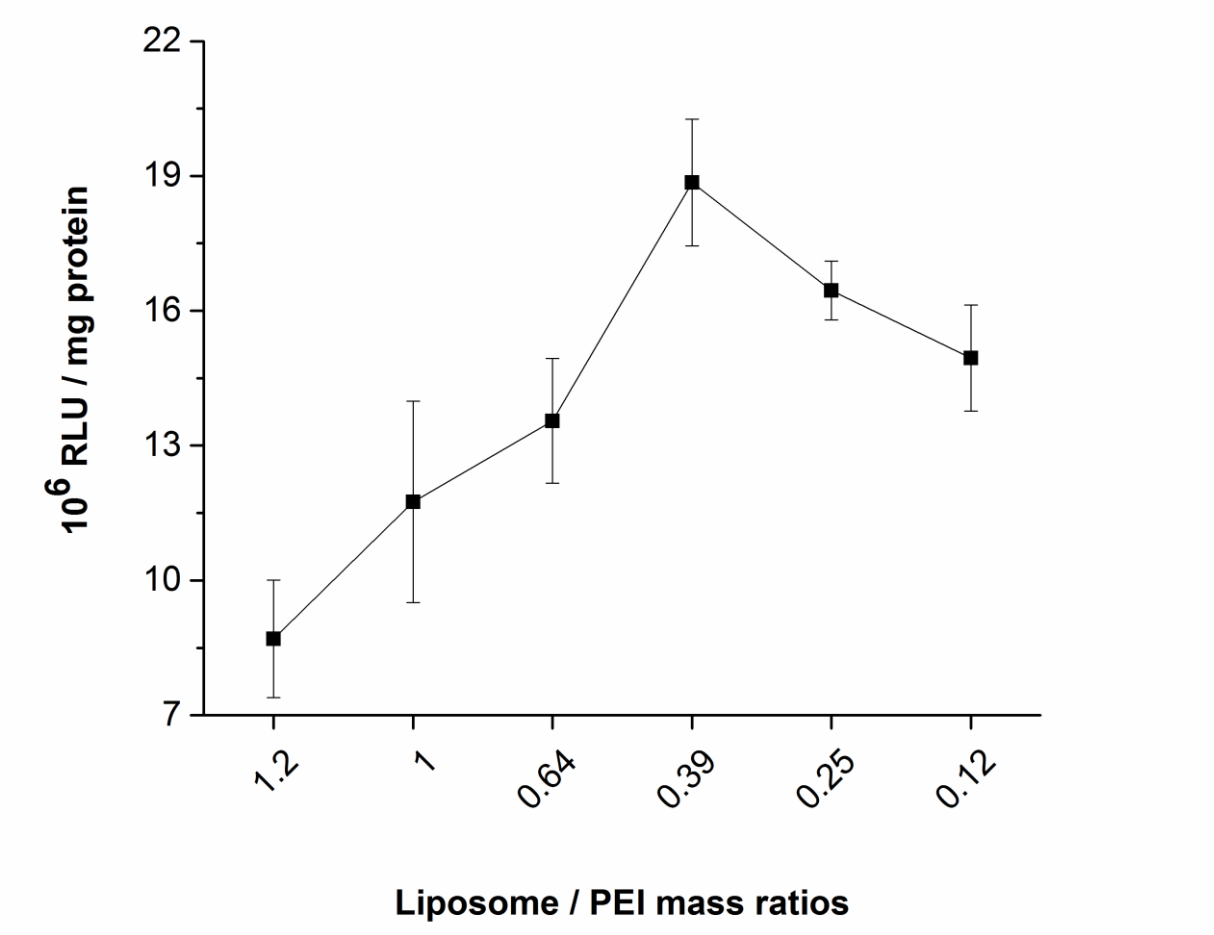

Figure 18: Optimisation of the liposome/PEI mass ratios of DOPE/DPPC/Cholesterol-linear PEI lipopolyplexes

Subsequent experiments involved optimising the stoichiometry of the DDC lipopolyplexes (

Figure 18). The experiments started off with a liposome/PEI mass ratio of 1.2 and then proceeded in decreasing ratios until an optimal ratio was achieved. After a series of experiments with different ratios, the mass ratio of 0.39 which showed a tenfold increase in transfection efficiency was deemed to be optimal. This suggests that at this ratio, the number of liposomes available to complex with the polyplexes was optimal. As seen in the graph, above this ratio, there is a decrease in the transfection efficiency, similar is the case with ratios below 0.39. This might be pointing towards an abundance or deficit of liposomes available for complexation, which was also seen in previous studies [75]. This ratio was therefore used in all subsequent experiments involving lipopolyplexes.

To confirm the transfection and to determine the transfection efficiency of lipopolyplexes in other tumour cells lines which would be used for knockdown experiments. HeLa, EA.hy926 and A549 cells were used

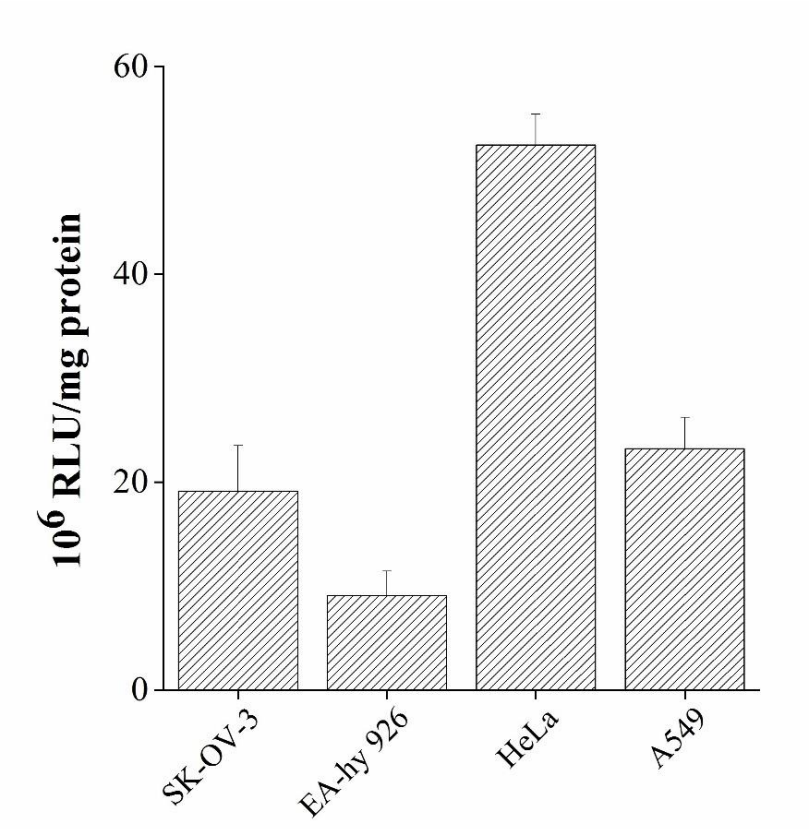

Figure 19: Transfection efficiency across various cells lines with linear PEI lipopolyplexes

Results from the transfections in various cells lines show that transfection efficiency varies across cell lines (Figure 19). Not just the delivery vehicle, but also the cells play an important role in the transfection efficiency. Factors such as the promoter used in the plasmid, size of the promoter sequence also play a role in expression of reporter gene. This is in agreement with a previous studies mentioning the role of promoter, transgene and cell line in determining the transfection efficiency [157]. Delivery vehicles need to be optimised to efficiently transfect across different cell lines for e.g. by attaching the delivery vehicles with ligands or antibodies depending upon the cells. Therefore, it is almost impossible to formulate a delivery vehicles which works with equal efficiency across all cell lines.

3.4.2 Uptake pathway analysis

The major internalisation route for non-viral gene delivery vehicles into the cells is through endocytosis. In endocytosis, a part of the cell membrane engulfs the delivery vehicle which is either electrostatically attached to cell membrane or is in the vicinity of the cell. Subsequently, a vesicle comprising membrane components, detaches off from the cell membrane and enters the cytoplasm to form an endosome. It is this vesicle the delivery system needs to overcome in order to be released into the cell. Different forms of endocytic pathways exist and different delivers vehicles utilise different pathways to enter the cell. The use for inhibitors for individual pathways helps understand the exact mechanism of cellular internalisation of the delivery vehicles. In this work, several different inhibitors of endocytic pathways were utilised. Dynasore, an inhibitor of dynamin 2 protein, interferes with the dynamin dependent endocytosis. Filipin III derived from *Streptomyces filipensis* was used as an inhibitor for caveolae mediated and lipid-raft mediated endocytosis and chlorpromazine was used for inhibiting clathrin mediated endocytosis.

The exact internalisation pathway and the mechanism of uptake could be identified using the inhibitors. Since serum has a detrimental effect on the inhibitory effects, experiments were conducted in its absence. To rule out any possible interaction of complexes with inhibitors, the cells were washed prior to incubation with complexes. Due to their dose dependent toxicity, inhibitors were used in concentrations reported to be safe in previous studies [75].

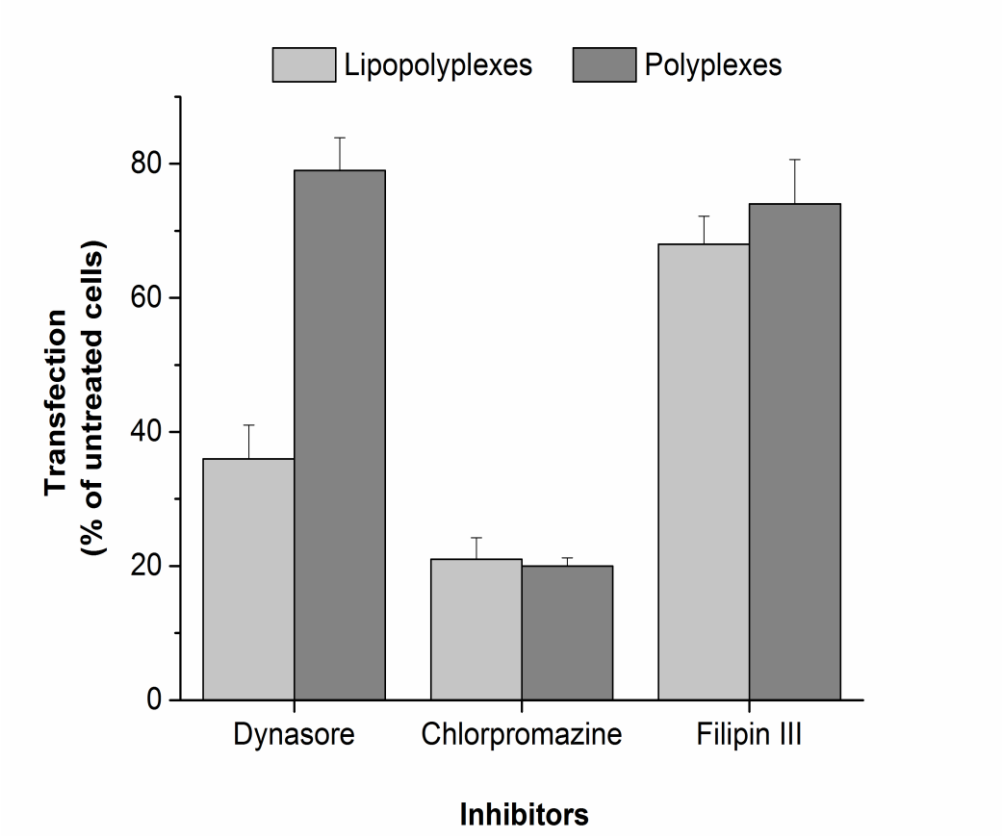

Figure 20: Transfection in SK-OV-3 cells in presence of specific endocytosis pathway inhibitors

Transfection efficiency of cells without inhibits was considered as 100 % and the results are expressed in correspondence to untreated cells. Results obtained from pathway analysis in SK-OV-3 cells show a certain level of reduction in the transfection efficiency of lipopolyplexes in presence of all the three inhibitors (Figure 20). In agreement with previous studies, the transfection efficiency of lipopolyplexes decreased in the presence of chlorpromazine, suggesting a clathrin mediated internalisation pathway [75]. Additionally, lipopolyplexes also seem to be internalised by dynamin dependent endocytosis. Internalisation of polyplexes, appears to occur mainly via clathrin mediated endocytosis. The data from polyplexes is however ambiguous with respective to their inhibition compared to other studies reporting a dose dependent inhibition via all major pathways [158]. As such, the uptake mechanism is dependent on the cell line and hence the data should be regarded cautiously. Studies reporting the uptake mechanism of PEI are conflicting in terms of internalisation pathway. Schäfer et. al reported a caveolae independent mechanism of uptake for PEI in SK-OV-3 cells whereas another study by Gabrielson et.al reported a caveolae dependent endocytosis of PEI in HeLa cells [75, 159].

As reported previously, pathway inhibitors appear to have a non-specific mechanism to inhibition which is influenced by several factors, therefore, the data obtained needs to be interpreted with caution [160]. It can be inferred from that results that lipopolyplexes only utilise the clathrin mediated endocytosis but also dynamin dependent endocytosis which gives them an edge over polyplexes in terms of internalisation.

3.5 Physical methods of enhancing gene transfer

The data obtained from pathway analysis prompted the investigation of a suitable method for improving the release of the lipopolyplexes from the endosome. In general, only a fraction of delivery vehicles reach the target cells, of these a fraction makes it into the cells and a fraction of the internalised vehicles escape the endosome. To enhance this endosomal escape, light and ultrasound have been made used in this work. While administering light is a minimally invasive technique, ultrasound is a completely non-invasive technique.

3.5.1 Photo-chemical internalisation

With an aim at improving the endosomal release, through light, curcumin loaded liposomes were used for the complexation with polyplexes. PCI mediated introduction of luciferase reported gene has been studied using a compact portable prototype LED device designed for photodynamic studies in multiwell plate formats [133]. The irradiation intensity used for the PCI experiments was completely harmless to the cells. The irradiation device used for this work sits onto microtiter plates covering the entire surface. By varying the current intensity and time, irradiation dose could be adjusted. In previous studies, gene delivery vehicles and photosensitisers have been administered individually or chemically linked to the delivery vehicle [94, 97, 98]. This work involves a composite delivery system, capable of introducing both the photoactive agent and the genetic material together.

Irradiation was performed after incubating the cells for 4 h with curcumin loaded lipopolyplexes and lipopolyplexes, taking into consideration the average time for endocytosis (1 - 4 h) [161]. Luciferase assay of the irradiated cells showed at least a threefold increase in the transfection efficiency upon irradiation (Figure 21). Different irradiation intensities yielded different results. This was in consistence with previous studies reporting the influence of irradiation dose on PCI [162]. An intensity of 1 J/cm^2 proved to be the best in terms of transfection efficiency.

Un-irradiated cells (dark) containing curcumin lipopolyplexes did not show any increase in the transfection efficiency, clearly indicating that the increase in the transfection efficiency was related to irradiation. Similarly, lipopolyplexes without curcumin also did not show a difference in transfection efficiency upon irradiation, pointing towards the PCI effect mediated by curcumin. The results suggest an endocytic vesicle permeabilisation upon irradiation of cells internalised with curcumin loaded lipopolyplexes. Similar effects were observed in previous studies, studying co-delivery of photosensitiser and genetic material [94, 98].

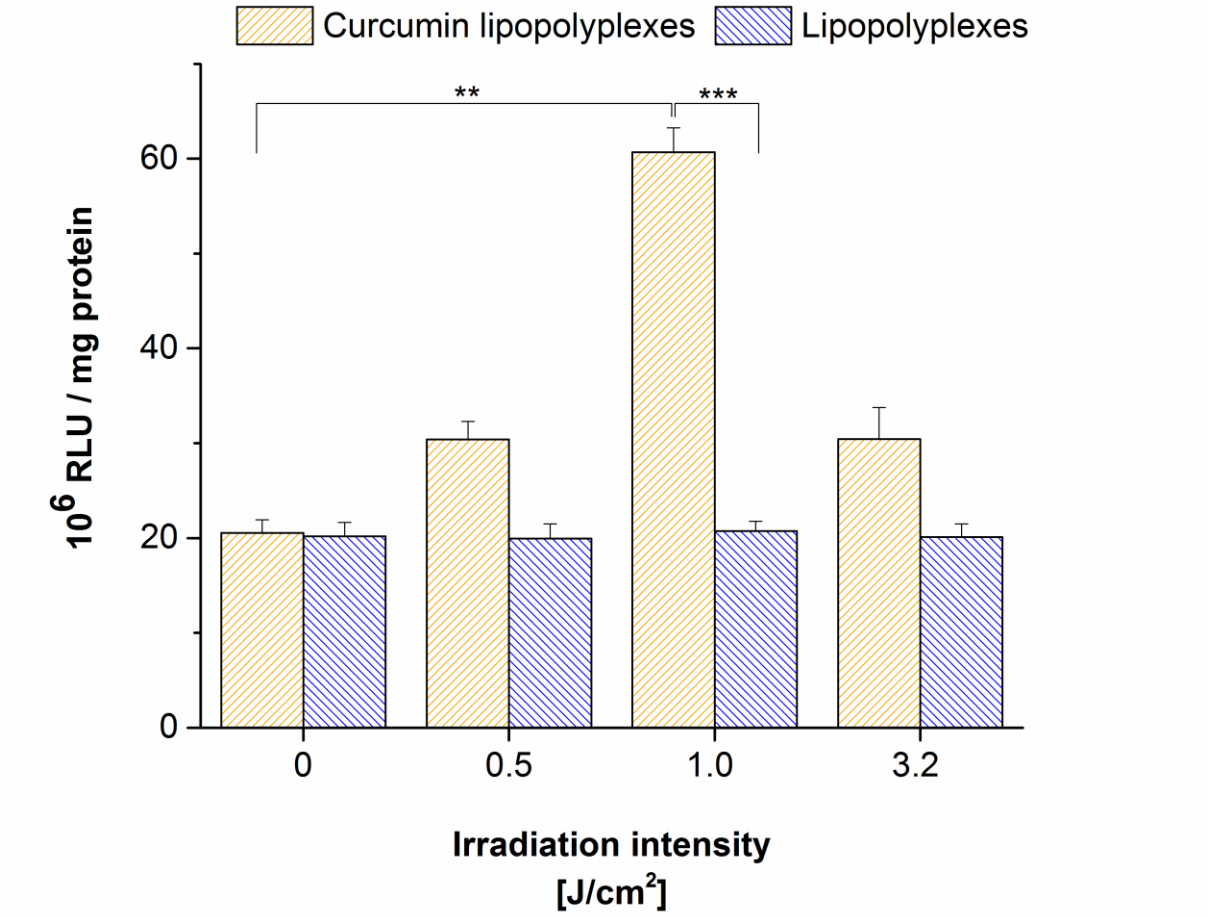

Figure 21: Comparison of photo-enhanced effects on curcumin loaded linear PEI lipopolyplexes and lipopolyplexes (0 denotes unirradiated cells)

3.5.2 Ultrasound enhanced gene transfer

Similar to photo-chemical internalisation, UEGT is a physical method aimed at enhancing gene transfer. Studies pertaining to UEGT have suggested that UEGT works by creating reversible cavities (cavitation) in the cell membrane allowing gene transfer [163, 164]. A prerequisite for this, however is the presence of gas filled microbubbles or gas filled particles that are sonogenic (acoustically active) [103, 109]. Lipopolyplexes were evaluated for their gene transfer potential using ultrasound.

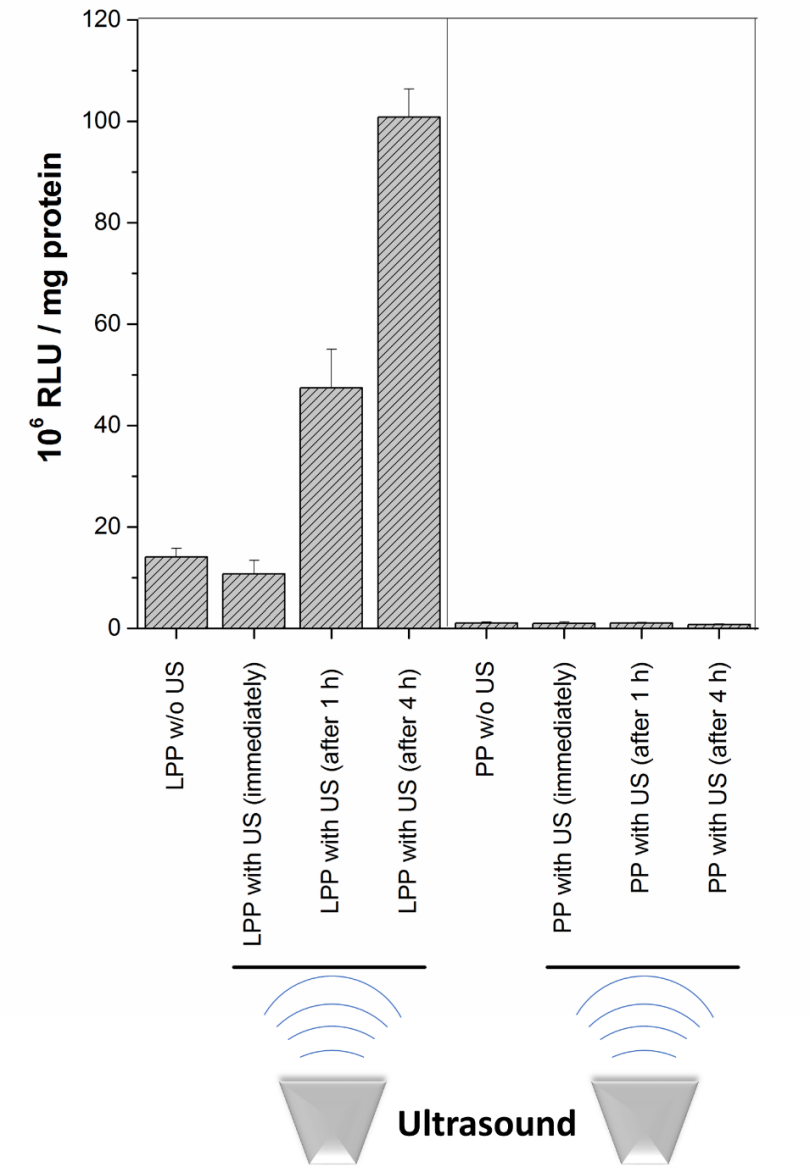

Figure 22: Ultrasound enhanced gene transfer at different time periods in SK-OV-3 cells with ultrasound application at different time intervals

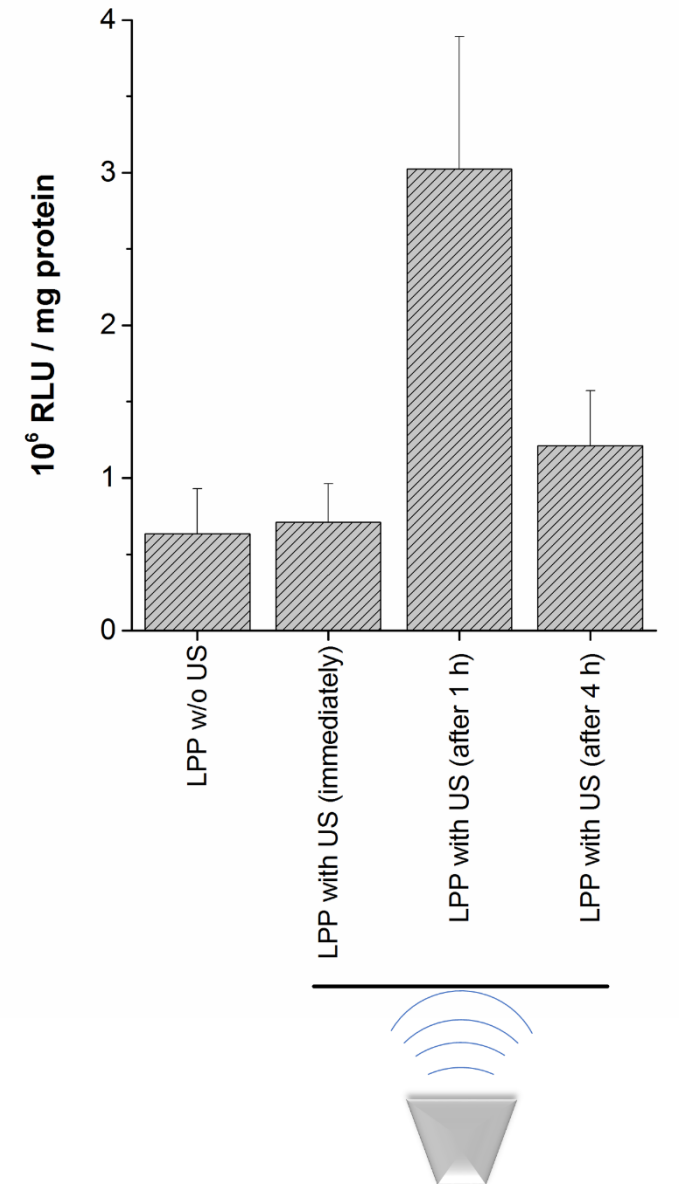

Figure 23: Ultrasound enhanced gene transfer in PCS-100-012™ cells with ultrasound application at different time intervals

The linear transducer used in the UEGT experiments was capable of delivering ultrasound at a frequency of 15 Mhz. Penetration depth was adjusted to 1.1 cm which was the gap between the surface of the petri dish and the position of the transducer (in growth medium). During the UEGT experiments, the mechanical index, which is a measure of the bio-effects cavitation, was at 1.5 which is below the maximum allowed level recommended by the regulatory authorities in Europe [165].

The results obtained from the UEGT experiments were unexpected regarding the timing of ultrasound exposure. Immediate exposure to ultrasound after incubation did not yield any benefit in SK-OV-3 cells (Figure 22). On the contrary, exposure to ultrasound after 1 and 4 h time periods yielded a significant increase in the transfection efficiency, with exposure after 4 h showing a fivefold increase.

In case of primary PCS-100-012™ aortic smooth muscle cells, transfection was improved after ultrasound exposure following 1 h of incubation with lipopolyplexes (Figure 23). Ultrasound exposure following 4 h incubation was not as effective as with SK-OV-3 cells. The results not only suggest a faster internalisation mechanism of PCS-100-012™ cells but also point towards a different uptake pathway. The transfection efficiency of polyplexes with or without ultrasound was relatively low in PCS-100-012™ cells (data not shown).

The results point towards an improved release from the endosome similar to PCI experiments. A cavitation effect could be excluded since no substantial effect was observed upon ultrasound exposure soon after incubation. Comparable results proposing an endosomal rupture were seen in another study suggesting the influx of Ca^{+} ions into the cell upon ultrasound exposure leading to endosomal acidification and subsequent release [166]. This, was however, not the case with polyplexes which did not show any substantial improvement at all, leading to ambiguity in the exact mechanism of action.

3.6 Transfection visualisation

To observe the intracellular expression of the reporter gene, and to confirm the transfection efficiency using a different reporter gene system, pEGFP-N1 plasmid DNA expressing green fluorescence protein was used. Expression of GFP was visualised using confocal laser scanning microscopy.

Micrographs from the cells transfected with lipopolyplexes and polyplexes show successful GFP expression (Figure 24). DAPI was used to counterstain the nuclei in order to localise the cells during microscopy. Compared to the micrographs of polyplexes, the micrographs of lipopolyplexes show more number of cells expressing GFP. The amount of GFP expressed per cell (qualitatively) is also higher in case of lipopolyplexes.

Both polyplexes and lipopolyplexes have successfully entered the cells and have undergone intracellular dissociation to release pEGFP-N1 which has successfully transcribed and been translated into green fluorescence protein.

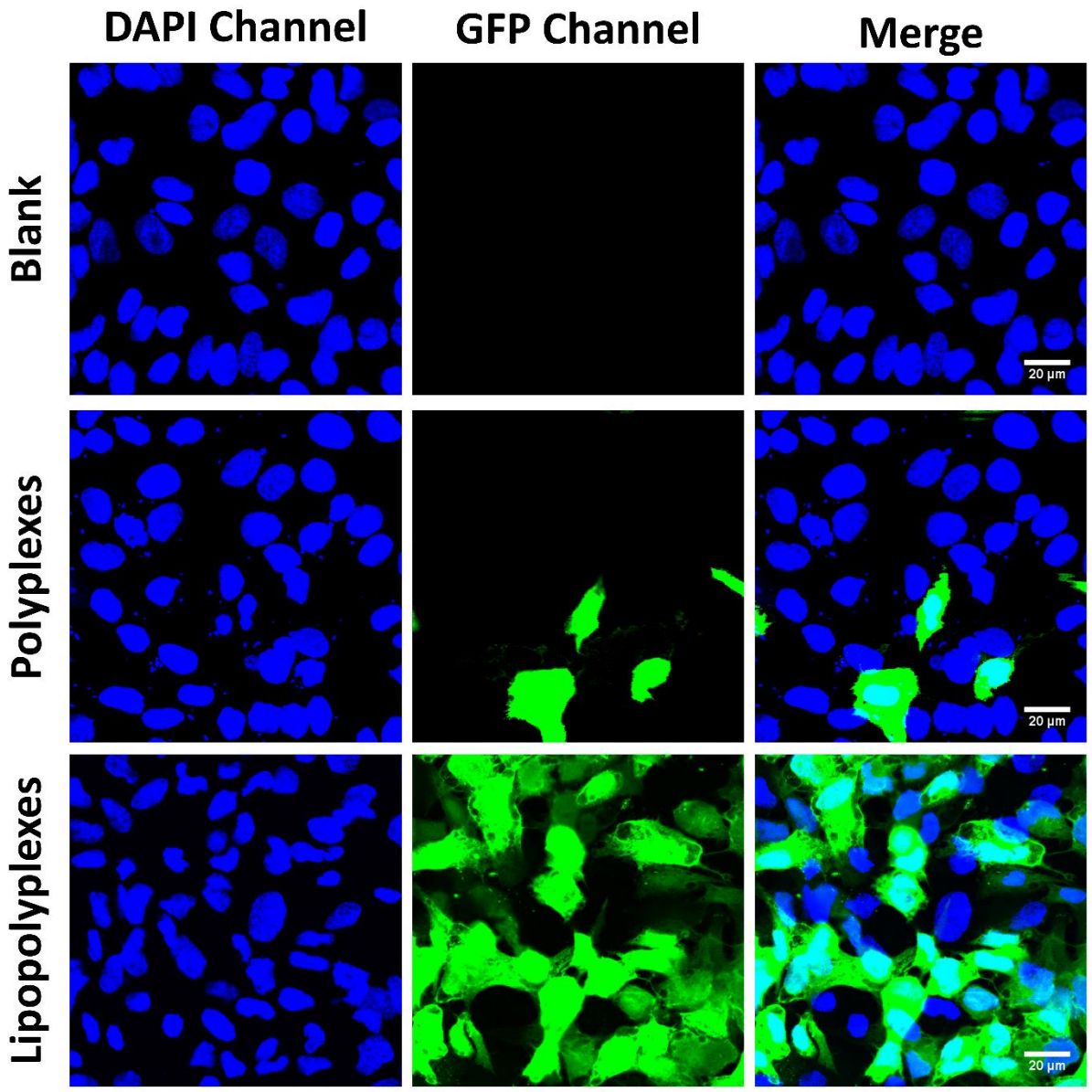

Figure 24: Visualisation of GFP expression in SK-OV-3 cell transfected with linear PEI polyplexes and lipopolyplexes; scale bar 20 µm

3.7 Knockdown studies

An ideal gene delivery vehicle should be able to deliver various kinds of nucleic acids with considerable efficiency. Most commercially available gene delivery vehicles, termed transfection reagents, fall short in this aspect. Most manufacturers offer different transfection reagent for different nucleic acids and to further complicate things, different transfection reagents for different cell lines are offered. Transfections with siRNA is cumbersome with regard to the special needs in terms of equipment and reagents. An RNAse free environment is required to rule out the effect of the nucleases on the siRNA. Buffers, reagents, equipment that comes into contact with the siRNA should all be RNAse free to ensure reliable results. Only the complexation buffer (10 mM HEPES; pH 7.4) and the pipette tips used in this work were RNAse free.

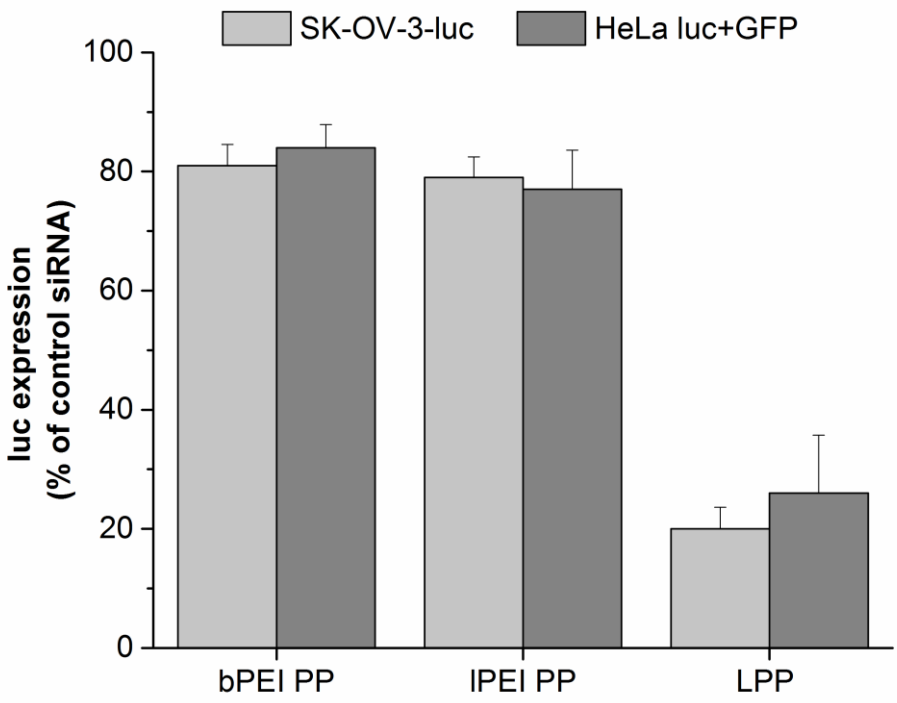

Figure 25: RNA interference in luciferase expressing SK-OV-3-luc and HeLa luc+GFP cell lines

To assess the RNAi potential of the delivery vehicles, a stable luciferase expressing SK-OV-3 cell line and a HeLa cell line co-expressing luciferase and GFP was used. siRNA often leads to off-target effects complicating the interpretation of results. To determine the siRNA activity without misinterpreting the results, appropriate controls should be used. In this work, a control siRNA siCtrl with no human or animal targets was employed. To target the GL3 luciferase gene in SK-OV-3-luc cells, luciferase GL3 duplex siRNA was used. In case of HeLa luc+GFP cells expressing firefly luciferase, Anti-luc siRNA 1 was used. The two cell lines showed different luciferase activity upon siRNA transfection. In a stark contrast with transfection experiments, where the difference in luciferase activity between SK-OV-3 and HeLa cells was huge, knockdown experiments yielded different results (Figure 19 and Figure 25). If the results of the HeLa were to be considered, knockdown efficiency in SK-OV-3 was greater compared to its transfection efficiency. This should however, be interpreted with caution due to the different mechanisms of action. Plasmid DNA needs to make its way to the nucleus in order to induce gene expression. The target biomolecule for siRNA is its complimentary mRNA which is transcribed into the cytosol, making it an easier target [167]. In terms of knockdown efficiency, the lipopolyplexes showed a far better transfection efficiency compared to lPEI polyplexes which were marginally better than their bPEI counterparts.

In order to replicate the knockdown efficiency using a target gene, endothelial EA.hy926 cells were used. Endothelial cells express E-selectin as an inflammatory response. In this work, inflammation was induced using TNF-α. E-selectin, an endothelial leukocyte adhesion molecule, plays a major role inflammation. As a response to inflammation, endothelial cells express E-selectin, which mediates leukocyte binding and subsequent infiltration (extravasation into the inflamed tissue [113]. This mechanism of E-selectin is exploited by the tumour cells to mimic the leukocytes and metastasise. Several studies also suggest that tumour cells might directly express factors and selectin ligands that induce E-selectin expression leading to a chain reaction. This in turn is associated with progression of tumours and infiltration of migrating cancer cells through endothelial vessels [168-171]. These factors make E-selectin an important therapeutic target to counter inflammatory diseases and inflammation associated tumour metastasis.

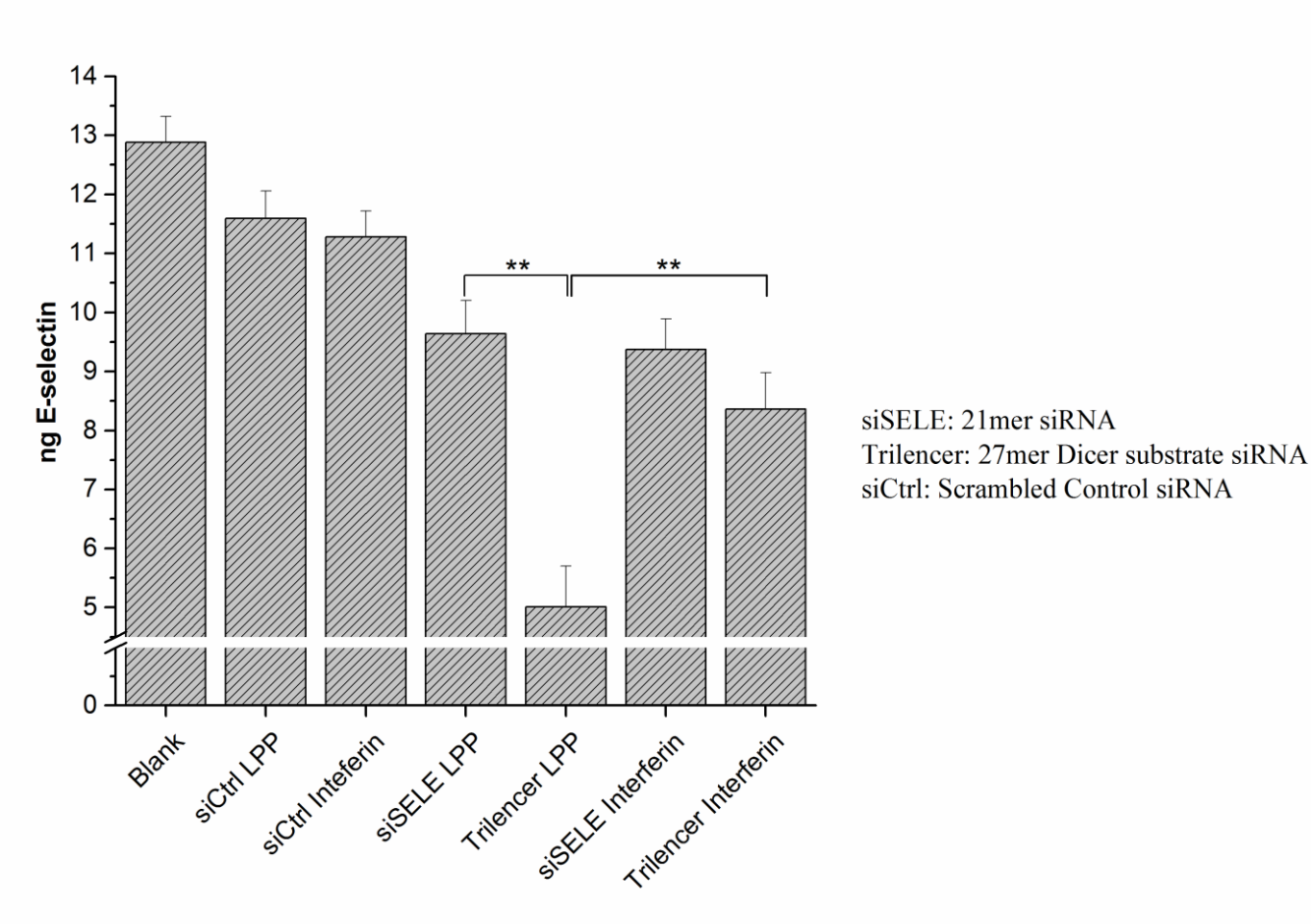

Figure 26: E-selectin knockdown in EA.hy926 cells, with two different siRNA directed against E-selectin

ELISA experiments following incubation of EA.hy926 cells with lipopolyplexes containing two different types of siRNA's yielded contrasting results. As a control a scrambled siRNA, siCtrl was used and as positive control for transfection, commercially available siRNA transfection reagent INTERFERin® was used. While the double stranded siRNA against SELE gene showed a slight reduction on E-selectin expression, the 27mer Trilencer dsiRNA showed a dramatic reduction in the expression (Figure 26). This points towards the role of dsiRNA in processing the siRNA post transfection, which is consistent with the studies reporting its improved role in RNAi compared to siRNA [172, 173]. Compared to the commercial siRNA transfection reagent, the lipopolyplexes showed better knockdown, especially with dsiRNA.

Although no strict RNAse free conditions were maintained (due to practical restrictions viz. extrusion equipment, glassware and other consumables) during the preparation of liposomes and PEI for the experiments, the RNAi studies with lipopolyplexes still showed significant bioactivity, pointing towards the role of lipopolyplexes from preventing the siRNA from degradation against nucleases.

3.8 *In vitro* Cytotoxicity studies

A major aspect in delivery of biomolecules, often understudied is the toxicity of the delivery vehicles. Cytotoxicity is the main obstacle for utilising non-viral gene delivery vehicles for a therapeutic setup. Toxicity studies help assess the safety of the delivery vehicles. Determination of a safe dose or a safe concentration could be done using toxicity tests. Toxicity of delivery vehicles could be both immediate or dependent on time. LDH and MTT assays have been used to determine the acute toxicity and time dependent toxicity of the complexes respectively.

3.8.1 Membrane toxicity

LDH assay measures the amount of lactose dehydrogenase released by cells into the medium (following cell membrane damage) as a measure of cytotoxicity. This usually occurs during the initial incubation period with the delivery vehicles. Most commercial non-viral vectors suggest changing the medium 4 h after incubation with cells to reduce the cytotoxic effect of the delivery vehicles. For this work, however, the medium was left until the time point of evaluation. Therefore, for the LDH assay, L929 cells were incubated for 48 h with the complexes.

Severe damage to the cell membrane could be seen in case of bPEI polyplexes (Figure 27). This is in agreement with previous studies linking the high charge density of PEI to cell membrane destabilisation and cellular necrosis [78, 79]. In case of lPEI polyplexes, cytotoxicity was considerably lower than its branched counterpart, which is in consistence with studies comparing the cytotoxicity of branched and linear polyethylenimine [174, 175]. Comparatively, lipopolyplexes formulated using bPEI were more cytotoxic than their linear counterparts, which were minimally cytotoxic. This could be attributed to the shielding effect liposomes impart to the polyplexes. As reported previously, the cytotoxicity of PEI is mainly due to its cationic charge density [79]. Liposomal encapsulation, especially with anionic liposomes, is an

outstanding approach in reducing the surface charge of PEI, without complex structural modifications and without compromising its transfection efficiency.

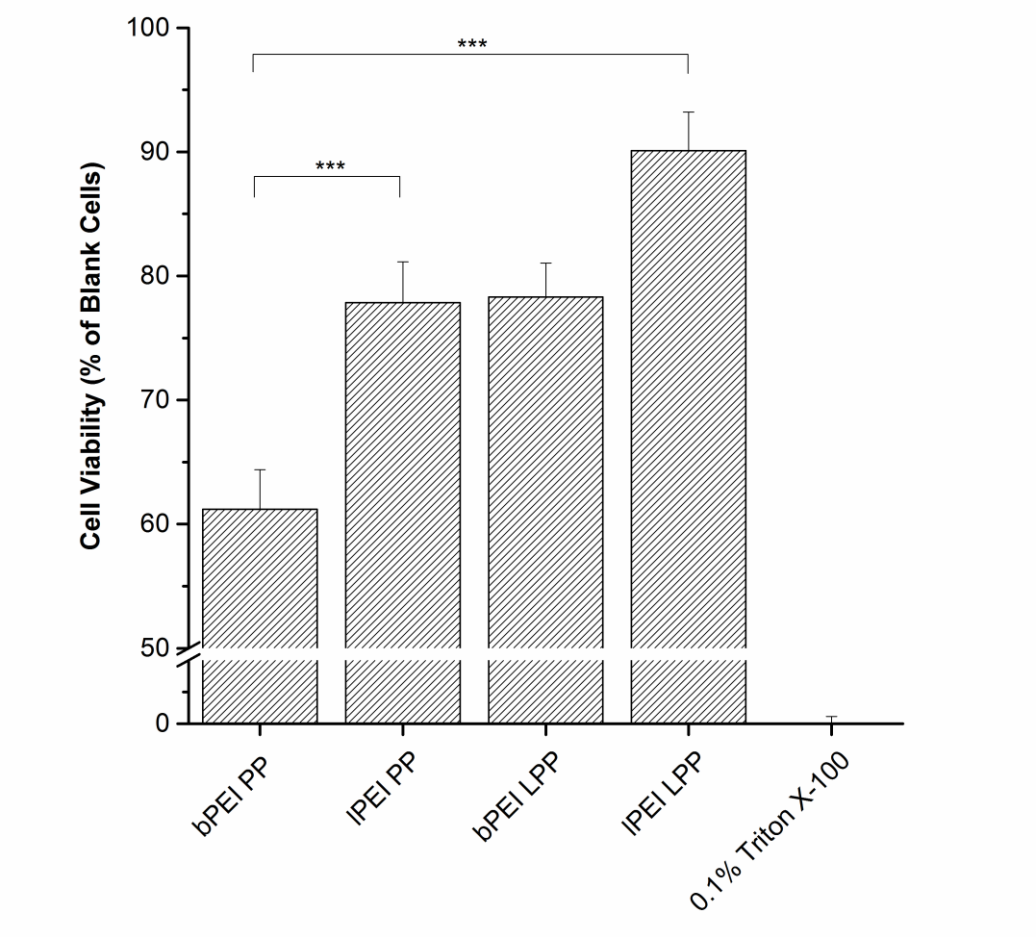

Figure 27: LDH assay of polyplexes and lipopolyplexes with branched and linear PEI. Triton X-100 ™ used as positive control.

3.8.2 Time dependent cytotoxicity

MTT assay was used to determine the cell viability as a function of time. Viable cells metabolise MTT into formazan crystals, which upon solubilisation with DMSO could be measured spectrophotometrically. To get a deeper insight into the time related toxicity of the complexes, MTT assay was performed after 4, 8, 16, 24, 36 and 48 h. L929 cells incubated with complexes were assayed at the aforementioned time periods to determine the cell viability.

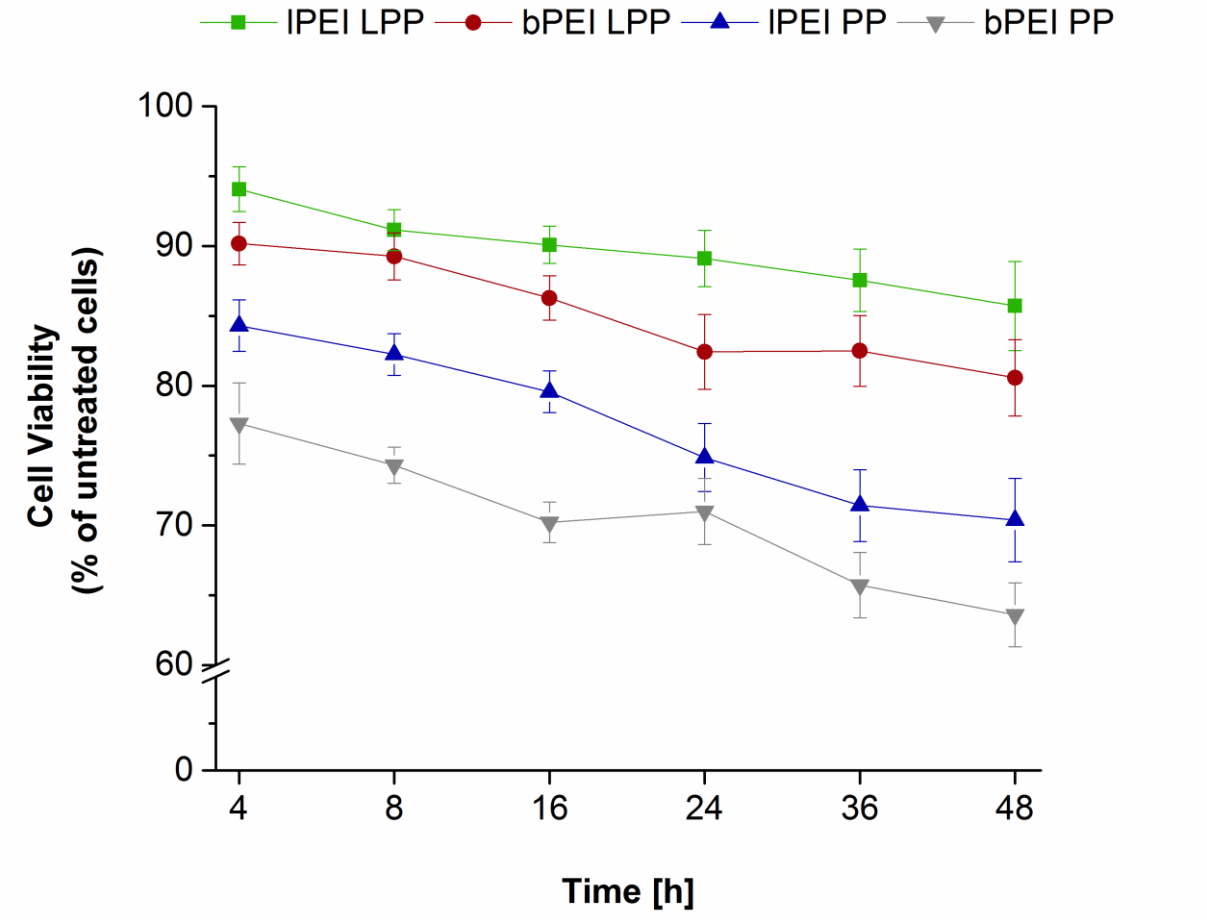

Figure 28: Cell viability of branched and linear PEI polyplexes and lipopolyplexes at time intervals ranging from 4 to 48 h

Similar to LDH assay results, MTT results show the highest toxicity in case of bPEI (Figure 28). The toxicity effect of bPEI is seen within 4 h of incubation, confirming the charge related cell membrane degradation reported previously [78]. This was similar in case of lPEI too, however, to a lesser extent. Viability of bPEI lipopolyplexes was less than their lPEI counterparts, but better than that of lPEI polyplexes. lPEI lipopolyplexes showed the highest cell viability even after 48 h of incubation. Viability of all the complexes inversely proportional to time, decreasing gradually with increasing incubation periods. The difference in the initial toxicity at 4 h in between polyplexes and lipopolyplexes confirms the liposomal shielding effect. The results of the cytotoxicity studies are consistent with a previous study reporting the liposomal shielding of PEI [75].

3.9 Haemocompatibility studies

Haemocompatibility studies offer an excellent platform in determining the compatibility of any non-viral delivery system. *In vitro* cytotoxicity tests give only a partial picture of the cytotoxicity scenario, which is limited to cells. Upon delivery, the first point of contact for non-viral vectors is blood. Blood is a mixture of a multitude of constituents. Interaction with the red blood cells or erythrocytes is a critical factor which determines the biocompatibility of delivery vehicles. Similarly, the delivery systems should also be compatible with the plasma, a major component of blood, containing clotting factors. Any unmonitored alteration to the pathways of haemostasis could have deleterious effects on the patient. Therefore, a clear understanding of the interaction of the delivery vehicles with blood is important in deeming a delivery system biocompatible. Haemocompatibility tests are also a bridge between *in vitro* and *in vivo* studies, wherein, they help determine the safe and ethical use of the delivery vehicles, saving a lot a of time, personnel and investment.

3.9.1 Haemolysis assay

Erythrocytes are the building blocks of the complex human biological system. They contain haemoglobin, which plays a vital role in the transport of oxygen and CO_2, to and from the tissues. Haemolysis assay give the measure of damage to the erythrocytes, by measuring the amount of haemoglobin released. Haemoglobin from the erythrocytes, binds with oxygen to form oxyhaemoglobin, whose absorbance could be recorded spectrophotometrically at 540 nm.

1 % Triton X-100™ was used as positive control for haemolysis due it ability to completely lyse the cells [176]. The absorbance values of oxyhaemoglobin from Triton X-100™ samples were considered as 100 % cell lysis. Due to its high charge density, bPEI polyplexes, readily lysed the erythrocytes leading to a release in haemoglobin (Figure 29). Interestingly, lPEI polyplexes showed a much less haemolytic potential, pointing towards a charge related lysis haemolytic effect of bPEI. Once again, encapsulation of the polyplexes with liposomes proved beneficial with both bPEI and lPEI lipopolyplexes. The haemolysis effect observed with lipopolyplexes is very low and taking into consideration, the ratio (v/v) of erythrocytes to injected delivery vehicles in the human body, is negligible.

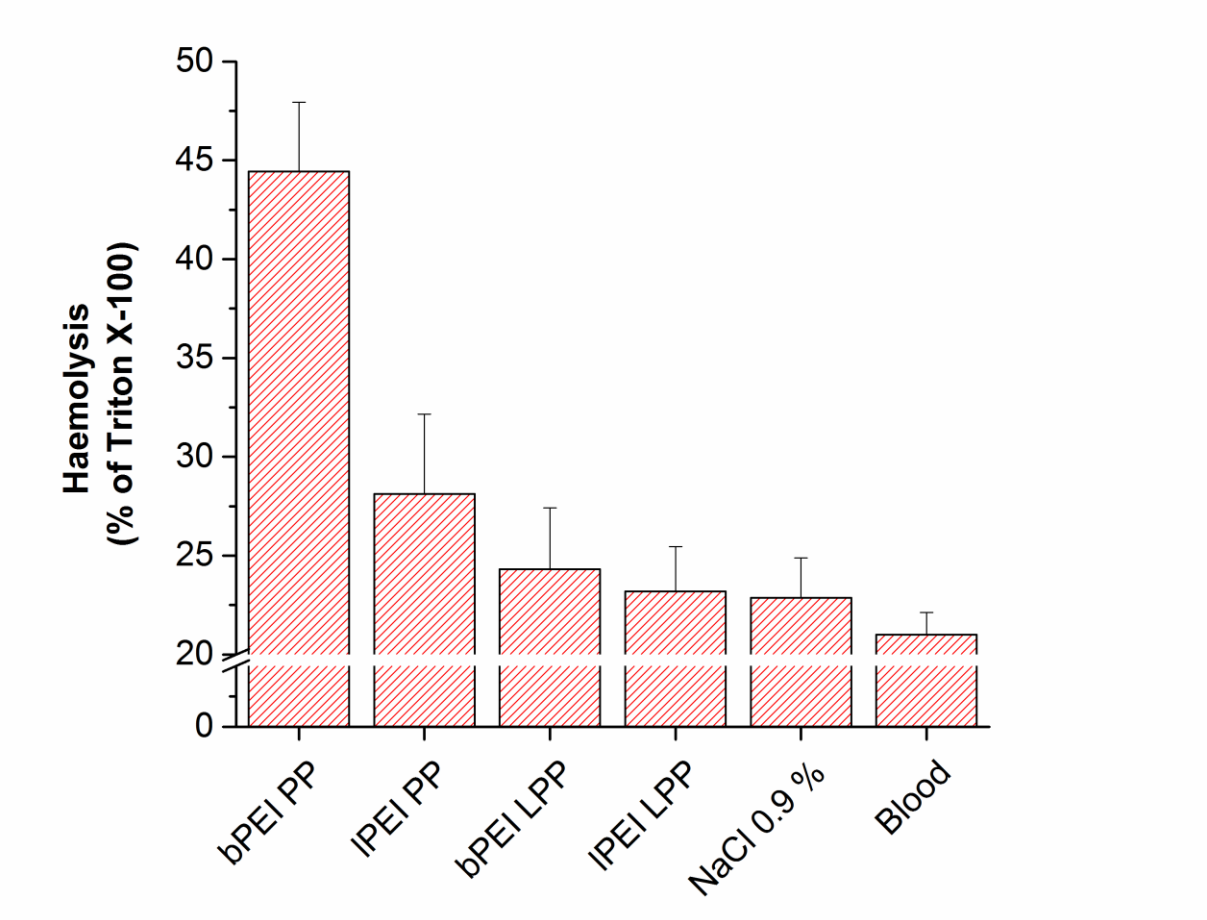

Figure 29: Haemolysis assay of the complexes, complexes showing haemolysis of above 20 % (untreated blood) were considered to show haemolytic potential

3.9.2 Activated partial thromboplastin time test

Normally a diagnostic tool for monitoring patients undergoing anticoagulant therapy, the aPTT test is valuable in determining the effect of the delivery vehicles on coagulation. Although a deviation from normal aPTT values does not pose immediate risk, when unmonitored, could prove fatal on a long run. aPTT test is often neglected and very rarely utilised in biocompatibility studies. With the aim of developing an efficient delivery system which is also biocompatible, aPTT test was performed in this work to determine the effect of the complexes on coagulation.

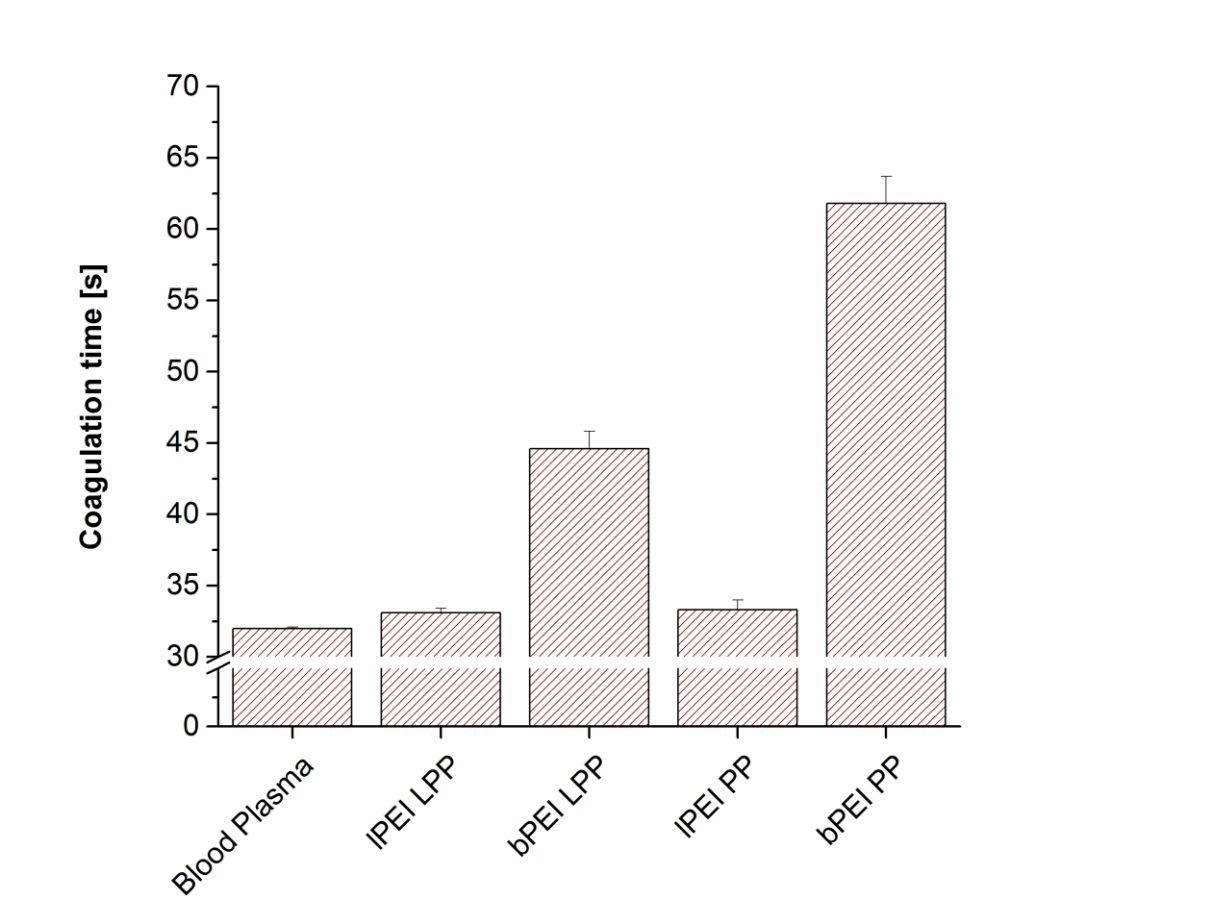

Figure 30: Activated partial thromboplastin time test of the complexes. Coagulation times between 30 and 40 s are considered normal, with above 45 s suggesting considerable interference with coagulation

Fresh blood plasma was used to determine the aPTT values. aPTT time of blood plasma was measured to be 32 ± 0.1 s and was found to be in the normal range [177]. Values between 30 - 40 s are considered acceptable and values above 70 s signifies spontaneous bleeding [137]. The aPTT time for bPEI polyplexes was higher than all the other complexes (Figure 30). This confirms the results obtained from toxicity and haemolysis tests, showing branched PEI polyplexes to be sparingly biocompatible. Both lPEI polyplexes and lipopolyplexes did not interfere with the coagulation time. Similar to the haemolysis assay, use of liposomes to encapsulate the polyplexes, reduced the aPTT time. This effect, however, was pronounced in case of bPEI polyplexes. It is worthwhile to mention that the lipopolyplexes, performed well in both toxicity and haemocompatibility tests, thereby proving its biocompatibility.

3.10 *In vivo* chick chorioallantoic membrane

In most cases, testing of delivery vehicles on animal models is quite inappropriate considering the ethical issues. Studies often directly use an animal models without performing specific *in vitro* and *ex vivo* tests, which give a picture of the biocompatibility of the delivery vehicles. *In vitro* efficiency and toxicity, in many cases in not reproducible with *in vivo* conditions. Therefore, a need for an alternative, which help reduce the animal tests is of utmost importance. The chick chorioallantoic membrane model offers an excellent ethical and cost effective alternative predictive platform. Several studies have used the CAM model for studying biomaterials, angiogenesis, tumour growth and tissue engineering [127, 129, 178, 179]. In this work, CAM model has been utilised to determine the efficacy and toxicity of the lipopolyplexes *in vivo*.

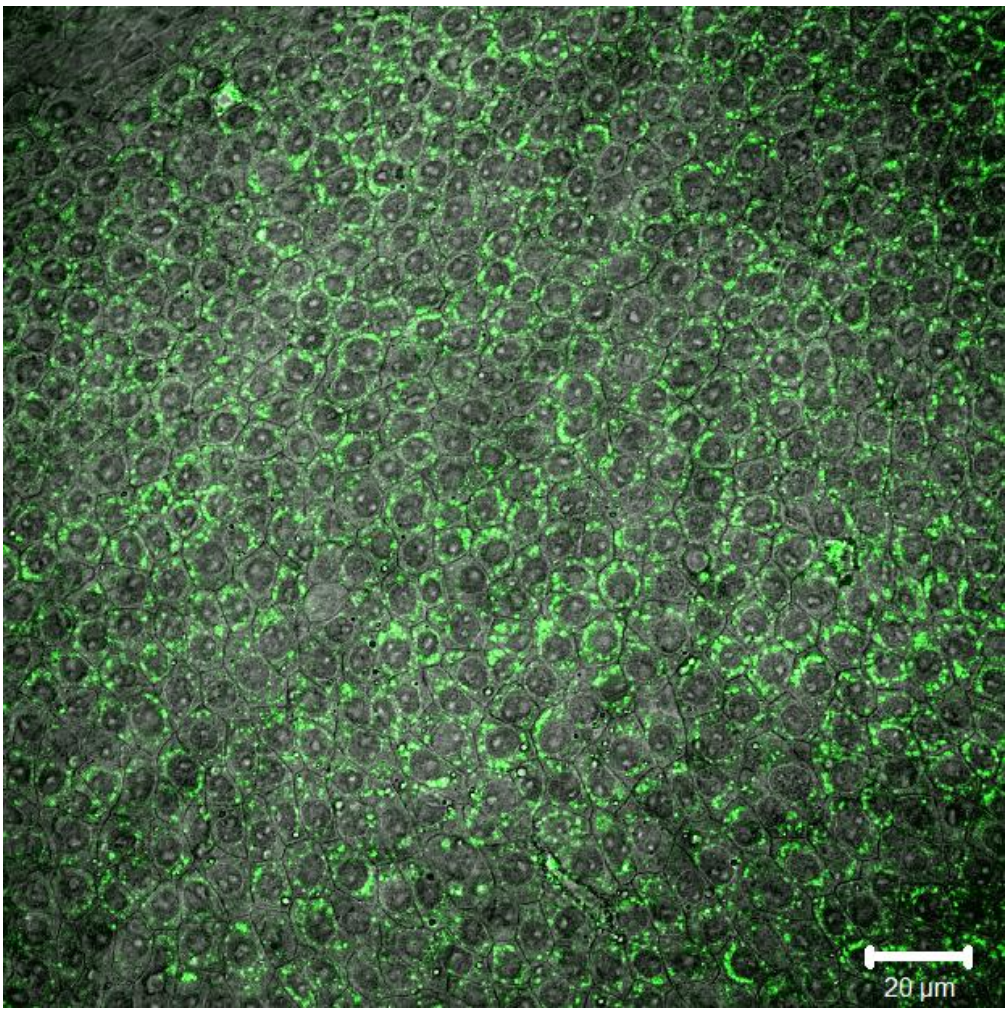

Figure 31: CLSM micrograph showing GFP expression in a CAM section 48 h post transfection

Transfection of the CAM model was performed by injecting 100 µL of lPEI lipopolyplexes (N/P 9.5) containing 0.8 µg of pEGFP-N1 on egg development day 11 (EDD 11). On EDD 13 the CAM layer cut out and observed for green fluorescent protein expression under a CLSM (Figure 31). The image shows GFP expression in what appears to be epithelial cells of the CAM. The pronounced expression of GFP is seen in almost each and every cell of the micrograph. Although other layers of CAM also showed GFP expression, due to practical limitations, a clear micrograph of the transfected inner layers of the CAM was not possible.

For the toxicity studies, 6 eggs were injected with LPPs (lPEI; N/P 9.5) containing 2 µg of HT-DNA into the blood vessels on EDD 11, the eggs were observed at regular intervals until the time point of appearance of distinct biological structures. No toxicity, or retardation in the embryogenesis was observed and therefore was a confirmation that the lipopolyplexes had no toxic effects on the development of the egg. Together with the results from the GFP expression, it could be safely concluded that the lipopolyplexes maintained their transfection efficiency *in vivo* at the same time being non-toxic to the eggs.

Part IV: Summary and outlook

4.1 Summary and outlook

Supported with a strong literature background, this thesis elaborately describes the perspectives of an efficient, biocompatible delivery system capable of transfecting both *in vitro* and *in vivo* with minimal toxicity. A detailed study of the lipopolyplexes was performed to evaluate its efficacy and capabilities yielding consistent results.

The introduction part of the thesis deals with aspects such as gene delivery, RNA interference and vectors used for the delivery. Non-viral vectors, especially polymer and liposomal based gene delivery vehicles are reviewed. These formed the basis for the composite nanocarrier system, lipopolyplex used in this study. Advantages and disadvantages of liposomal and polymer based gene delivery systems are reviewed. Composition, structural characteristics and physicochemical properties of lipopolyplexes are discussed. Physical methods for enhancing the gene transfer using lipopolyplexes via photochemical internalisation and ultrasound enhanced gene transfer are described. A therapeutic anti-inflammatory model to evaluate the efficacy of the lipopolyplexes has been described. The necessity of toxicity and haemocompatibility studies for the evaluation of delivery vehicles have been summarised. Chorioallantoic membrane model has been described with the aim to prove the biocompatibility and efficacy of the lipopolyplexes *in vivo*.

In the results part, preparation and formulation of the liposomes, polyplexes and lipopolyplexes has been described in detail. Physicochemical characterisation of the delivery vehicles using dynamic light scattering and laser Doppler velocimetry has revealed a stable, monodisperse formulation within the size range suitable for cellular internalisation. Influence of factors such as liposomal composition, N/P ratio of polyplexes, liposome/PEI mass ratio of lipopolyplexes and storage conditions on size and zeta potential have been described. The results obtained show that the lipopolyplexes are stable even after a month of storage with minimal loss in biological activity.

To give a deeper insight into the structure of the lipopolyplexes, extensive electron microscopic characterisation has been performed. Morphological characteristics were described using atomic force microscopy. The size of the lipopolyplexes obtained by dynamic light scattering has been confirmed using micrographs from electron and atomic force microscopy.

Scanning electron micrographs show a defined spherical morphology of the lipopolyplexes which is a characteristic of their parent liposomes. The micrographs from the transmission electron microscopy using gold coupled PEI elucidate the multicomponent polyplex-in-liposome structure of the lipopolyplexes. Freeze fracture technique has been utilised to obtain replica images showing structural characteristics of the lipopolyplexes. Atomic force micrographs confirmed the shape of the lipopolyplexes.

Transfection studies have been performed to determine the efficiency of the complexes. Compared to the polyplexes, lipopolyplexes, especially those formulated using linear PEI showed a tremendous increase in expression of luciferase gene. The increased gene expression has been confirmed using confocal laser scanning microscopy with green fluorescence protein expression. The effect of photochemical enhancement has been studied using curcumin loaded lipopolyplexes which showed improved transfection efficiencies followed by irradiation using a prototype LED device. Similar effects were observed upon application of ultrasound in ultrasound enhanced gene transfer experiments. The potential of lipopolyplexes to be delivered via different methods depending on the target has been explained using physical enhancement methods. Applicability of such methods for delivering genetic material into difficult to transfect primary cells using lipopolyplexes has been reported.

Toxicity studies describing the membrane damage and time dependent toxicity of the complexes have been discussed in detail. The membrane integrity studies compare the cytotoxic potential of polyplexes and lipopolyplexes. The decreased cytotoxic potential upon addition of liposomes to polyplexes helps understand the shielding effect of liposomes on PEI. Time dependent toxicity studies comparing the cell viability of cells transfected using polyplexes and lipopolyplexes show a substantial improvement in the cell viability upon liposomal encapsulation of polyplexes.

Haemocompatibility studies were performed to determine the biocompatibility and potential of the lipopolyplexes for *in vivo* use. Lipopolyplexes are shown to have a decreased haemolytic potential compared to the polyplexes. Similarly, aPTT studies show that lipopolyplexes, on contrary to polyplexes, especially bPEI polyplexes, do not interfere with coagulation. The haemocompatibility studies revealed the lipopolyplexes to be biocompatible and therefore safe for intravenous administration.

In vivo chick chorioallantoic model (CAM) has been used as an alternative to animal models. The CAM studies showed that the lipopolyplexes were also able to transfect *in vivo* with a considerable transfection efficiency. The GFP expression was visualised by confocal laser scanning microscopy of the CAM section. The *in vivo* toxicity assay, wherein the lipopolyplexes were injected into the blood stream, show no deleterious effect on the development of the embryo and the egg, confirming the safety profile of lipopolyplexes.

The investigations carried out in this work have shown that the combination of lPEI polyplexes with DOPE/DPPC/Cholesterol liposomes is a promising candidate in DNA and siRNA delivery both *in vitro* and *in vivo*. The liposomal shielding effect, which reduces the surface charge of the PEI, has been reported to be the key for the increased efficiency and low toxicity of the lipopolyplexes.

A clear understanding into the mechanisms of action regarding photochemical internalisation and ultrasound enhanced gene transfer is needed to further optimise the methods. This could be achieved using markers for cell death pathways. Use of fluorescence probes for specific cellular organelles together with confocal microscopic investigations would help understand the enhancement mechanisms involved. Further investigation into the beneficial properties of the lipopolyplexes for therapeutic gene delivery could lead to the development of a safe delivery system for clinical purposes.

Together with the reliable results and elaborate characterisation, this thesis work presents a potential composite nanocarrier as a worthy contender for gene therapy.

4.2 Zusammenfassung und Ausblick

Die vorliegende Arbeit beschreibt ausführlich die Perspektiven eines effizienten und biokompatiblen Gentransfersystems, welches sowohl *in vitro* als auch *in vivo* verwendbar ist. Zur Überprüfung der Wirksamkeit und Einsatzfähigkeit der Lipopolyplexe wurden im Vorfeld eingehende physikalisch chemische Charakterisierungen durchgeführt. Einen ausführlichen Überblick über die potentiellen Möglichkeiten des Gentransfers, die RNA-Interferenz und sogenannte Nicht-virale Vektoren werden in der Einleitung gegeben. Einleitend sind zunächst die nicht-virale Vektoren, insbesondere die Polymer- und Liposomale Transfersysteme dargestellt. Diese Transfersysteme bilden die Grundlage für das zusammengesetzte, in dieser Arbeit vorgestellte, Nanoträgersystem „Lipopolyplex“. Anschließend erfolgt eine Diskussion über ihre strukturellen Eigenschaften. Moderne physikalische Methoden (Ultraschall bzw. Photodynamik), welche zur Verbesserung des Gentransfers mit Lipopolyplexen dienen können, werden ebenfalls dargestellt. Bei diesen Methoden handelt es sich insbesondere um die photochemische Internalisierung (PCI, Photodynamik) und der durch Ultraschall verstärkte Gentransfer (UEGT). Darüber hinaus wird ein therapeutisches antiinflammatorisches Modell zur Bewertung der Wirksamkeit von Lipopolyplexen als erster therapeutischer Ansatz dargestellt. Zusätzlich werden die Notwendigkeit der Toxizitäts- und Hämokompatibilitätsstudien für die Evaluierung von Gentransfersysteme beschrieben und zusammengefasst. Ein weiteres Modell, das sogenannte Chorioallantoismembran Modell (CAM) diente der in vivo Charakterisierung, der Biokompatibilität und der Effizienz der Lipopolyplexen.

Die Herstellung und Formulierung von Liposomen, Polyplexen und Lipopolyplexen wurde ausführlich in Part II (2.2 Experiments) beschrieben. Mit Hilfe der dynamischen Lichtstreuung und des Laser-Doppler-Velocimetrie konnte die physikalisch-chemische Charakterisierung der Gentransfersysteme bestimmt werden. Die daraus resultierenden Ergebnisse ergaben eine stabile, monodisperse Formulierung (hydrodynamischer Durchmesser 201.1 ± 5.9; PDI 0.19) innerhalb der für die zelluläre Internalisierung geeigneten Größenbereiche (≤ 200 nm). Der Einfluss von Faktoren wie Lipidzusammensetzung, N/P-Verhältnis von Polyplexen, Liposom/PEI-Massenverhältnisse von Lipopolyplexen und deren Lagerbedingungen auf die Größe und das Zeta-Potential wurden ausführlich untersucht. Dabei wurde festgestellt, dass die N/P-Verhältnis einen großen Einfluss auf Zeta Potential hatte. Die Ergebnisse zeigen, dass die

Lipopolyplexe auch nach einem Monat Lagerung stabil sind und einen minimalen Verlust an ihrer biologischen Aktivität haben.

Um einen tieferen Einblick in die Struktur der Lipopolyplexe zu gewinnen, wurde eine umfangreiche elektronenmikroskopische Charakterisierung in Kombination mit der Rasterkraftmikroskopie durchgeführt. Die bestimmten Größen der unterschiedlichen Lipopolyplexe waren innerhalb der Methoden vergleichbar. Die rasterelektronenmikroskopischen Aufnahmen zeigten eine definierte kugelförmige Morphologie, die üblicherweise für die Ausgangs-Liposomen charakteristisch ist. Die mikroskopischen Aufnahmen der Transmissionselektronenmikroskopie wurden unter der Verwendung von goldgekoppeltem PEI durchgeführt um eine Differenzierung zwischen dem Polymer und dem Lipid vornehmen zu können. Die entstandenen Bilder verdeutlichen die Mehrschichten Struktur „Polyplex-in-Liposome“ der Lipopolyplexe. Die strukturellen Oberflächeneigenschaften (mit Replika Technik) konnten mittels der Gefrierbruch Elektronenmikroskopie visualisiert werden. Die rasterkraftmikroskopischen Aufnahmen bestätigen die Form der Lipopolyplexe.

Um die Effizienz der Komplexe (Polyplexe und Lipopolyplexe) nachzuweisen, wurden weitere Transfektionsstudien durchgeführt. Im Vergleich zu den Polyplexen wiesen die Lipopolyplexe, insbesondere die, welche mit linearem PEI hergestellt wurden, eine enorme Zunahme der Expression des Luciferasegens auf. Die erhöhte Genexpression konnte mittels konfokalem Laser-Scanning-Mikroskops durch den Einsatz von Grün fluoreszierenden Proteinexpression bestätigt werden.

Die Wirkung der photochemischen Verstärkung (Photochemical Internalisation) wurde unter Verwendung von Curcumin beladenen Lipopolyplexen untersucht. Die Ergebnisse zeigten nach der Bestrahlung mit einer Prototyp-LED-Leuchte eine verbesserte Transfektionseffizienz. Ähnliche Effekte konnten bei der Anwendung von Ultraschall (Ultrasound enhanced gene transfer) erzeugt werden. Die Anwendbarkeit von Verfahren, die zur Bereitstellung von genetischem Material in schwierig transfizierbaren Primärzellen dienen, konnten unter der Verwendung von Lipopolyplexen bestätigt werden.

Membranschäden und die zeitabhängige Zytotoxizität von Komplexen wurde anhand verschiedenster Toxizitätsstudien festgestellt. Die Membranintegritätsstudien vergleichen das zytotoxische Potential von Polyplexen und Lipopolyplexen. Darüber hinaus konnte bewiesen werden, dass durch die Zugabe von Liposomen der zytotoxische Effekt von Polyplexen signifikant abnimmt. Die Ursache liegt in der Abschirmung der Ladungsdichte von PEI. Weitere zeitabhängige Toxizitätsstudien vergleichen die bereits mit Polyplexen und Lipopolyplexen transfizierten Zellen miteinander. Diese Ergebnisse zeigten eine deutliche Erhöhung der Zellviabilität durch die liposomale Verkapselung von Polyplexen.

Hämokompatibilitätsstudien verdeutlichten die Biokompatibilität und das Potential der Lipopolyplexe für *in vivo* Verwendungen. Im Vergleich zu Polyplexen haben Lipopolyplexe ein deutlich vermindertes hämolytisches Potential. Ähnliche Ergebnisse zeigten die aPTT-Studien. Lipopolyplexe beeinflussen im Gegensatz zu den Polyplexen (insbesondere bPEI-Polyplexe), nicht die Koagulation des Blutes. Die Hämokompatibilitätsstudien zeigten, dass die Lipopolyplexe biokompatibel und daher für eine intravenöse Verabreichung gut geeignet sind.

Das *in vivo* Chorioallantoismembran Modell wurde als Alternative zu Tiermodellen verwendet. Die CAM Studien zeigten, dass sich Lipopolyplexe auch in vivo transfizieren lassen. Diese wurden durch die GFP Expression in den CAM-Aufnahmen bestätigt. Die *in vivo* Toxizitätsstudien im CAM Modell mit Lipopolyplexen zeigten keinerlei schädliche Wirkung auf die Entwicklung des Embryos und des Eies und bestätigen damit das Sicherheitsprofil von Lipopolyplexen.

Zusammenfassend kann eingeschätzt werden, dass die hier erstellte Kombination von lPEI-Polyplexen und DOPE/ DPPC/Cholesterol-Liposomen ein vielversprechender Kandidat für die DNA- und siRNA-Transfer in einer modernen Gentherapie ist. Die Abschirmwirkung der Liposomen reduziert die Oberflächenladung des PEIs. Dieses Phänomen spielt hierbei eine große Rolle für die erhöhte Effizienz und geringe Toxizität der Lipopolyplexe.

Ein besseres Verständnis der Wirkungsmechanismen, hinsichtlich der photochemischen Internalisierung und des ultraschallverstärkten Gentransfers sind jedoch erforderlich, um die Methoden weiter zu optimieren. Eine Möglichkeit wäre den Weg des Zelltodes mittels spezieller Markern zu ermitteln. Die Verwendung von Fluoreszenzproben für spezifische

zelluläre Organellen, unterstützt mit konfokalen mikroskopischen Untersuchungen bietet eine gute und solide Methode die beteiligten Mechanismen zu verstehen. Weitere Untersuchungen der positiven Eigenschaften der Lipopolyplexe könnten zur Entwicklung eines sicheren Abgabesystems für die klinische Anwendung des therapeutischen Gentransfers führen.

Zusammen mit den hier zuverlässig erzeugten Ergebnissen und der umfangreichen Charakterisierung stellt diese Dissertation ein potentielles Composite-Nanocarrier-System für die Gentherapie dar.

Part V: Appendix

5.1 References

[1] M. Collins, A. Thrasher, Gene therapy: progress and predictions, Proc Biol Sci, 282 (2015).

[2] E. Bender, Gene therapy: Industrial strength, Nature, 537 (2016).

[3] D.M. Dykxhoorn, D. Palliser, J. Lieberman, The silent treatment: siRNAs as small molecule drugs, Gene Ther, 13 (2006) 541-552.

[4] G.D. Ferrari S, Alton EW., Barriers to and new approaches for gene therapy and gene delivery in cystic fibrosis, 54 (2002) 1373–1393.

[5] F.D. Ledley, Pharmaceutical approach to somatic gene therapy, Pharm Res, 13 (1996) 1595-1614.

[6] R.C. Mulligan, The basic science of gene therapy, Science, 260 (1993) 926-932.

[7] I.M. Verma, Gene therapy: hopes, hypes, and hurdles, Mol Med, 1 (1994) 2-3.

[8] I.M. Verma, N. Somia, Gene therapy -- promises, problems and prospects, Nature, 389 (1997) 239-242.

[9] N. Somia, I.M. Verma, Gene therapy: trials and tribulations, Nature Reviews Genetics, 1 (2000) 91-99.

[10] M.S. Fox, J.W. Littlefield, Reservations Concerning Gene Therapy, Science, (1971).

[11] A. Fire, S. Xu, M.K. Montgomery, S.A. Kostas, S.E. Driver, C.C. Mello, Potent and specific genetic interference by double-stranded RNA in Caenorhabditis elegans, Nature, 391 (1998) 806-811.

[12] S.M. Hammond, E. Bernstein, D. Beach, G.J. Hannon, An RNA-directed nuclease mediates post-transcriptional gene silencingin Drosophila cells, Nature, 404 (2000) 293-296.

[13] M. Tijsterman, R.H. Plasterk, Dicers at RISC; the mechanism of RNAi, Cell, 117 (2004) 1-3.

[14] D.-H. Kim, M.A. Behlke, S.D. Rose, M.-S. Chang, S. Choi, J.J. Rossi, Synthetic dsRNA Dicer substrates enhance RNAi potency and efficacy, Nature Biotechnology, 23 (2004) 222-226.

[15] M. Amarzguioui, J.J. Rossi, Principles of Dicer substrate (D-siRNA) design and function, Methods Mol Biol, 442 (2008) 3-10.

[16] A. Aigner, Delivery Systems for the Direct Application of siRNAs to Induce RNA Interference (RNAi) In Vivo, J Biomed Biotechnol, 2006 (2006).

[17] I. Slivac, D. Guay, M. Mangion, J. Champeil, B. Gaillet, Non-viral nucleic acid delivery methods, Expert Opin Biol Ther, 17 (2017) 105-118.

[18] A. Ewe, O. Panchal, S.R. Pinnapireddy, U. Bakowsky, S. Przybylski, A. Temme, A. Aigner, Liposome-polyethylenimine complexes (DPPC-PEI lipopolyplexes) for therapeutic siRNA delivery in vivo, Nanomedicine, (2016).

[19] C. Janich, S.R. Pinnapireddy, F. Erdmann, T. Groth, A. Langner, U. Bakowsky, C. Wolk, Fast therapeutic DNA internalization - A high potential transfection system based on a peptide mimicking cationic lipid, Eur J Pharm Biopharm, (2016).

[20] M.N.V.R. Kumar, U. Bakowsky, C.M. Lehr, Nanoparticles as Non-Viral Transfection Agents, in: Nanobiotechnology, Wiley-VCH Verlag GmbH & Co. KGaA, 2005, pp. 319-342.

[21] I.S. Zuhorn, V. Oberle, W.H. Visser, J. Engberts, U. Bakowsky, E. Polushkin, D. Hoekstra, Phase behavior of cationic amphiphiles and their mixtures with helper lipid influences lipoplex shape, DNA translocation, and transfection efficiency, Biophys J, 83 (2002) 2096-2108.

[22] I.S. Zuhorn, U. Bakowsky, E. Polushkin, W.H. Visser, M.C.A. Stuart, J.B.F.N. Engberts, D. Hoekstra, Nonbilayer phase of lipoplex–membrane mixture determines endosomal escape of genetic cargo and transfection efficiency, Molecular Therapy, 11 (2005) 801-810.

[23] M. Morille, C. Passirani, A. Vonarbourg, A. Clavreul, J.P. Benoit, Progress in developing cationic vectors for non-viral systemic gene therapy against cancer, Biomaterials, 29 (2008) 3477-3496.

[24] K. Tabatt, C. Kneuer, M. Sameti, C. Olbrich, R.H. Muller, C.M. Lehr, U. Bakowsky, Transfection with different colloidal systems: comparison of solid lipid nanoparticles and liposomes, J Control Release, 97 (2004) 321-332.

[25] H. Yin, R.L. Kanasty, A.A. Eltoukhy, A.J. Vegas, J.R. Dorkin, D.G. Anderson, Non-viral vectors for gene-based therapy, Nature Reviews Genetics, 15 (2014) 541-555.

[26] C. Kneuer, C. Ehrhardt, H. Bakowsky, M.N. Kumar, V. Oberle, C.M. Lehr, D. Hoekstra, U. Bakowsky, The influence of physicochemical parameters on the efficacy of non-viral DNA transfection complexes: a comparative study, J Nanosci Nanotechnol, 6 (2006) 2776-2782.

[27] D.D. Lasic, Liposomes : from physics to applications, Elsevier, Amsterdam; New York, 1993.

[28] F. Szoka, Jr., D. Papahadjopoulos, Comparative properties and methods of preparation of lipid vesicles (liposomes), Annu Rev Biophys Bioeng, 9 (1980) 467-508.

[29] M.I. Angelova, Liposome Electroformation, in: Perspectives in Supramolecular Chemistry, John Wiley & Sons, Ltd., 1999, pp. 26-36.

[30] I. Levacheva, O. Samsonova, E. Tazina, M. Beck-Broichsitter, S. Levachev, B. Strehlow, M. Baryshnikova, N. Oborotova, A. Baryshnikov, U. Bakowsky, Optimized thermosensitive liposomes for selective doxorubicin delivery: formulation development, quality analysis and bioactivity proof, Colloids Surf B Biointerfaces, 121 (2014) 248-256.

[31] J. Schäfer, Liposome, in: Corel Draw, 2010.

[32] D.D. Lasic, F.J. Martin, Stealth Liposomes, CRC Press, 1995.

[33] P.R. Cullis, A. Chonn, S.C. Semple, Interactions of liposomes and lipid-based carrier systems with blood proteins: Relation to clearance behaviour in vivo, Adv Drug Deliv Rev, 32 (1998) 3-17.

[34] K. Hoekstra, J. van Renswoude, R. Tomasini, G. Scherphof, Interaction of phospholipid vesicles with rat hepatocytes: further characterization of vesicle-cell surface interaction; use of serum as a physiological modulator, Membr Biochem, 4 (1981) 129-147.

[35] G. Scherphof, F. Roerdink, M. Waite, J. Parks, Disintegration of phosphatidylcholine liposomes in plasma as a result of interaction with high-density lipoproteins, Biochim Biophys Acta, 542 (1978) 296-307.

[36] J. Wilschut, D. Hoekstra, Membrane fusion: lipid vesicles as a model system, Chem Phys Lipids, 40 (1986) 145-166.

[37] P.L. Felgner, T.R. Gadek, M. Holm, R. Roman, H.W. Chan, M. Wenz, J.P. Northrop, G.M. Ringold, M. Danielsen, Lipofection: a highly efficient, lipid-mediated DNA-transfection procedure, Proc Natl Acad Sci U S A, 84 (1987) 7413-7417.

[38] J.T. Dingle, P.J. Jacques, I.H. Shaw, Lysosomes in applied biology and therapeutics, in: C. Toothill (Ed.) Lysosomes in biology and pathology, Headington Hill Hall, 1981, pp. 74-74.

[39] I.M. Hafez, P.R. Cullis, Roles of lipid polymorphism in intracellular delivery, Adv Drug Deliv Rev, 47 (2001) 139-148.

[40] F. Aqil, R. Munagala, J. Jeyabalan, M.V. Vadhanam, Bioavailability of phytochemicals and its enhancement by drug delivery systems, Cancer Lett, 334 (2013) 133-141.

[41] S.S. Bansal, M. Goel, F. Aqil, M.V. Vadhanam, R.C. Gupta, Advanced Drug Delivery Systems of Curcumin for Cancer Chemoprevention, (2011).

[42] V. Oberle, U. Bakowsky, I.S. Zuhorn, D. Hoekstra, Lipoplex formation under equilibrium conditions reveals a three-step mechanism, Biophys J, 79 (2000) 1447-1454.

[43] L. Wasungu, D. Hoekstra, Cationic lipids, lipoplexes and intracellular delivery of genes, J Control Release, 116 (2006) 255-264.

[44] I.S. Zuhorn, J.B.F.N. Engberts, D. Hoekstra, Gene delivery by cationic lipid vectors: overcoming cellular barriers, European Biophysics Journal, 36 (2007) 349-362.

[45] J. Marshall, N.S. Yew, S.J. Eastman, C. Jiang, R.K. Scheule, S.H. Cheng, Cationic Lipid-Mediated Gene Delivery to the Airways, 1 ed., Elsevier, 1999.

[46] C.R. Dass, P.F. Choong, Targeting of small molecule anticancer drugs to the tumour and its vasculature using cationic liposomes: lessons from gene therapy, in: Cancer Cell Int, 2006, pp. 17.

[47] H. Lv, S. Zhang, B. Wang, S. Cui, J. Yan, Toxicity of cationic lipids and cationic polymers in gene delivery, J Control Release, 114 (2006) 100-109.

[48] S. Khiati, N. Pierre, S. Andriamanarivo, M.W. Grinstaff, N. Arazam, F. Nallet, L. Navailles, P. Barthelemy, Anionic nucleotide--lipids for in vitro DNA transfection, Bioconjug Chem, 20 (2009) 1765-1772.

[49] S.D. Patil, D.G. Rhodes, D.J. Burgess, Anionic liposomal delivery system for DNA transfection, in: AAPS J, 2004, pp. 13-22.

[50] J. Smisterova, A. Wagenaar, M.C. Stuart, E. Polushkin, G. ten Brinke, R. Hulst, J.B. Engberts, D. Hoekstra, Molecular shape of the cationic lipid controls the structure of cationic lipid/dioleylphosphatidylethanolamine-DNA complexes and the efficiency of gene delivery, J Biol Chem, 276 (2001) 47615-47622.

[51] H. Farhood, N. Serbina, L. Huang, The role of dioleoyl phosphatidylethanolamine in cationic liposome mediated gene transfer, Biochim Biophys Acta, 1235 (1995) 289-295.

[52] M.C. Garnett, Gene-delivery systems using cationic polymers, Crit Rev Ther Drug Carrier Syst, 16 (1999) 147-207.

[53] D.Y. Kwoh, C.C. Coffin, C.P. Lollo, J. Jovenal, M.G. Banaszczyk, P. Mullen, A. Phillips, A. Amini, J. Fabrycki, R.M. Bartholomew, S.W. Brostoff, D.J. Carlo, Stabilization of poly-L-lysine/DNA polyplexes for in vivo gene delivery to the liver, Biochim Biophys Acta, 1444 (1999) 171-190.

[54] U.K. Laemmli, Characterization of DNA condensates induced by poly(ethylene oxide) and polylysine, Proc Natl Acad Sci U S A, 72 (1975) 4288-4292.

[55] T.G. Park, J.H. Jeong, S.W. Kim, Current status of polymeric gene delivery systems, Adv Drug Deliv Rev, 58 (2006) 467-486.

[56] O. Boussif, F. Lezoualc'h, M.A. Zanta, M.D. Mergny, D. Scherman, B. Demeneix, J.P. Behr, A versatile vector for gene and oligonucleotide transfer into cells in culture and in vivo: polyethylenimine, Proc Natl Acad Sci U S A, 92 (1995) 7297-7301.

[57] R.V. Benjaminsen, M.A. Mattebjerg, J.R. Henriksen, S.M. Moghimi, T.L. Andresen, The possible "proton sponge " effect of polyethylenimine (PEI) does not include change in lysosomal pH, Mol Ther, 21 (2013) 149-157.

[58] J.-P. Behr, The Proton Sponge: a Trick to Enter Cells the Viruses Did Not Exploit, (1997).

[59] A. Akinc, M. Thomas, A.M. Klibanov, R. Langer, Exploring polyethylenimine-mediated DNA transfection and the proton sponge hypothesis, J Gene Med, 7 (2005) 657-663.

[60] M. Neu, D. Fischer, T. Kissel, Recent advances in rational gene transfer vector design based on poly(ethylene imine) and its derivatives, J Gene Med, 7 (2005) 992-1009.

[61] S. Werth, B. Urban-Klein, L. Dai, S. Hobel, M. Grzelinski, U. Bakowsky, F. Czubayko, A. Aigner, A low molecular weight fraction of polyethylenimine (PEI) displays increased transfection efficiency of DNA and siRNA in fresh or lyophilized complexes, J Control Release, 112 (2006) 257-270.

[62] M. Grzelinski, B. Urban-Klein, T. Martens, K. Lamszus, U. Bakowsky, S. Hobel, F. Czubayko, A. Aigner, RNA interference-mediated gene silencing of pleiotrophin through polyethylenimine-complexed small interfering RNAs in vivo exerts antitumoral effects in glioblastoma xenografts, Hum Gene Ther, 17 (2006) 751-766.

[63] L.A. Dailey, E. Kleemann, T. Merdan, H. Petersen, T. Schmehl, T. Gessler, J. Hanze, W. Seeger, T. Kissel, Modified polyethylenimines as non viral gene delivery systems for aerosol therapy: effects of nebulization on cellular uptake and transfection efficiency, J Control Release, 100 (2004) 425-436.

[64] C. Brus, H. Petersen, A. Aigner, F. Czubayko, T. Kissel, Physicochemical and biological characterization of polyethylenimine-graft-poly(ethylene glycol) block copolymers as a delivery system for oligonucleotides and ribozymes, Bioconjug Chem, 15 (2004) 677-684.

[65] A. Aigner, D. Fischer, T. Merdan, C. Brus, T. Kissel, F. Czubayko, Delivery of unmodified bioactive ribozymes by an RNA-stabilizing polyethylenimine (LMW-PEI) efficiently down-regulates gene expression, Gene Ther, 9 (2002) 1700-1707.

[66] C. Brus, H. Petersen, A. Aigner, F. Czubayko, T. Kissel, Efficiency of polyethylenimines and polyethylenimine-graft-poly (ethylene glycol) block copolymers to protect oligonucleotides against enzymatic degradation, Eur J Pharm Biopharm, 57 (2004) 427-430.

[67] D. Fischer, T. Bieber, Y. Li, H.P. Elsasser, T. Kissel, A novel non-viral vector for DNA delivery based on low molecular weight, branched polyethylenimine: effect of molecular weight on transfection efficiency and cytotoxicity, Pharm Res, 16 (1999) 1273-1279.

[68] T. Merdan, K. Kunath, H. Petersen, U. Bakowsky, K.H. Voigt, J. Kopecek, T. Kissel, PEGylation of poly(ethylene imine) affects stability of complexes with plasmid DNA under in vivo conditions in a dose-dependent manner after intravenous injection into mice, Bioconjug Chem, 16 (2005) 785-792.

[69] T. Endres, M. Zheng, A. Kılıç, A. Turowska, M. Beck-Broichsitter, H. Renz, O.M. Merkel, T. Kissel, Amphiphilic Biodegradable PEG-PCL-PEI Triblock Copolymers for FRET-Capable in Vitro and in Vivo Delivery of siRNA and Quantum Dots, (2014).

[70] T. Merdan, J. Callahan, H. Petersen, K. Kunath, U. Bakowsky, P. Kopeckova, T. Kissel, J. Kopecek, Pegylated polyethylenimine-Fab' antibody fragment conjugates for targeted gene delivery to human ovarian carcinoma cells, Bioconjug Chem, 14 (2003) 989-996.

[71] O.M. Merkel, M.A. Mintzer, J. Sitterberg, U. Bakowsky, E.E. Simanek, T. Kissel, Triazine dendrimers as non-viral gene delivery systems: Effects of molecular structure on biological activity, Bioconjug Chem, 20 (2009) 1799-1806.

[72] O. Samsonova, C. Pfeiffer, M. Hellmund, O.M. Merkel, T. Kissel, Low Molecular Weight pDMAEMA-block-pHEMA Block-Copolymers Synthesized via RAFT-Polymerization: Potential Non-Viral Gene Delivery Agents?, Polymers, 3 (2011) 693-718.

[73] G. Borchard, Chitosans for gene delivery, Adv Drug Deliv Rev, 52 (2001) 145-150.

[74] J. Haas, M.N. Ravi Kumar, G. Borchard, U. Bakowsky, C.M. Lehr, Preparation and characterization of chitosan and trimethyl-chitosan-modified poly-(epsilon-caprolactone) nanoparticles as DNA carriers, AAPS PharmSciTech, 6 (2005) E22-30.

[75] J. Schäfer, S. Hobel, U. Bakowsky, A. Aigner, Liposome-polyethylenimine complexes for enhanced DNA and siRNA delivery, Biomaterials, 31 (2010) 6892-6900.

[76] C. Peetla, A. Stine, V. Labhasetwar, Biophysical interactions with model lipid membranes: applications in drug discovery and drug delivery, Mol Pharm, 6 (2009) 1264-1276.

[77] M. Thomas, J.J. Lu, Q. Ge, C. Zhang, J. Chen, A.M. Klibanov, Full deacylation of polyethylenimine dramatically boosts its gene delivery efficiency and specificity to mouse lung, Proc Natl Acad Sci U S A, 102 (2005) 5679-5684.

[78] S.M. Moghimi, P. Symonds, J.C. Murray, A.C. Hunter, G. Debska, A. Szewczyk, A two-stage poly(ethylenimine)-mediated cytotoxicity: implications for gene transfer/therapy, Mol Ther, 11 (2005) 990-995.

[79] K. Regnström, E.G.E. Ragnarsson, M. Köping-Höggård, E. Torstensson, H. Nyblom, P. Artursson, PEI - a potent, but not harmless, mucosal immuno-stimulator of mixed T-helper cell response and FasL-mediated cell death in mice, Gene Therapy, 10 (2003) 1575-1583.

[80] M. Breunig, U. Lungwitz, R. Liebl, A. Goepferich, Breaking up the correlation between efficacy and toxicity for nonviral gene delivery, Proc Natl Acad Sci U S A, 104 (2007) 14454-14459.

[81] E. Blanco, H. Shen, M. Ferrari, Principles of nanoparticle design for overcoming biological barriers to drug delivery, Nature Biotechnology, 33 (2015) 941-951.

[82] A.P. Dabkowska, D.J. Barlow, A.V. Hughes, R.A. Campbell, P.J. Quinn, M.J. Lawrence, The effect of neutral helper lipids on the structure of cationic lipid monolayers, J R Soc Interface, 9 (2012) 548-561.

[83] J. Zabner, A.J. Fasbender, T. Moninger, K.A. Poellinger, M.J. Welsh, Cellular and molecular barriers to gene transfer by a cationic lipid, J Biol Chem, 270 (1995) 18997-19007.

[84] D.E.J.G.J. Dolmans, D. Fukumura, R.K. Jain, Photodynamic therapy for cancer, Nature Reviews Cancer, 3 (2003) 380-387.

[85] T.J. Dougherty, C.J. Gomer, B.W. Henderson, G. Jori, D. Kessel, M. Korbelik, J. Moan, Q. Peng, Photodynamic therapy, J Natl Cancer Inst, 90 (1998) 889-905.

[86] F. Stewart, P. Baas, W. Star, What does photodynamic therapy have to offer radiation oncologists (or their cancer patients)?, Radiother Oncol, 48 (1998) 233-248.

[87] P.J. Lou, H.R. Jager, L. Jones, T. Theodossy, S.G. Bown, C. Hopper, Interstitial photodynamic therapy as salvage treatment for recurrent head and neck cancer, Br J Cancer, 91 (2004) 441-446.

[88] C. Pais-Silva, D. de Melo-Diogo, I.J. Correia, IR780-loaded TPGS-TOS micelles for breast cancer photodynamic therapy, European Journal of Pharmaceutics and Biopharmaceutics, 113 (2017) 108-117.

[89] M.A. Biel, Photodynamic therapy of head and neck cancers, Methods Mol Biol, 635 (2010) 281-293.

[90] P.K. Selbo, A. Hogset, L. Prasmickaite, K. Berg, Photochemical internalisation: a novel drug delivery system, Tumour Biol, 23 (2002) 103-112.

[91] K. Berg, M. Folini, L. Prasmickaite, P.K. Selbo, A. Bonsted, B.O. Engesaeter, N. Zaffaroni, A. Weyergang, A. Dietze, G.M. Maelandsmo, E. Wagner, O.J. Norum, A. Hogset, Photochemical internalization: a new tool for drug delivery, Curr Pharm Biotechnol, 8 (2007) 362-372.

[92] K. Berg, A. Weyergang, L. Prasmickaite, A. Bonsted, A. Hogset, M.T. Strand, E. Wagner, P.K. Selbo, Photochemical internalization (PCI): a technology for drug delivery, Methods Mol Biol, 635 (2010) 133-145.

[93] T. Ohtsuki, S. Miki, S. Kobayashi, T. Haraguchi, E. Nakata, K. Hirakawa, K. Sumita, K. Watanabe, S. Okazaki, The molecular mechanism of photochemical internalization of cell penetrating peptide-cargo-photosensitizer conjugates, Scientific Reports, Published online: 21 December 2015; | doi:10.1038/srep18577, (2015).

[94] M.J. Shieh, C.L. Peng, P.J. Lou, C.H. Chiu, T.Y. Tsai, C.Y. Hsu, C.Y. Yeh, P.S. Lai, Non-toxic phototriggered gene transfection by PAMAM-porphyrin conjugates, J Control Release, 129 (2008) 200-206.

[95] A. Puri, Phototriggerable Liposomes: Current Research and Future Perspectives, Pharmaceutics, 6 (2014) 1-25.

[96] P. Shum, J.M. Kim, D.H. Thompson, Phototriggering of liposomal drug delivery systems, Adv Drug Deliv Rev, 53 (2001) 273-284.

[97] M. Folini, K. Berg, E. Millo, R. Villa, L. Prasmickaite, M.G. Daidone, U. Benatti, N. Zaffaroni, Photochemical internalization of a peptide nucleic acid targeting the catalytic subunit of human telomerase, Cancer Res, 63 (2003) 3490-3494.

[98] A. Ndoye, J.L. Merlin, A. Leroux, G. Dolivet, P. Erbacher, J.P. Behr, K. Berg, F. Guillemin, Enhanced gene transfer and cell death following p53 gene transfer using photochemical internalisation of glucosylated PEI-DNA complexes, J Gene Med, 6 (2004) 884-894.

[99] I. Donald, J. Macvicar, T.G. Brown, Investigation Of Abdominal Masses By Pulsed Ultrasound, The Lancet, 271 (1958) 1188-1195.

[100] D.E. FitzGerald, J.E. Drumm, Non-invasive measurement of human fetal circulation using ultrasound: a new method., (1977).

[101] P. Freeman, The role of ultrasound in the assessment of the trauma patient, Aust J Rural Health, 7 (1999) 85-89.

[102] W.G. Pitt, G.A. Husseini, B.J. Staples, Ultrasonic Drug Delivery – A General Review, Expert Opin Drug Deliv, 1 (2004) 37-56.

[103] C. Olbrich, P. Hauff, F. Scholle, W. Schmidt, U. Bakowsky, A. Briel, M. Schirner, The in vitro stability of air-filled polybutylcyanoacrylate microparticles, Biomaterials, 27 (2006) 3549-3559.

[104] J. Brussler, E. Marxer, A. Becker, R. Schubert, J. Schummelfeder, C. Nimsky, U. Bakowsky, Correlation of structure and echogenicity of nanoscaled ultrasound contrast agents in vitro, Colloids Surf B Biointerfaces, 117 (2014) 206-215.

[105] S. Mitragotri, Healing sound: the use of ultrasound in drug delivery and other therapeutic applications, Nature Reviews Drug Discovery, 4 (2005) 255-260.

[106] M. Joersbo, J. Brunstedt, Sonication: A new method for gene transfer to plants, Physiologia Plantarum, 85 (1992) 230-234.

[107] J. Sundaram, B.R. Mellein, S. Mitragotri, An Experimental and Theoretical Analysis of Ultrasound-Induced Permeabilization of Cell Membranes, in: Biophys J, 2003, pp. 3087-3101.

[108] A. Rahim, S.L. Taylor, N.L. Bush, G.R. ter Haar, J.C. Bamber, C.D. Porter, Physical parameters affecting ultrasound/microbubble-mediated gene delivery efficiency in vitro, Ultrasound Med Biol, 32 (2006) 1269-1279.

[109] N. Nomikou, A.P. McHale, Microbubble-enhanced ultrasound-mediated gene transfer--towards the development of targeted gene therapy for cancer, Int J Hyperthermia, 28 (2012) 300-310.

[110] S. Wirtz, M.F. Neurath, Gene transfer approaches for the treatment of inflammatory bowel disease, Gene Therapy, 10 (2003) 854-860.

[111] S.W. Tas, M.J. Vervoordeldonk, P.P. Tak, Gene Therapy Targeting Nuclear Factor-κB: Towards Clinical Application in Inflammatory Diseases and Cancer, Curr Gene Ther, 9 (2009) 160-170.

[112] T. Collins, A. Williams, G.I. Johnston, J. Kim, R. Eddy, T. Shows, M.A. Gimbrone, Jr., M.P. Bevilacqua, Structure and chromosomal location of the gene for endothelial-leukocyte adhesion molecule 1, J Biol Chem, 266 (1991) 2466-2473.

[113] V. Kumar, R.S. Cotran, T. Collins, S.L. Robbins, Robbins Pathological Basis of Disease., 7th ed., WB Saunders, Philadelphia, PA, 1999.

[114] G.L. Nicolson, Cancer metastasis: tumor cell and host organ properties important in metastasis to specific secondary sites, Biochim Biophys Acta, 948 (1988) 175-224.

[115] K. K.J., V. T.K., Isotherms of Dipalmitoylphosphatidylcholine (DPPC) Monolayers: Features Revealed and Features Obscured - ScienceDirect, Journal of Colloid and Interface Science, (1996).

[116] B.d. Kruijff, P.R. Cullis, A.J. Verkleij, Non-bilayer lipid structures in model and biological membranes, Trends in Biochemical Sciences, 5 (1980) 79-81.

[117] I. Wrobel, D. Collins, Fusion of cationic liposomes with mammalian cells occurs after endocytosis, Biochim Biophys Acta, 1235 (1995) 296-304.

[118] G. Bastiat, M. Lafleur, Phase Behavior of Palmitic Acid/Cholesterol/Cholesterol Sulfate Mixtures and Properties of the Derived Liposomes, The Journal of Physical Chemistry B, (2007).

[119] K. Crook, B.J. Stevenson, M. Dubouchet, D.J. Porteous, Inclusion of cholesterol in DOTAP transfection complexes increases the delivery of DNA to cells in vitro in the presence of serum, Gene Ther, 5 (1998) 137-143.

[120] D.S. Zhuk, P.A. Gembitskii, V.A. Kargin, Advances in the chemistry of Polyethyleneimine (Polyaziridine), Russian Chemical Reviews, 34 (1965) 515-527.

[121] I.M. Klotz, G.P. Royer, I.S. Scarpa, Synthetic derivatives of polyethyleneimine with enzyme-like catalytic activity (synzymes), Proc Natl Acad Sci U S A, 68 (1971) 263-264.

[122] S. Fiedler, R. Wirth, Transformation of bacteria with plasmid DNA by electroporation, Anal Biochem, 170 (1988) 38-44.

[123] C.J. Edgell, C.C. McDonald, J.B. Graham, Permanent cell line expressing human factor VIII-related antigen established by hybridization, Proc Natl Acad Sci U S A, 80 (1983) 3734-3737.

[124] Biological evaluation of medical devices Part 5: Tests for in vitro cytotoxicity, in: IS0 10 993-5, EN 30 993-5, 199, 2009.

[125] British Standard Institution Evaluation of medical devices for biological hazards part 10., in: BS 5736: part 1, 1988.

[126] R. Zange, T. Kissel, Comparative in vitro biocompatibility testing of polycyanoacrylates and poly(d,l-lactide-co-glycolide) using different mouse fibroblast (L929) biocompatibility test models, European Journal of Pharmaceutics and Biopharmaceutics, 44 (1997) 149-157.

[127] C.D. Scher, M.U. Hematology-Oncology Division Children's Hospital Medical Center Boston, M.U. Sidney Farber Cancer Center Department of Pediatrics Harvard Medical School Boston, C. Haudenschild, M. Klagsbrun, The chick chorioallantoic membrane as a model system for the study of tissue invasion by viral transformed cells, Cell, 8 (1976) 373-382.

[128] D. Ribatti, A. Gualandris, M. Bastaki, A. Vacca, M. Iurlaro, L. Roncali, M. Presta, New model for the study of angiogenesis and antiangiogenesis in the chick embryo chorioallantoic membrane: the gelatin sponge/chorioallantoic membrane assay, J Vasc Res, 34 (1997) 455-463.

[129] J. Jedelska, B. Strehlow, U. Bakowsky, A. Aigner, S. Hobel, M. Bette, M. Roessler, N. Franke, A. Teymoortash, J.A. Werner, B. Eivazi, R. Mandic, The chorioallantoic membrane assay is a promising ex vivo model system for the study of vascular anomalies, In Vivo, 27 (2013) 701-705.

[130] W. Guo, R.J. Lee, Receptor-targeted gene delivery viafolate-conjugated polyethylenimine, AAPS PharmSci, 1 (1999) 20-26.

[131] V. Bonasera, S. Alberti, A. Sacchetti, Protocol for high-sensitivity/long linear-range spectrofluorimetric DNA quantification using ethidium bromide, Biotechniques, 43 (2007) 173-174, 176.

[132] R.L. Steere, Electron microscopy of structural detail in frozen biological specimens, J Biophys Biochem Cytol, 3 (1957) 45-60.

[133] L. Duse, Untersuchungen einer Prototyp LED-Leuchte zur Photodynamischen Therapie mit photosensibilisator-haltigen Liposomen, in: Department of Pharmaceutics and Biopharmaceutics, Technische Hochschule Mittelhessen, Gießen, 2016.

[134] P.K. Smith, R.I. Krohn, G.T. Hermanson, A.K. Mallia, F.H. Gartner, M.D. Provenzano, E.K. Fujimoto, N.M. Goeke, B.J. Olson, D.C. Klenk, Measurement of protein using bicinchoninic acid, Anal Biochem, 150 (1985) 76-85.

[135] M.P. Bevilacqua, J.S. Pober, D.L. Mendrick, R.S. Cotran, M.A. Gimbrone, Identification of an inducible endothelial-leukocyte adhesion molecule, Proc Natl Acad Sci U S A, 84 (1987) 9238-9242.

[136] T. Mosmann, Rapid colorimetric assay for cellular growth and survival: Application to proliferation and cytotoxicity assays, 65 (1983) 55–63.

[137] M. Wintrobe, Wintrobe's Clinical Hematology, 9 ed., Lea & Febiger, Philadelphia, 1993.

[138] R. Duncan, M. Bhakoo, M.-L. Riley, A. Tuboku-Metzger, Soluble Polymeric Drug Carriers: Haematocompatibility, Birkhäuser, Basel, 1991.

[139] A. Ozcetin, A. Aigner, U. Bakowsky, A chorioallantoic membrane model for the determination of anti-angiogenic effects of imatinib, Eur J Pharm Biopharm, 85 (2013) 711-715.

[140] I.M. Tucker, J.C.W. Corbett, J. Fatkin, R.O. Jack, M. Kaszuba, B. MacCreath, F. McNeil-Watson, Laser Doppler Electrophoresis applied to colloids and surfaces, Colloids and Surfaces: A, 20 (2015) 215-226.

[141] D. Goula, J.S. Remy, P. Erbacher, M. Wasowicz, G. Levi, B. Abdallah, B.A. Demeneix, Size, diffusibility and transfection performance of linear PEI/DNA complexes in the mouse central nervous system, Gene Ther, 5 (1998) 712-717.

[142] A. von Harpe, H. Petersen, Y. Li, T. Kissel, Characterization of commercially available and synthesized polyethylenimines for gene delivery, J Control Release, 69 (2000) 309-322.

[143] M.J. Hope, R. Nayar, L.D. Mayer, P.R. Cullis, Reduction of Liposome Size and Preparation of Unilamellar Vesicles by Extrusion Techniques, in: G. Gregoriadis (Ed.) Liposome Technology, CRC Press, 1993.

[144] N. Duzgunes, Liposomes, Part D, 1 ed., Academic Press, 2004.

[145] I. Mellman, Endocytosis and molecular sorting, Annu Rev Cell Dev Biol, 12 (1996) 575-625.

[146] T.W. Prow, W.A. Rose, N. Wang, L.M. Reece, Y. Lvov, J.F. Leary, T. Vo-Dinh, W.S. Grundfest, D.A. Benaron, G.E. Cohn, Biosensor-controlled gene therapy/drug delivery with nanoparticles for nanomedicine, Advanced Biomedical and Clinical Diagnostic Systems III, 5692 (2005) 199.

[147] A. Rolland, S.M. Sullivan, Pharmaceutical Gene Delivery Systems (Drugs and the Pharmaceutical Sciences), 1 ed., CRC Press, 2003.

[148] D. Fischer, Y. Li, B. Ahlemeyer, J. Krieglstein, T. Kissel, In vitro cytotoxicity testing of polycations: influence of polymer structure on cell viability and hemolysis, Biomaterials, 24 (2003) 1121-1131.

[149] V. Pector, J. Backmann, D. Maes, M. Vandenbranden, J.M. Ruysschaert, Biophysical and structural properties of DNA.diC(14)-amidine complexes. Influence of the DNA/lipid ratio, J Biol Chem, 275 (2000) 29533-29538.

[150] H. Lodish, A. Berk, S.L. Zipursky, P. Matsudaira, D. Baltimore, J. Darnell, Biomembranes: Structural Organization and Basic Functions, in: Molecular Cell Biology, W. H. Freeman, 2000.

[151] J. Schaefer, C. Schulze, E.E. Marxer, U.F. Schaefer, W. Wohlleben, U. Bakowsky, C.M. Lehr, Atomic force microscopy and analytical ultracentrifugation for probing nanomaterial protein interactions, ACS Nano, 6 (2012) 4603-4614.

[152] J. Sitterberg, A. Ozcetin, C. Ehrhardt, U. Bakowsky, Utilising atomic force microscopy for the characterisation of nanoscale drug delivery systems, Eur J Pharm Biopharm, 74 (2010) 2-13.

[153] H. Engelberg, Plasma heparin levels. Correlation with serum cholesterol and low-density lipoproteins, Circulation, 23 (1961) 573-577.

[154] A.L. Parker, D. Oupicky, P.R. Dash, L.W. Seymour, Methodologies for monitoring nanoparticle formation by self-assembly of DNA with poly(l-lysine), Anal Biochem, 302 (2002) 75-80.

[155] J.W. Wiseman, C.A. Goddard, D. McLelland, W.H. Colledge, A comparison of linear and branched polyethylenimine (PEI) with DCChol/DOPE liposomes for gene delivery to epithelial cells in vitro and in vivo, Gene Therapy, 10 (2003) 1654-1662.

[156] M. Emerson, L. Renwick, S. Tate, S. Rhind, E. Milne, H.A. Painter, A.C. Boyd, G. McLachlan, U. Griesenbach, S.H. Cheng, D.R. Gill, S.C. Hyde, A. Baker, E.W. Alton, D.J. Porteous, D.D. Collie, Transfection efficiency and toxicity following delivery of naked plasmid DNA and cationic lipid-DNA complexes to ovine lung segments, Mol Ther, 8 (2003) 646-653.

[157] A. Raup, V. Jérôme, R. Freitag, C.V. Synatschke, A.H.E. Müller, Promoter, transgene, and cell line effects in the transfection of mammalian cells using PDMAEMA-based nano-stars, Biotechnology Reports, 11 (2016) 53-61.

[158] O.L. Mozley, A Mechanistic Dissection of Polyethylenimine Mediated Transfection of Chinese Hamster Ovary Cells, (2013).

[159] N.P. Gabrielson, D.W. Pack, Efficient polyethylenimine-mediated gene delivery proceeds via a caveolar pathway in HeLa cells, J Control Release, 136 (2009) 54-61.

[160] A.I. Ivanov, Pharmacological inhibition of endocytic pathways: is it specific enough to be useful?, Methods Mol Biol, 440 (2008) 15-33.

[161] N. Oh, J.H. Park, Endocytosis and exocytosis of nanoparticles in mammalian cells, Int J Nanomedicine, 9 (2014) 51-63.

[162] A. Hogset, L. Prasmickaite, P.K. Selbo, M. Hellum, B.O. Engesaeter, A. Bonsted, K. Berg, Photochemical internalisation in drug and gene delivery, Adv Drug Deliv Rev, 56 (2004) 95-115.

[163] M. Tomizawa, F. Shinozaki, Y. Motoyoshi, T. Sugiyama, S. Yamamoto, M. Sueishi, Sonoporation: Gene transfer using ultrasound, World J Methodol, 3 (2013) 39-44.

[164] E.C. Unger, E. Hersh, M. Vannan, T.O. Matsunaga, T. McCreery, Local drug and gene delivery through microbubbles, Prog Cardiovasc Dis, 44 (2001) 45-54.

[165] G. ter Haar, Ultrasonic imaging: safety considerations, in: Interface Focus, 2011, pp. 686-697.

[166] D. Omata, Y. Negishi, S. Yamamura, S. Hagiwara, Y. Endo-Takahashi, R. Suzuki, K. Maruyama, M. Nomizu, Y. Aramaki, Involvement of Ca(2)(+) and ATP in enhanced gene delivery by bubble liposomes and ultrasound exposure, Mol Pharm, 9 (2012) 1017-1023.

[167] D.J. Gary, N. Puri, Y.Y. Won, Polymer-based siRNA delivery: perspectives on the fundamental and phenomenological distinctions from polymer-based DNA delivery, J Control Release, 121 (2007) 64-73.

[168] S.R. Barthel, J.D. Gavino, L. Descheny, C.J. Dimitroff, Targeting selectins and selectin ligands in inflammation and cancer, Expert Opin Ther Targets, 11 (2007) 1473-1491.

[169] N. Matsuura, T. Narita, C. Mitsuoka, N. Kimura, R. Kannagi, T. Imai, H. Funahashi, H. Takagi, Increased concentration of soluble E-selectin in the sera of breast cancer patients, Anticancer Res, 17 (1997) 1367-1372.

[170] T. Narita, N. Kawakami-Kimura, N. Matsuura, J. Hosono, R. Kannagi, Corticosteroids and medroxyprogesterone acetate inhibit the induction of E-selectin on the vascular endothelium by MDA-MB-231 breast cancer cells, Anticancer Res, 15 (1995) 2523-2527.

[171] U. Bakowsky, G. Schumacher, C. Gege, R.R. Schmidt, U. Rothe, G. Bendas, Cooperation between lateral ligand mobility and accessibility for receptor recognition in selectin-induced cell rolling, Biochemistry, 41 (2002) 4704-4712.

[172] B. Carneiro, A.C. Braga, M.N. Batista, M. Harris, P. Rahal, Evaluation of canonical siRNA and Dicer substrate RNA for inhibition of hepatitis C virus genome replication--a comparative study, PLoS One, 10 (2015) e0117742.

[173] D.J. Foster, S. Barros, R. Duncan, S. Shaikh, W. Cantley, A. Dell, E. Bulgakova, J. O'Shea, N. Taneja, S. Kuchimanchi, C.B. Sherrill, A. Akinc, G. Hinkle, A.C. Seila White, B.

Pang, K. Charisse, R. Meyers, M. Manoharan, S.M. Elbashir, Comprehensive evaluation of canonical versus Dicer-substrate siRNA in vitro and in vivo, RNA, 18 (2012) 557-568.

[174] V. Kafil, Y. Omidi, Cytotoxic Impacts of Linear and Branched Polyethylenimine Nanostructures in A431 Cells, Bioimpacts, 1 (2011) 23-30.

[175] M.S. Shim, Y.J. Kwon, Acid-Responsive Linear Polyethylenimine for Efficient, Specific, and Biocompatible siRNA Delivery, Bioconjugate Chemistry, (2009).

[176] G.E. Deibler, M.S. Holmes, P.L. Campbell, J. Gans, Use of triton X-100 as a hemolytic agent in the spectrophotometric measurement of blood O2 saturation, J Appl Physiol, 14 (1959) 133-136.

[177] J.G. Lenahan, S. Frye, G.E. Phillips, Use of the Activated Partial Thromboplastin Time in the Control of Heparin Administration, Clinical Chemistry, 12 (1966) 263-268.

[178] P. Nowak-Sliwinska, T. Segura, M.L. Iruela-Arispe, The chicken chorioallantoic membrane model in biology, medicine and bioengineering, Angiogenesis, 17 (2014) 779-804.

[179] A. Vargas, M. Zeisser-Labouebe, N. Lange, R. Gurny, F. Delie, The chick embryo and its chorioallantoic membrane (CAM) for the in vivo evaluation of drug delivery systems, Adv Drug Deliv Rev, 59 (2007) 1162-1176.

5.2 List of abbreviations

AFM	Atomic Force Microscopy
AGO	Argonuate
aPTT	Activated Partial Thromboplastin Time
EDD	Egg Development Day
BCA	Bicinchoninic Acid
bp	Base Pairs
bPEI	Branched PEI
CAM	Chorioallantoic Membrane
CCD	Charged Coupled Device
CLSM	Confocal Laser Scanning Microscopy
CMOS	Complementary Metal-Oxide-Semiconductor
CMV	Cytomegalovirus
DAPI	4',6-diamidino-2-phenylindole
DDC	DOPE, DPPC, Cholesterol
DLS	Dynamic Light Scattering
DMEM	Dulbecco's Modified Eagle's Medium
DMRIE	1,2-dimyristyloxy-propyl-3-dimethyl-hydroxy ethyl ammonium bromide
DMSO	Dimethylsulphoxide
DNA	Deoxyribonucleic Acid
DODC	DOTAP, DPPC, Cholesterol
DOGS	1,2-di-(9Z-octadecenoyl)-*sn*-glycero-3- [(N- (5-amino-1-carboxypentyl) iminodiacetic acid) succinyl
DOPE	1,2-dioleoyl-sn-glycero-3-phosphoethanolamine

DOTAP	1,2-dioleoyl-3-trimethylammonium-propane
DOTIM	(1-[2-(9-(Z)-octadecenoyloxy)ethyl] -2-(8-(Z)-heptadecenyl) -3 (hydroxyethyl) imidazolinium chloride
DOTMA	1,2-di-O-octadecenyl-3-trimethylammonium propane
DPPC	Dipalmitoylphosphatidylcholine
dsiRNA	Dicer Substrate Short Interfering Ribonucleic Acid
EGF	Endothelial Growth Factor
EGFP	Enhanced Green Fluorescence Protein
ELISA	Enzyme-Linked Immunosorbent Assay
EMA	European Medicines Agency
FDA	Food and Drug Administration
FGF	Fibroblast Growth Factor
GFP	Green Fluorescence Protein
HeNe	Helium Neon
HEPES	4-(2-hydroxyethyl)-1-piperazineethanesulfonic acid
HRP	Horseradish Peroxidase
HT-DNA	Herring Testes deoxyribonucleic acid
IGF	Insulin-Like Growth Factor
IMDM	Iscove's Modified Dulbecco's Medium
IU	International Units
LDH	Lactate Dehydrogenase
LDV	Laser Doppler Velocimetry
LED	Light Emitting Diode
lPEI	Linear Polyethylenimine
LPP	Lipopolyplex

MCDB	Molecular, Cellular and Developmental Biology (medium)
MI	Mechanical Index
mRNA	Messenger Ribonucleic Acid
MTT	3-(4,5-dimethylthiazol-2-yl)-2,5-diphenyltetrazolium bromide
OD	Optical Density
PAMAM	Polyamidoamine
PBS	Phosphate Buffered Saline
PCI	Photochemical Internalisation
PDI	Polydispersity Index
pDMAEMA	Poly (2-dimethylaminoethyl methacrylate)
pDNA	Plasmid Deoxyribonucleic Acid
PDT	Photodynamic Therapy
PEG	Polyethylene Gylcol
PEI	Polyethylenimine
PLGA	Poly (lactic-co-glycolic acid)
PLL	Poly-L-lysine
PP	Polyplex
RISC	Ribonucleic Acid Induced Silencing Complex
RLU	Relative Luminescence Units
RNA	Ribonucleic Acid
RNAi	Ribonucleic Acid Interference
RT	Room Temperature
SAINT	N-methyl-4(dioleyl)methylpyridiniumchloride
SD	Standard Deviation

SELE	E-selectin
SEM	Scanning Electron Microscope
siCtrl	Control Short Interfering Ribonucleic Acid
siRNA	Short Interfering Ribonucleic Acid
SOC	Super Optimal Broth with Catabolite Repression
TBE	Tris(hydroxymethyl)aminomethane/Borate/ Ethylenediaminetetraacetic acid
TEM	Transmission Electron Microscope
TNF	Tumour Necrosis Factor
Tris	Tris(hydroxymethyl)aminomethane
UEGT	Ultrasound Enhanced Gene Transfer
VEGF	Vascular Endothelial Growth Factor
WD	Working Distance

5.3 Research output

1.) L. Duse, **S.R. Pinnapireddy**, B. Strehlow, J. Jedelská, U. Bakowsky; Can Curcumin loaded Liposomes together with LED's improve the quality of Photodynamic Therapy? Submitted manuscript

2.) E. Baghdan, **S. R. Pinnapireddy**, B. Strehlow, K. Engelhardt, J. Schäfer, U. Bakowsky; Lipid coated Chitosan-DNA nanoparticles for enhanced gene delivery. Submitted manuscript; Equally contributing author

3.) M. Möhwald, **S. R. Pinnapireddy**, B. Wonnenberg, M. Pourasghar, M.Jurisic, A. Jung, C. F. Straube, T. Tschernig, U. Bakowsky, M. Schneider; Aspherical, Nanostructured Microparticles for Targeted Gene Delivery to Alveolar Macrophages. Submitted Manuscript; Equally contributing author

4.) **S.R. Pinnapireddy**, L. Duse, B. Strehlow, J. Schäfer, U. Bakowsky; Composite liposome-PEI/nucleic acid lipopolyplexes for safe and efficient gene delivery and gene knockdown. Submitted Manuscript, under consideration.

5.) F. Yang, R. Riedel, P. Pino, B. Pelaz, A.H. Said, M. Soliman, **S.R. Pinnapireddy**, N. Feliu, W.J. Parak, U. Bakowsky, N. Hampp; Real-time, label-free monitoring of cell viability based on cell adhesion measurements with an atomic force microscope, Journal of Nanobiotechnology, 15 (2017) 23.

6.) K.H. Engelhardt, **S.R. Pinnapireddy**, E. Baghdan, J. Jedelská, U. Bakowsky, Transfection Studies with Colloidal Systems Containing Highly Purified Bipolar Tetraether Lipids from Sulfolobus acidocaldarius, Archaea, 2017 (2017).

7.) C. Janich, **S.R. Pinnapireddy**, F. Erdmann, T. Groth, A. Langner, U. Bakowsky, C. Wolk; Fast therapeutic DNA internalization - A high potential transfection system based on a peptide mimicking cationic lipid, Eur J Pharm Biopharm, (2016).

8.) A. Ewe, O. Panchal, **S.R. Pinnapireddy**, U. Bakowsky, S. Przybylski, A. Temme, A. Aigner; Liposome-polyethylenimine complexes (DPPC-PEI lipopolyplexes) for therapeutic siRNA delivery in vivo, Nanomedicine, (2016).

9.) B. Strehlow, U. Bakowsky, **S.R. Pinnapireddy**, J. Kusterer, G. Mielke, M. Keusgen; A Novel Microparticulate Formulation with Allicin In Situ Synthesis, Journal of Pharmaceutics & Drug Delivery Research, 2016 (2016).

5.4 Presentations

1.) Next Generation Nanocarriers & Future Trends in Gene Therapy - *Lecture*: **Shashank R. Pinnapireddy**; Special Session, Controlled Release Society, German Chapter (2^{nd} - 3^{rd} March 2017), Marburg, Germany.

2.) Photo-enhanced gene delivery using composite lipopolyplexes - *Poster Presentation*: **Shashank R. Pinnapireddy**, Lili Duse, Udo Bakowsky; Controlled Release Society, German Chapter (2^{nd} - 3^{rd} March 2017), Marburg, Germany.

3.) Gene delivery using non-viral vectors - *Lecture*: **Shashank R. Pinnapireddy**; Department of Pharmaceutical Chemistry, AG Steinmetzer Lab (18^{th} January 2017), Marburg, Germany.

4.) Photo-enhanced gene delivery using curcumin embedded composite lipopolyplexes - *Oral Presentation*: **Shashank R. Pinnapireddy**; GPEN (9^{th} - 12^{th} November 2016), Lawrence, USA.

5.) Ultrafection - a novel liposomal based biophysicochemical gene delivery strategy for safe and efficient gene transfer - *Oral Presentation*: **Shashank R. Pinnapireddy**; 24^{th} Mountain Sea Liposome Workshop (5^{th} - 9^{th} October 2015), Ameland, Netherlands.

6.) RNAi and gene delivery mediated via novel Lipopolyplexes - *Poster Presentation*: **Shashank R. Pinnapireddy**, Boris Strehlow, Jens Schäfer, Udo Bakowsky; Controlled Release Society Annual Meeting (26^{th} - 29^{th} July 2015), Edinburgh, Scotland.

7.) Gene Delivery and Knockdown using Novel Lipopolyplexes - *Poster Presentation*: **Shashank R. Pinnapireddy**, Udo Bakowsky; DPhG Jahrestagung (24^{th} - 26^{th} September 2014), Frankfurt, Germany.

8.) Novel Lipopolyplexes for Gene delivery and Gene knockdown - *Poster presentation*: **Shashank R. Pinnapireddy**, Udo Bakowsky; GPEN (24^{th} - 30^{th} August 2014), Helsinki, Finland.

5.5 Curriculum Vitae

PERSONAL DETAILS

Name	Shashank Reddy Pinnapireddy
Date of Birth	23 February 1990
Place of Birth	Hyderabad, India
Marital Status	Unmarried
Nationality	Indian

EDUCATION AND TRAINING

Mar 2017 - Present	Project Leader, Genetic Engineering and Biosafety Dept. of Pharmaceutics and Biopharmaceutics, University of Marburg, Marburg (Germany)
Mar 2016 - Present	Group Leader, Gene Therapy Dept. of Pharmaceutics and Biopharmaceutics, University of Marburg, Marburg (Germany)
Aug 2013 - Present	PhD Dept. of Pharmaceutics and Biopharmaceutics, University of Marburg, Marburg (Germany)
Oct 2011 - Jul 2013	Master of Engineering, Biomedical Engineering University of Halle/Anhalt University of Applied Sciences, Halle an der Saale (Germany)
Mar 2011 - Apr 2011	Internship Aurobindo Pharma Ltd., Hyderabad (India)
Oct 2007 - Jun 2011	Bachelor of Pharmacy Jawaharlal Nehru Technological University, Hyderabad (India)

SCHOOLING

Jun 2005 - Apr 2007	Intermediate Education Board of Intermediate Education, Hyderabad (India)
Jun 2001 - Apr 2005	Secondary Education St. Patrick’s High School (SSC Board), Secunderabad (India)